Development of Expression Systems for Various Forms of Human Nitric Oxide Synthase Isozymes

by

Chinhyun (Erica) Lee

A thesis
presented to the University of Waterloo
in fulfillment of the
thesis requirement for the degree of
Master of Science
in
Chemistry

Waterloo, Ontario, Canada, 2015

Author's Declaration

I hereby declare that I am the sole author of this thesis. This is a true copy of the thesis, including any required final revisions, as accepted by my examiners.

I understand that my thesis may be made electronically available to the public.

Chinhyun (Erica) Lee

Abstract

Nitric oxide (NO) is one of the important biological molecules which has functions in neurotransmission, vasodilation, and immune responses. However, excess levels of NO have been associated with neurodegenerative and inflammation-related diseases. Nitric oxide synthase (NOS) is the enzyme that catalyzes the synthesis of NO from L-arginine in biological systems, and has been a potential target for inhibition. Three isoforms of NOS exist in mammalian systems: neuronal NOS (nNOS), endothelial NOS (eNOS), and inducible NOS (iNOS). While nNOS and eNOS are named according to where they are expressed, iNOS is named by its inducible expression. The structures of the active sites of the three isoforms are determined to be similar.

This has been posing a challenge in the development of NOS inhibitors, because inhibition of eNOS has been shown to ultimately lead to hypertension and atherosclerosis. To overcome this, researchers have examined a wide variety of possible inhibitors. Binding of the inhibitors to non-human NOS isoforms was often studied by crystallography and by mutagenesis studies. However, none of the inhibitors have been approved for clinical applications.

In this study, expression systems for different forms of human NOS isozymes were investigated. This involved molecular cloning of expression vectors for human full-length NOS isozymes and their oxygenase domains. It has been demonstrated that preparations of oxygenase domains is easier giving good yields due to their smaller size compared to the holoenzymes. After confirmation of the molecular cloning of the expression vectors by restriction enzyme digestions and by DNA sequencing, expression and purification of the oxygenase domains were attempted. As N-terminal histidine tags were present in the

oxygenase domains, protein purifications were carried out in nickel affinity columns. For the human nNOS oxygenase domain with the CaM-binding region, the protein was also purified by a glutathione column as a second purification step with the addition of glutathione S-transferase-tagged calmodulin (GST-TEV-CaM). It is shown that the oxygenase domains are well expressed but further protein purification is required.

Lastly, expression and purification of GST-TEV-CaM were developed and optimal cleavage reaction conditions of GST-TEV-CaM by TEV protease were studied. From this study, optimal cleavage reaction condition is identified for GST-TEV-CaM which can be used in the purification of various forms of human NOS isozymes. These studies will allow optimization of purification of human forms of NOS oxygenase domains and holoenzymes for binding studies with NOS inhibitors.

Acknowledgements

I would like to thank my supervisor Dr. Guy Guillemette for his guidance, support, and patience throughout my studies. I am grateful for the opportunity to work in his laboratory and the knowledge he provided me.

I would like to also thank my committee members, Dr. Thorsten Dieckmann and Dr. Gary Dmitrienko, for reading and reviewing my thesis.

I am grateful to my past and present lab mates: Valentina Taiakina, Mike Piazza, Jenna Collier, Maggie Zhou, Ryan Cho, Simon Guillemette, Edmund Luk, Kevin Pottruff, John Lape, and Matthew Nguyen for their help and for providing an enjoyable lab environment. Thank you to my friends in the department as well for their friendship and support during my studies.

Special thanks go to my family for their love and support. Thank you.

Dedication

To my family

for your love and support throughout my studies

Table of Contents

List of Figures

List of Tables

List of Abbreviations

δ-ALA	δ-aminolevulinic acid
CaM	Calmodulin
eNOS	Endothelial nitric oxide synthase
FAD	Flavin-adenine dinucleotide
FMN	Flavin mononucleotide
GST-TEV-CaM	Glutathione S-transferase-tagged calmodulin
heNOS	Human full-length eNOS
heNOSox	Human eNOS oxygenase domain without CaM-binding motif
heNOSoxyCaM	Human eNOS oxygenase domain with CaM-binding motif
hiNOS	Human full-length Δ70 iNOS
hiNOSox	Human Δ70 iNOS oxygenase domain without CaM-binding motif
hiNOSoxyCaM	Human Δ70 iNOS oxygenase domain with CaM-binding motif
hnNOS	Human full-length nNOS
hnNOSox	Human nNOS oxygenase domain without CaM-binding motif
hnNOSoxyCaM	Human eNOS oxygenase domain with CaM-binding motif
iNOS	Inducible nitric oxide synthase
IPTG	Isopropyl β-D-1-thiogalactopyranoside
LB	Luria-Bertani broth
L-NNA	*N*-nitro-L-arginine
NADPH	Nicotinamide adenine dinucleotide phosphate
NHA	N^{ω}-hydroxy-L-arginine
nNOS	Neuronal nitric oxide synthase
NO	Nitric oxide
NOS	Nitric oxide synthase
PCR	Polymerase chain reaction
SLIC	Sequence- and ligation-independent cloning
TB	Terrific broth
BH_4	Tetrahydrobiopterin
TEV	Tobacco Etch Virus

Chapter 1

Introduction

1.1 Nitric Oxide in Biological Systems

Nitric oxide (NO) is a highly reactive free radical, which consists of a nitrogen and an oxygen atom (Bretscher et al., 2003). In biological systems, it is an essential molecule that participates in various physiological processes. In the nervous system, it is produced as a signaling molecule for neurotransmission. It is also found in endothelial cells, in which it is involved in the regulation of blood pressure. Last but not least, it plays an important role in the immune system by being present in high amounts and exhibiting cytotoxic effects against infections and tumour cells (Joubert & Malan, 2011).

Our body is able to produce this molecule and its production appears to require tight regulation, as insufficient or excessive production demonstrates pathological role in several disease states. Low concentrations of NO in neurons and endothelial cells have been related to hypertension, atherosclerosis, and other cardiovascular diseases. On the other hand, excess NO has been observed in patients with neurodegenerative diseases such as Parkinson's and Alzheimer's diseases (Xue et al., 2010). In the immune system, overproduction of NO seems to be linked to inflammation, immune-type diabetes, and rheumatoid arthritis (Garcin et al., 2008). Due to its roles mentioned, there is significant interest in finding ways to control NO production.

1.2 Nitric Oxide Synthase

Nitric oxide synthase (NOS) is the enzyme that is responsible for the synthesis of NO molecules in biological system.

1.2.1 NOS Isoforms

Three isoforms of NOS are identified in mammalian systems, which are neuronal NOS (nNOS), endothelial NOS (eNOS), and inducible NOS (iNOS). nNOS carries out NO synthesis in the central nervous system, while eNOS takes part in the regulation of smooth muscle relaxation. iNOS received its term 'inducible' from its inducible expression in macrophages in contrast to nNOS and eNOS, whose expressions are constitutive (Joubert & Malan, 2011). Another feature that nNOS and eNOS share is that their enzymatic reactions are subject to formation of complexes with Ca^{2+}/calmodulin. Calmodulin (CaM) is a calcium-sensing protein in cells, which can bind to and activate NOS. iNOS is quite different from nNOS and eNOS, whose activity is independent of calcium content in cells. The three isoforms, having different features, also show to derive from different genes and to have different subcellular localizations and inhibitor binding. Nonetheless, about 50% amino acid sequence homology was seen between the human isoforms (Alderton et al., 2001).

1.2.2 NOS Structure

Despite the differences in their primary amino acid sequences, the three isoforms were observed to be comprised of similar components. They are homodimeric proteins, in which each monomer consists of two domains (Joubert & Malan, 2011). The N-terminal domain displays oxygenase activity that has binding sites for a heme, tetrahydrobiopterin (BH_4), and its substrate, L-arginine. The C-terminal domain is a reductase domain which contains sites for flavin mononucleotide (FMN), flavin-adenine dinucleotide (FAD), and nicotinamide adenine dinucleotide phosphate (NADPH). The two active domains are connected by a calmodulin binding motif (Alderton et al., 2001).

The active site is found in the N-terminal oxygenase domain, to which heme and BH_4 are bound, and to which electrons from the reductase domain are finally transferred. Crystal structures of the isoforms reveal high conservation of residues in the active sites of all three isoforms, and this has posed a challenge in the design of isoform-selective inhibitors of NOS (Ji et al., 2010).

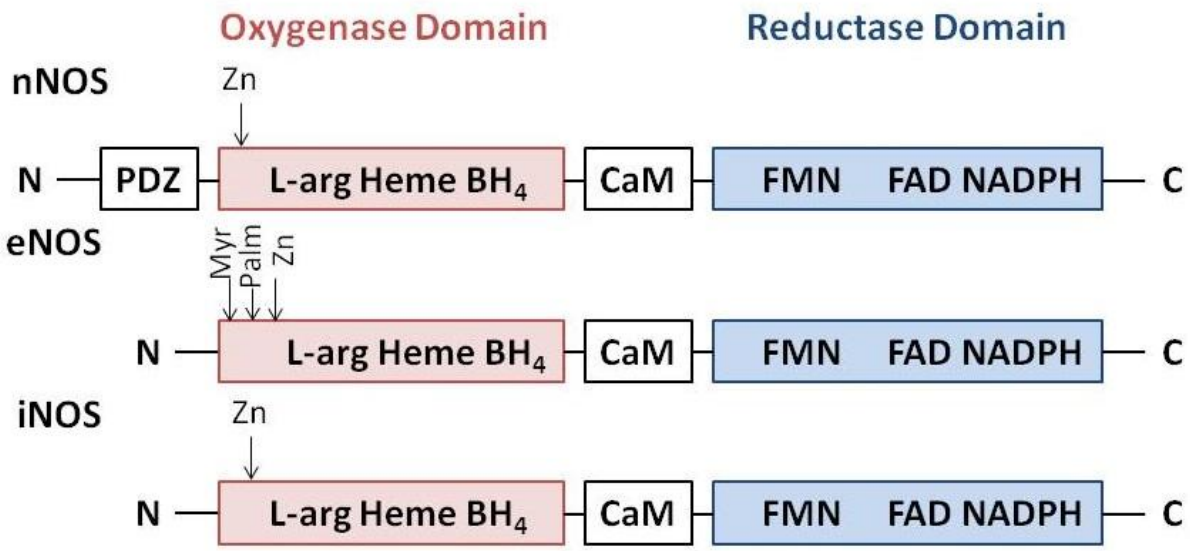

Figure 1.1 Illustration of the structures of NOS isoforms. This figure also indicates the locations of PSD-95 discs large/ZO-1 homology domain (PDZ), zinc-ligating cysteines (Zn), and myristoylation (Myr) and palmitoylation (Palm) sites. (Alderton et al., 2001)

1.2.3 NO Synthesis Reaction

For NO synthesis, the two domains that are present in each monomer have distinctive roles. The reductase domain, as its name suggests, reduces the other domain upon firstly accepting a hydride ion from NADPH producing $NADP^+$. Then, electrons are transferred from $FADH_2$ to FMNH·. $FMNH_2$ in the reductase domain lastly donates the electrons to the heme iron in the oxygenase domain where NO synthesis occurs (Alderton et al., 2001).

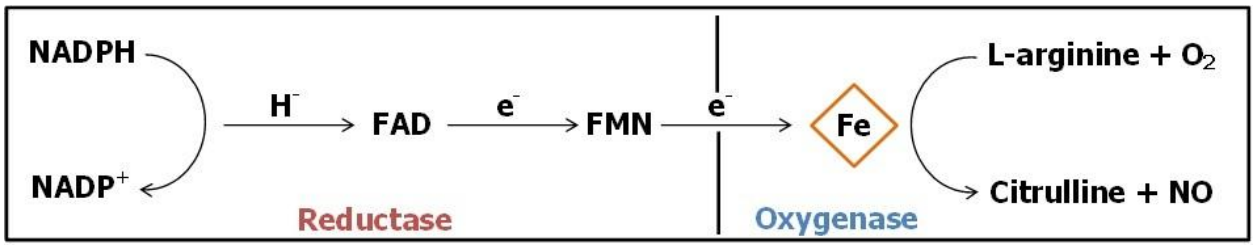

Figure 1.2 Overall NOS reaction

The oxygenase domain generates NO upon conversion of L-arginine into L-citrulline. The domain hydroxylates L-arginine at one of the guanidino nitrogens, using molecular oxygen (O_2) as co-substrate. This reaction forms the intermediate, N^{ω}-hydroxy-L-arginine (NHA). The reaction further continues to produce NO and L-citrulline from NHA (Hurshman & Marletta, 2002).

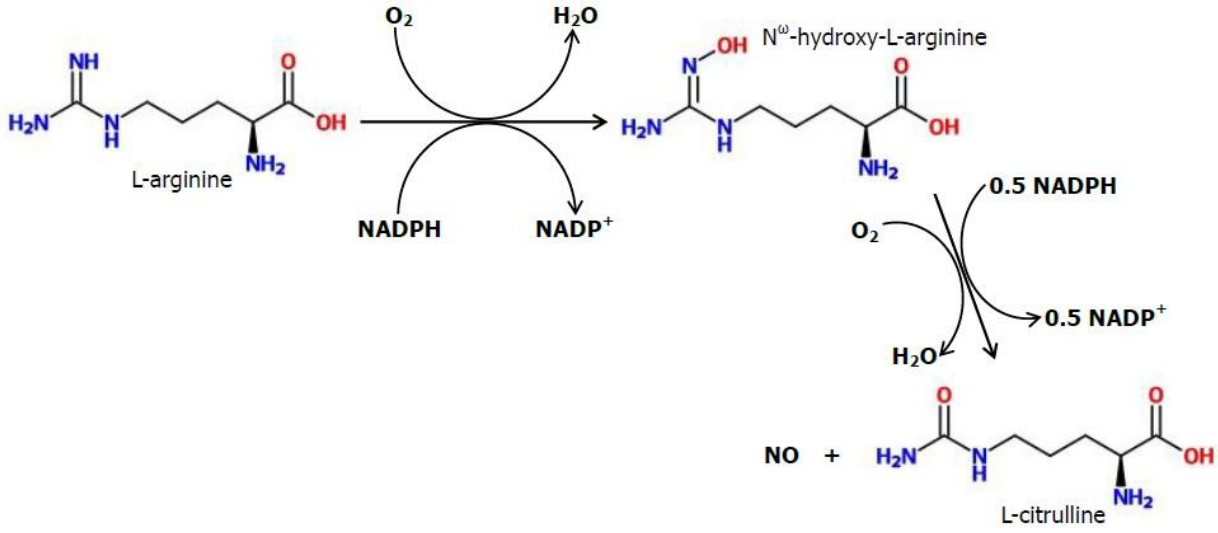

Figure 1.3 NO synthesis reaction at the oxygenase domain

1.3 NOS Inhibitors

Due to their aforementioned pathological effects by NO overproduction, nNOS and iNOS have been therapeutic targets for inhibition. However, inhibition of eNOS results in low levels of NO, which can lead to hypertension and other cardiovascular diseases. For these

reasons, studies on the development of isoform-selective inhibitors have been extensively performed, and numerous inhibitors have been generated. Based on their structures, the inhibitors are divided into two groups: amino acid-based inhibitors and non-amino acid-based inhibitors (Salerno et al., 2002).

1.3.1 Amino acid-based Inhibitors

L-Arginine analogues are one of the studied amino acid-based inhibitors, as they tend to be less toxic and potent *in vivo* with their similarity in structure to L-arginine. One disadvantage of these inhibitors was that they do not show high selectivity (Bretscher et al., 2003). Another example of amino acid-based inhibitors is *N*-nitro-L-arginine (L-NNA) (Fig. 1.4 (a)). This compound was demonstrated to inhibit NOS activity well but studies also revealed moderate selectivity. As well, it showed to have low solubility at neutral pH (Vitecek et al., 2012). Dipeptides were synthesized with L-NNA and as products, dipeptides such as D-Phe-D-Arg$^{NO}_2$ and L-Lys-D-Arg$^{NO}_2$-NH_2 were made whose selectivities for nNOS were high. The study also demonstrated that dipeptides containing basic amine side chains were effective against and selective for nNOS by forming non-covalent interactions (Salerno et al., 2002). However, being also selective for eNOS, the dipeptides were evaluated to be unsafe for clinical trials.

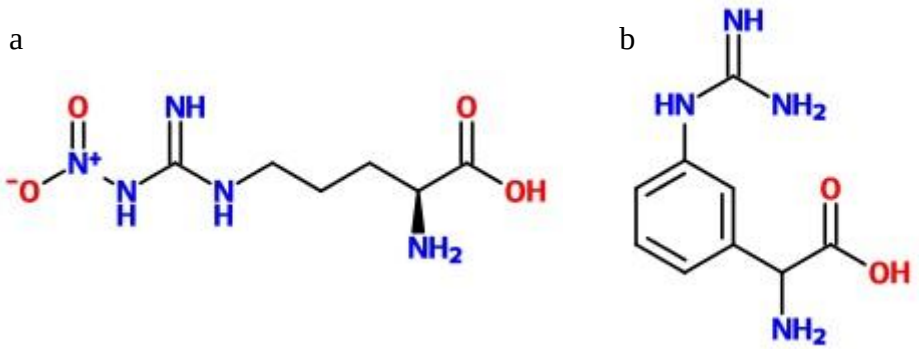

Figure 1.4 Examples of amino acid-based inhibitors. (a) N-nitro-L-arginine (b) m-guanidino-D, L-phenylglycine

1.3.2 Non-Amino acid-based Inhibitors

Non-amino acid-based inhibitors were also examined for design of NOS inhibitors with high selectivity and potency. Results from studies on these inhibitors presented that inhibition of NOS does not necessarily require the amino acid moiety. This group could be further broken down into two subgroups, the amidinic and heterocyclic compounds. Amidinic compounds, which encompass guanidines, isothioureas, and amidines, had efficient NOS inhibition (Salerno et al., 2002). Their structures could mimic that of L-arginine, which showed different selectivities with their diverse moieties. Similarly, studies demonstrated that heterocyclic compounds, such as indazoles, and imidazoles, could effectively inhibit NOS isoforms with excellent selectivity. However, a general relationship between inhibitor structures and their activities on the isoforms could not been identified so far. This seemed to be because the structures vary widely and the inhibitors have different mechanisms of action. As well, despite in-depth research, no inhibitor has been approved for clinical applications (Maddaford et al., 2009).

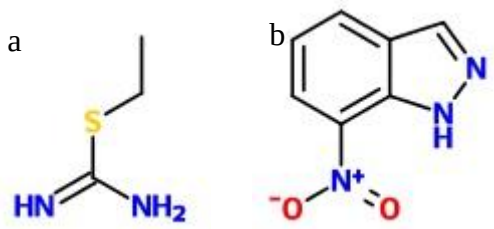

Figure 1.5 Examples of non-amino acid-based inhibitors. (a) S-ethylisothiourea (b) 7-nitroindazole

1.4 Challenges in the Development of NOS Inhibitors

Challenges in the development of isoform-selective NOS inhibitors include similar active sites among the isoforms, as well as difficulty in defining a structure-activity relationship of NOS inhibitors, as mentioned before. Furthermore, advancement in the development of effective NOS inhibitors appears to be slow due to insufficient information on inhibitor binding to NOS isoforms. Binding of NOS inhibitors has often been examined using crystallography, but several limitations on the technique have been suggested. Some examples are ambiguities with the identity or the position of a compound in the binding site, and the fact that biophysical information on the inhibitor binding, such as binding enthalpies and interaction types, cannot be obtained from crystal structures (Maddaford et al., 2009). There have been cases of inhibitor studies where crystal structures suggested promising bindings of inhibitors but other binding studies demonstrated poor activities of the inhibitors.

Studies on non-human NOS isoforms also seem to present a challenge. For many binding studies of NOS inhibitors, several mammalian NOS isoforms were used such as rat nNOS, bovine eNOS, and murine iNOS. Rat nNOS has been comprehensively studied due to its 90% sequence identity to human nNOS and its efficient purification method. However, other studies have shown that rat nNOS has different binding affinities to certain inhibitors from that of human nNOS, although the affinities for L-arginine were similar (Fang et al., 2009).

1.5 Anchored Plasticity Approach

In order to solve the problem with conserved active sites, Garcin et al. (2008) proposed a systematic and logical approach in investigating isoform-selective inhibitors, called the anchored plasticity approach. This approach analyzes inhibitor binding and enzyme structural

changes to discover isoform-selective binding modes. In this approach, an inhibitor is set or anchored in a conserved active site and then, upon addition of rigid substituents to the structure, formation of a novel isoform-specific pocket is explored. In the study by Garcin et al., this approach was demonstrated with an aminopyridine compound, shown in Figure 1.6 (a). From IC_{50} results, this compound was more potent to iNOS than to eNOS. Crystal structures revealed that while the amidine moiety of the compound binds and stacks with the heme in the active site, its side chain causes a conformational change in iNOS and creates a novel pocket. This seemed to have occurred by the movement of outer residues that interact with the residues in the active site. In iNOS, the residue that interacts with the active site residues, referred as the first-shell residue, was arginine, which seems to be able to freely rotate and form the novel pocket and additional hydrogen bonds (Fig. 1.6 (b)). However, in eNOS, the rotation of arginine in the first shell was seen to be restricted by third-shell residues, leucine and isoleucine, which are different from those in iNOS (Table 1.1). This was proposed to prevent eNOS from creating a pocket with additional hydrogen bonds decreasing its binding affinity. Similar results were observed with an iNOS mutant that is composed of eNOS third-shell residues, where the binding affinity of the inhibitor to the mutant was decreased (Garcin et al., 2008).

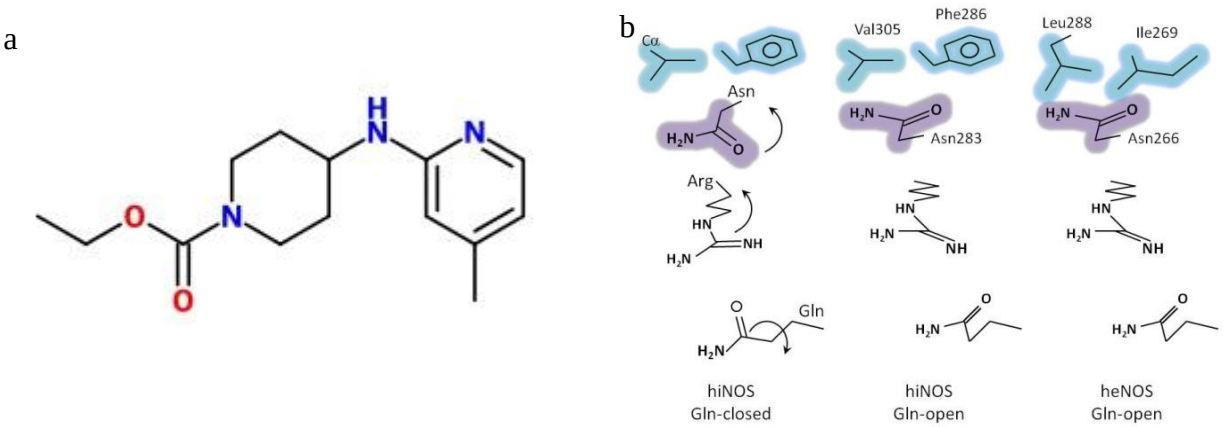

Figure 1.6 Aminopyridine compound whose NOS binding was studied by Garcin et al. (a) and a schematic diagram illustrating movement of residues in human Δ70 iNOS and eNOS upon its binding (b). Unhighlighted Gln and Arg are first shell residues while those in orange are second shell residues. Third shell residues are highlighted in green. In iNOS, binding of the compound induces Gln-open conformation which leads to rotations of Arg and Asn. eNOS cannot form the Gln-open conformation due to the presence of third shell residues, leucine and isoleucine. The Figure is modified from Garcin et al., 2008.

Table 1.1 Major residues that participate in creation of isoform-specific pockets in NOS. This table shows isoform-specific residues in the third shell that are different between NOS isoforms. Table is modified from Garcin et al., 2008.

NOS isoform	Active site	First shell				Second shell	Third shell	
Mouse iNOS	Glu371	Gln257	Tyr341	Arg260	Arg382	Thr277	Phe280	Leu299
Human iNOS	Glu377	Gln263	Tyr347	Arg266	Arg388	Asn283	Phe286	Val305
Bovine eNOS	Glu362	Gln248	Tyr332	Arg251	Arg373	Asn268	Ile271	Leu290
Human eNOS	Glu360	Gln246	Tyr330	Arg249	Arg371	Asn266	Ile269	Leu288

1.6 Research Objectives

The research objectives of this study were to produce human isoforms of NOS and study their interactions with NOS inhibitors for better understanding of isoform selectivity that will be useful in the development of NOS inhibitors with enhanced selectivity. The research aimed at testing the possibility that isoform specific binding to human NOS isozymes has been overlooked because of the general use of non-human mammalian recombinant enzymes. Most of the published studies have used recombinant bovine eNOS and rat nNOS, in addition to human iNOS. For this reason, new expression systems were developed in the lab for the human NOS isozymes. The investigation focussed on characterizing the new expression systems with the ultimate goal of using them to test the anchored plasticity approach for the identification of NOS isoform specific inhibitors.

In the past, various host cells have been used for the expression of mammalian NOS enzymes including yeast, insect cells, and bacteria (Roman et al., 1995). Of all the host cell systems used, it was discovered that bacterial cells gave the best results. Our lab has produced the human iNOS, rat nNOS and bovine eNOS but never the human forms of nNOS and eNOS. Our experience showed that the expression and purification of these enzymes was very labour intensive and gave low yields of recombinant protein. Accordingly, it was decided to try a parent plasmid with a stronger promoter in the hope of getting better expression and yields of the protein. Most P450-like proteins including NOS have been expressed in *E. coli* using the pCWori expression vector. pCWori is not a strong expression vector and it was decided to try using a vector with a strong promoter from the pET series.

Each of the active sites in NOS isozymes are composed of a dimer consisting of oxygenase domains from two NOS subunits. Previous studies have shown that active site

dimers can be generated from recombinant expression of the oxygenase domain alone (McMillan & Masters, 1995). Also, recombinant NOS oxygenase domain expression systems generally provide higher yields and require less complex expression and purification procedures (Rafferty et al., 1999). Consequently, for the initial screening of inhibitors that bind to the enzyme active site, expression systems consisting of the oxygenase domains for each of the three isoforms were generated. Expression systems for the human NOS holoenzymes will also be required to assay the enzymes activity in the presence of any lead compounds from the oxygenase investigation.

In order to further functionalize the recombinant forms of the NOS enzymes, expression systems for all three enzymes were generated that consisted of the catalytic oxygenase domain as well as the downstream calmodulin (CaM) binding domain that resides in between the oxygenase and reductase domains of NOS isozymes. These constructs were referred to as oxyCaM proteins and the CaM-binding region that could be used as an additional affinity tag for purification of the oxygenase domains and for protein immobilization. Chapter 2 describes the subcloning and characterization of all nine constructs.

Chapter 3 describes the initial attempts to express and purify the oxygenase domains of all three isoforms of human NOS. In chapter 4, an expression vector for GST-TEV-CaM was constructed and the recombinant protein was characterized. This fusion protein could be used in purification of NOS isoforms and oxygenase domains using a glutathione column. The expression vector for GST-TEV-CaM was created such that a Tobacco Etch Virus (TEV) protease site would be present between GST and CaM for removal of GST portion. Accordingly, different reaction conditions for optimization of the GST-TEV-CaM cleavage reaction were explored.

Chapter 2

Subcloning of Human NOS Isoforms and Oxygenase Domains

2.1 Introduction

In this chapter, molecular cloning of human NOS oxygenase domains and holoenzymes is described. Not all but most of the human NOS isoforms and oxygenase domains were cloned into pDS-78 while others were in a pCWori vector. pDS-78 was a modified version of the kanamycin resistant pET28a vector which has a cleavage site for TEV protease incorporated four amino acids after the N-terminal hexahistidine tag. The cleavage site, which is ENLYFQG, was added for removal of the N-terminal hexahistidine tag. pCWori, which contains an ampicillin resistance gene, is a commonly used vector for expression of NOS in *E. coli* and the protein expression from a pET vector was attempted in this study (Roman et al., 1995). A major difference between pCWori and pET is the promoter which controls mRNA transcription for the recombinant protein. In pCWori, the expression of the recombinant protein is under control of a tac promoter, a hybrid promoter of -35 region of a trp promoter and -10 region of a *lacUV5* promoter. The combination of the two regions is known to be a favourable binding site for *E. coli* RNA polymerase. Instead, pET has a T7 promoter which T7 RNA polymerase specifically recognizes (Zelasko et al., 2013).

The construction of phnNOSox, pheNOSox, and pCWori-hiNOSox was carried out by Jenna Collier (UW Co-op student) and Maggie Zhou (BSc. U of Waterloo, Summer student). The molecular cloning of phnNOSoxyCaM was carried out by the candidate, and that of pheNOSoxyCaM was performed by Kevin Pottruff (BSc. U of Waterloo). pCWori-hiNOSoxyCaM was created by Simon Guillemette (BSc. U of Waterloo, Summer student). The molecular cloning of phnNOS was carried out by Edmund Luk (UW Co-op student), while that

of pheNOS was done by Ryan Cho (BSc. U of Waterloo, Summer student). Jenna Collier (UW Co-op student) and Maggie Zhou (BSc. U of Waterloo, Summer student) also accomplished the construction of phiNOS.

2.2 Methods

2.2.1 phnNOSox

phnNOSox was the expression vector for the human nNOS oxygenase domain without CaM-binding region (hnNOSox). This vector contained the human nNOS oxygenase domain whose amino acid sequence ended just before the CaM-binding region in pDS-78. The cloning was accomplished by Polymerase chain reaction (PCR) amplification of the human nNOS oxygenase domain from the full-length human nNOS. The forward and reverse primers used were, respectively:

HnoxyFor 5’ GGAATTCATATGGAGGATCACATGTTCGGTG 3’

HnoxyStop 5’ ATCGATAAGCTTATCAGGTGCCTTTCCAGACATGCGTGTTCC 3’

NdeI and HindIII sites were present in the primers at 5’- and 3’-ends, respectively, and so were digested for insertion of the PCR product into pDS-78.

2.2.2 pheNOSox

Human eNOS oxygenase domain without the CaM-binding regioin (heNOSox) was cloned into pDS-78 as well and the cloning was done similarly to phnNOSox. heNOSox gene was PCR amplified and NdeI and HindIII sites that were present in the forward and reverse primers, respectively, were also incorporated by PCR.

eNoxFor 5’ GCGGAATTCATATGCACCACCACCACCACCACATGGGCAACTTGAAGA GCGTGGCC 3’

eNoxRev 5’ CAGGAAGCTTATCAGATGCCGGTGCCCTTGGCGG 3’

2.2.3 pCWori-hiNOSox

pCWori-hiNOSox was the expression vector for human Δ70 iNOS oxygenase domain without the CaM-binding region (hiNOSox) in which residues 1 – 70 were removed. This was because the region seems to be prone to proteases and hold rare codons. For its construction, a stop codon was introduced just downstream of human Δ70 iNOS oxygenase domain in the holoenzyme that is in the ampicillin resistant vector, pCWori by two-stage PCR site-directed mutagenesis (Wang & Malcolm, 1999). This mutagenesis protocol has an additional PCR stage to the original PCR site-directed mutagenesis protocol. Prior to the PCR stage with both forward and reverse primers that have the intended mutation, two PCRs, one with only the forward primer and another one with the reverse primer, are carried in separate tubes for 1 to 5 cycles. Afterwards, the two samples are mixed and are subjected to 15 PCR cycles as in the original PCR site-directed mutagenesis. Then, one adds the restriction enzyme, DpnI, which digests only methylated plasmids, the template, and uses the sample for bacterial transformation. In pCWori-hiNOSox, a HindIII site was incorporated at the 3'-end of the stop codon. As an additional HindIII site was present just downstream of the reductase domain, the mutagenesis could be confirmed by HindIII digestion, in which two fragments of 6.3 kb and 1.9 kb were generated. Then, HindIII digestion and a subsequent ligation reaction were performed for removal of the reductase domain. The removal was verified by HindIII digestion where a fragment of 1.9 kb was absent.

2.2.4 phnNOSoxyCaM

phnNOSoxyCaM, the expression vector for human nNOS oxygenase domain with the CaM-binding region (hnNOSoxyCaM), was also made by two-stage PCR site-directed mutagenesis. The template used in the PCR amplification was the pDS-78 vector containing

the full-length human nNOS and a stop codon and an EcoRI were incorporated at the 3'-end of CaM-binding region. This was accomplished with the forward and reverse primers:

HnNOSOxCamF 5' GGGGCAGGCTATGGCCTAGAATTCGAAAGCGACCATCCTCTAT GCC 3'

HnNOSOxCamR 5' GGCATAGAGGATGGTCGCTTTCGAATTCTAGGCCATAGCCTGC CCC 3'

After plasmid purification, the mutagenesis was verified by EcoRI digestion from which two DNA bands of 7.6 kb and 2.3 kb were seen.

2.2.5 pheNOSoxyCaM

For the expression vector coding human eNOS oxygenase domain with the CaM-binding region (heNOSoxyCaM), full-length human eNOS in pDS-78 was also subjected to PCR amplification for addition of a stop codon downstream of CaM-binding region by two-stage PCR site-directed mutagenesis. As well, a HindIII restriction site was added at the 3'-end of the stop codon to be used for confirmation of the intended mutation with the following primers:

HeNOSoxCamF 5' CATGGGCACGGTGATGGCGTAAGCTTTGAAGGCGACAATCCTGT ATGGCTCC 3'

HeNOSoxCamR 5' GGAGCCATACAGGATTGTCGCCTTCAAAGCTTACGCCATCACCG TGCCCATG 3'

HindIII digestion of a candidate vector generated an 8.8 kb and a 2.2 kb fragment which confirmed the presence of the intended mutation.

2.2.6 pCWori-hiNOSoxyCaM

The expression vector for human Δ70 iNOS oxygenase domain with the CaM-binding region (hiNOSoxyCaM), pCWori-hiNOSoxyCaM, was also constructed by two-stage PCR site-directed mutagenesis. Full-length human Δ70 iNOS in an ampicillin resistant pCWori vector was taken and a stop codon and a HindIII restriction site were introduced downstream of CaM-binding region. The forward and reverse primers used for the mutagenesis were:

HiNOSoxCamF 5' GACAATGGCGTCCCGAGTCTGAAGCTTCATCCTCTTTGCGACAG AGACAG 3'

HiNOSoxCamR 5' CTGTCTCTGTCGCAAAGAGGATGAAGCTTCAGACTCGGGACGCC ATTGTC 3'

The success of the mutagenesis was confirmed by HindIII digestion. The digestion resulted in a 1.8-kb and a 6.4-kb fragment, as expected.

2.2.7 phnNOS

pDS-78 vector containing the full-length human nNOS (hnNOS) coding region was prepared by one-step sequence- and ligation-independent cloning (SLIC) method (Jeong et al., 2012). This method involved PCR amplification of the full-length human nNOS. The primers used were:

HNfullfor 5' CTTGTATTTCCAGGGCCATATGGAGGATCACATGTTCGGTGTTCAGC 3'

HNfullrev 5' CAGCAGCTTACGATCTTCTTCCATATTAGGAGCTGAAAACCTCATCGG TGTCT 3'

The forward and reverse primers used were designed so that regions homologous to *Nde*I-cleaved vector ends are incorporated to the ends of the PCR product. Afterwards, the PCR product and cleaved vector were mixed at an insert-to-vector ratio of 2:1. One also added, to the mixture, T4 polymerase which has 3' to 5' exonuclease activity and creates 5' overhangs,

and incubated for 3.5 minutes at room temperature. This mixture was then used in bacterial transformation by heat shock in which DNA gaps would be repaired and the cloning would be completed.

2.2.8 pheNOS

The full-length human eNOS (heNOS) was cloned into pDS-78. Initially, the full-length human eNOS coding region was PCR amplified with the following primers:

Hefullfor 5’ CTTGTATTTCCATATGGGCAACTTGAAGAGCGTGGCCCAGGAG 3’

HefullrevEcoRI 5’ GCGGAATTCTCAGGGGCTGTTGGTGTCTGAGCCGGG 3’

While an NdeI site was already present in the PCR product amplified, the reverse primer in the PCR had an EcoRI site to add to the 5’ end. The PCR product as well as the vector, pDS-78, were then digested with NdeI and EcoRI, and were mixed in a ligation reaction. Subsequent bacterial transformation by heat shock was performed. This resulted in the full-length human eNOS coding region to be in the kanamycin resistant pDS-78 vector. Also, the human eNOS would be hexahistidine-tagged at its N-terminal end, when expressed in *E. coli* cells.

2.2.9 phiNOS

phiNOS, full-length human Δ70 iNOS (hiNOS) in pDS-78, was made digestion and ligation procedures. For its cloning, the full-length human Δ70 iNOS coding region was isolated from ampicillin resistant pCWOri vector by double digestion with NdeI and HindIII restriction enzymes. The region of interest was cut out such that its N-terminal hexahistidine tag from pCWOri vector was retained. Subsequently, it was inserted into a pDS-78 vector. This allowed the human Δ70 iNOS coding region to be in the kanamycin resistant pET28a vector.

2.3 Results

2.3.1 Expression Vectors for Human NOS Oxygenase Domains without CaM-binding region

Digestion of phnNOSox with NdeI and HindIII resulted in a 2.2-kb fragment which was the human nNOS oxygenase domain without the CaM-binding region and a 5.3-kb fragment, the pDS-78 vector. As well, complete sequencing of the oxygenase domain verified its subcloning without any mutations. From this result, it could be confirmed that the human nNOS oxygenase domain was successfully inserted into pDS-78 vector (Figure 2.1). (please refer to Appendix for vector sequences)

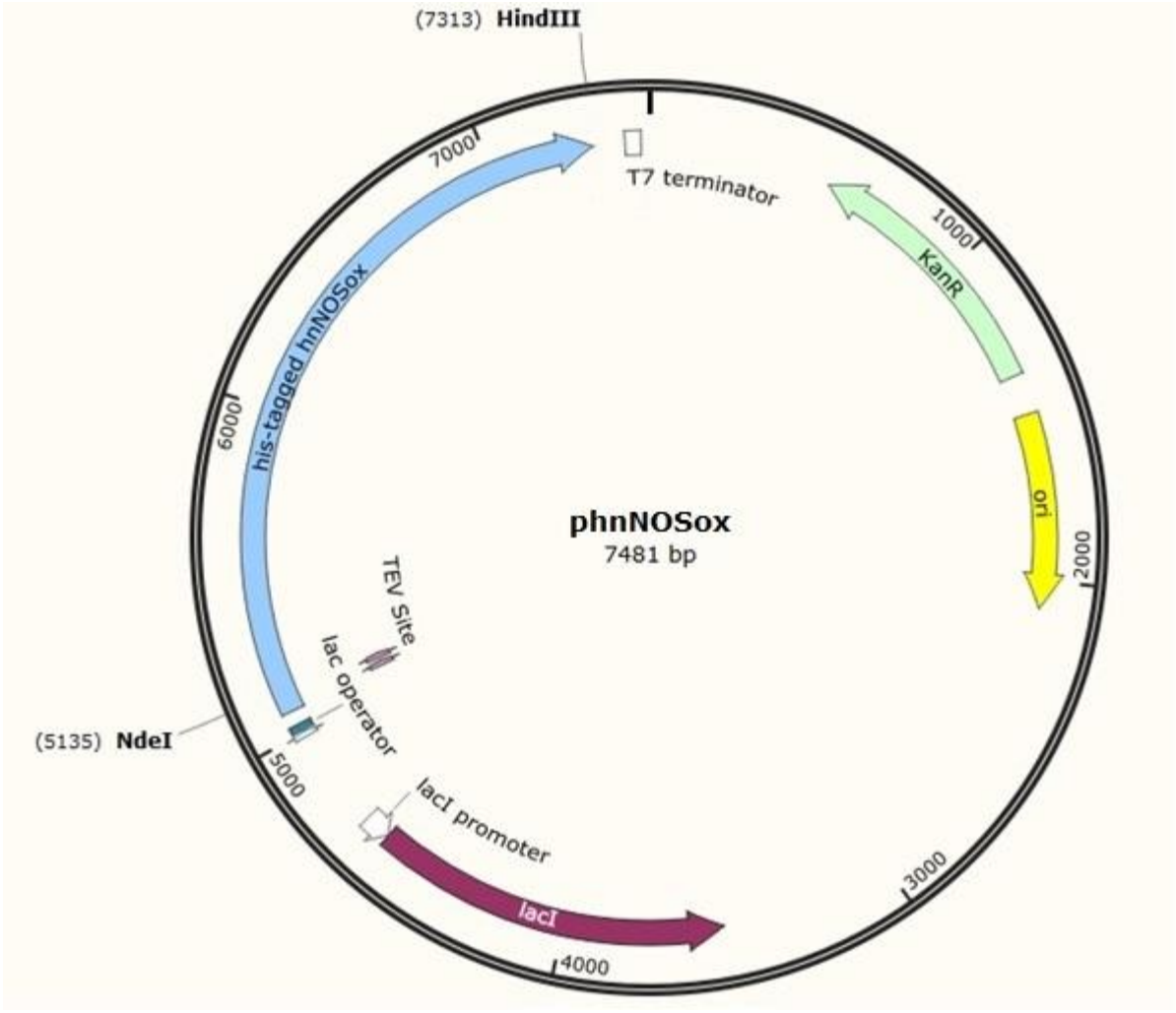

Figure 2.1 Vector map of phnNOSox coding human nNOS oxygenase domain without CaM-binding region. This figure is showing features present in the phnNOSox vector, such as the kanamycin resistant gene and *lacI* gene. It is also showing restriction enzyme sites that one used for subcloning of human nNOS oxygenase domain into pDS-78 vector.

The molecular cloning of human eNOS oxygenase domain without the CaM-binding region was verified by double digestion with NdeI and HindIII as well. The double digestion generated the 1.5-kb insert and 5.3-kb vector. The insert was also fully confirmed by sequencing. (Figure 2.2)

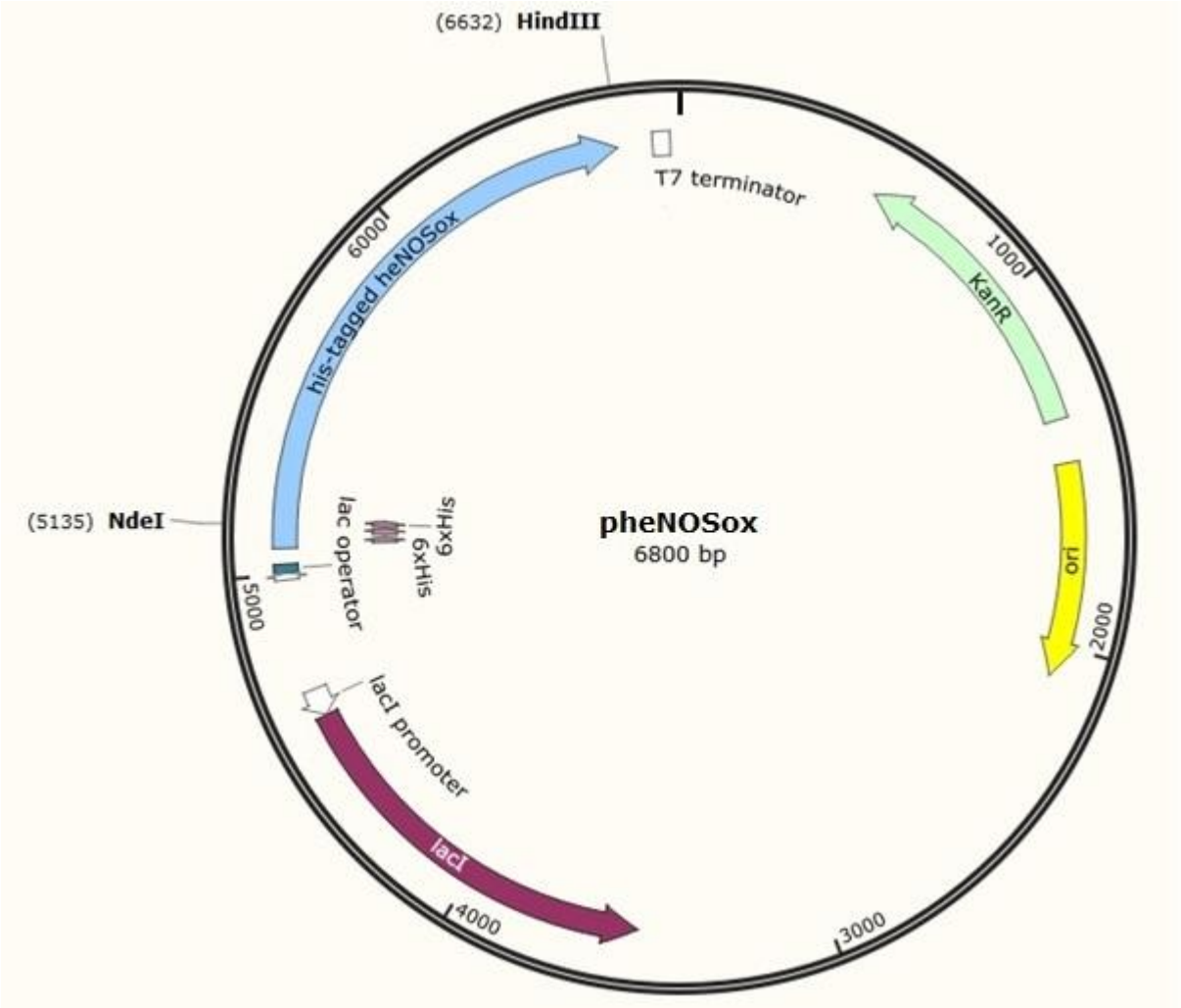

Figure 2.2 Vector map of pheNOSox coding human eNOS oxygenase domain without CaM-binding region. The insert was subcloned into kanamycin resistant pDS-78 vector at NdeI and HindIII sites, which are shown in this figure. Accordingly, N-terminal histidine tag and a TEV protease site was added to the insert.

Digestion of pCWori-hiNOSox with HindIII did not show a fragment of 1.9 kb which confirmed the removal of the reductase domain with the CaM-binding region and relegation of the vector. Also, the removal was confirmed by sequencing. However, the DNA sequences 1 – 165 and 1177 – 1206 were not examined and can be sequenced with primers pCWOri-fr and 1000iNOSfr. (please refer to the Appendix for DNA sequences)

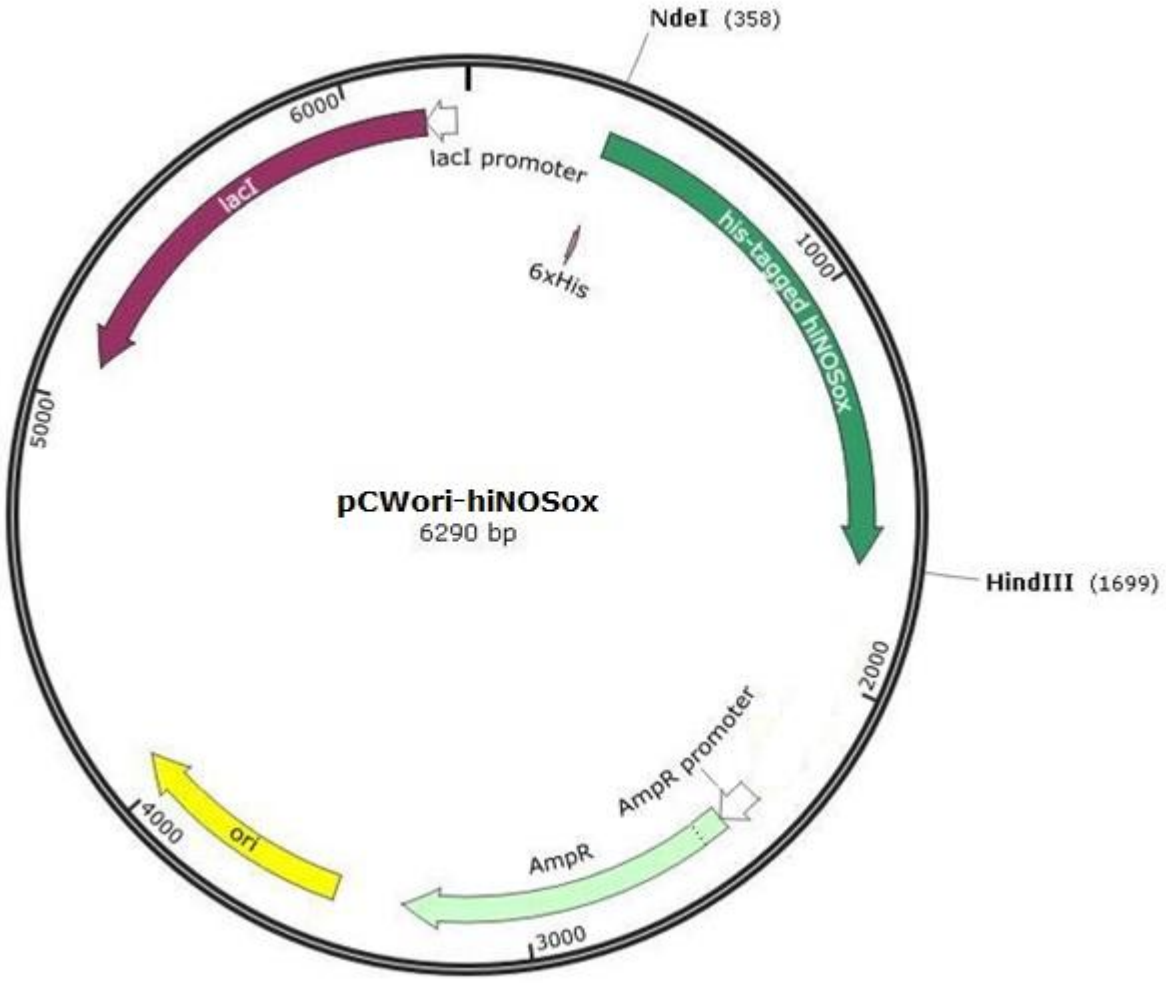

Figure 2.3 Vector map of pCWori-hiNOSox coding human Δ70 iNOS oxygenase domain without CaM-binding region. In pCWori-hiNOSox, human Δ70 iNOS oxygenase domain is in a pCWori vector. The domain in this vector is histidine-tagged at its N-terminus and does not contain a TEV protease cleavage site between the domain and the tag. This vector has an ampicillin resistance gene.

2.3.2 Expression Vectors for Human NOS Oxygenase Domains with CaM-binding region

For phnNOSoxyCaM, the presence of a mutation could be recognized by digestion of the vector with EcoRI. The digestion generated two fragments of 2.3kb and 7.6 kb. The insert was fully sequenced and a mutation at G726W was found.

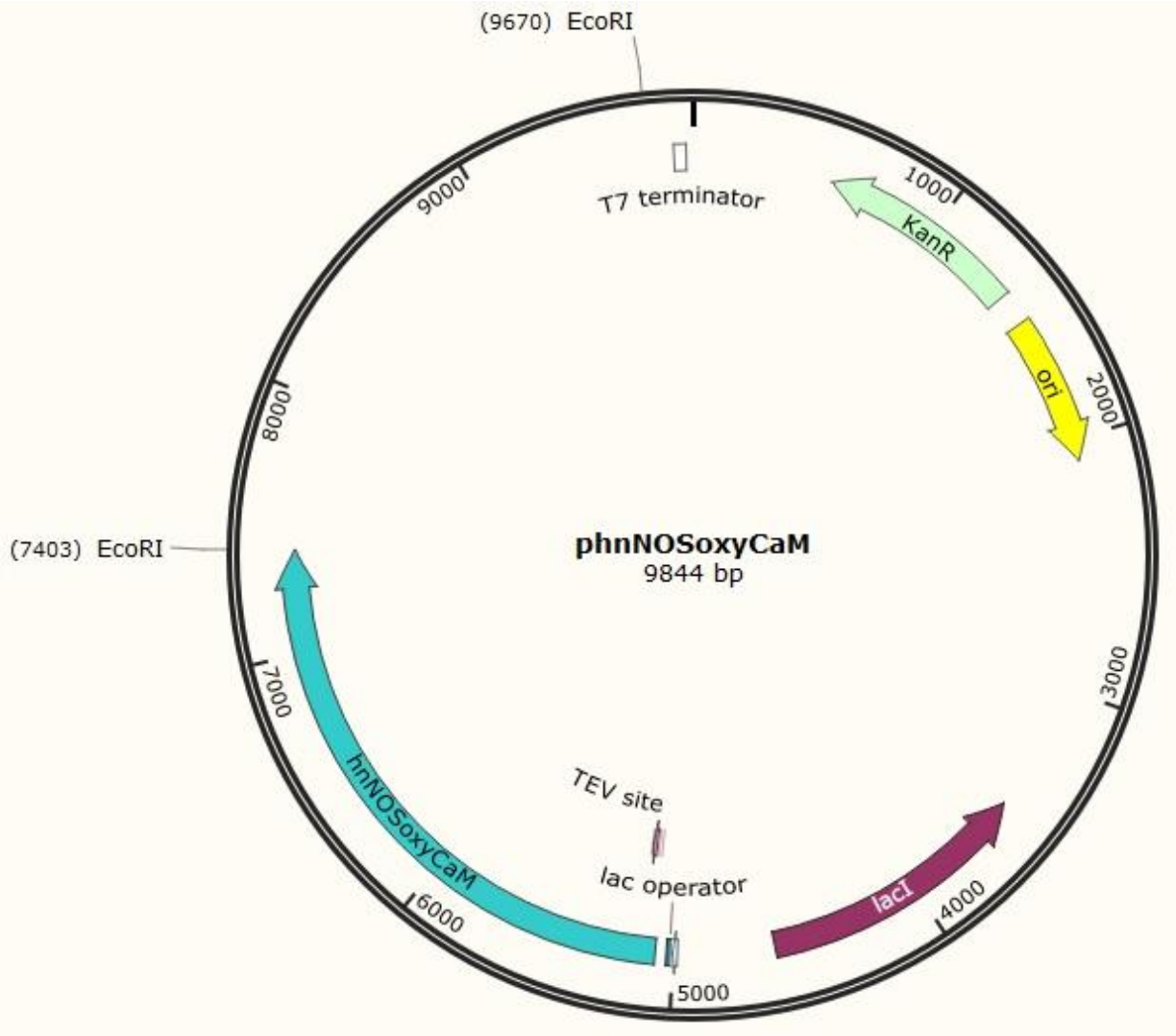

Figure 2.4 Vector map of phnNOSoxyCaM coding human nNOS oxygenase domain with CaM-binding region. A stop codon and an EcoRI restriction site were introduced to phnNOS for expression of human nNOS oxygenase domain with CaM-binding region. Accordingly, it contains features present in phnNOS, such as N-terminal histidine tag, TEV protease site, and the kanamycin resistance gene, but protein translation of the nNOS would stop just downstream of the CaM-binding region.

Digestion of pheNOSoxyCaM with HindIII produced a 2.1-kb and a 6.8-kb fragment. This result demonstrated that the intended mutation, the addition of a stop codon and a HindIII site, occurred successfully. The insert was also verified by sequencing where no mutation was found.

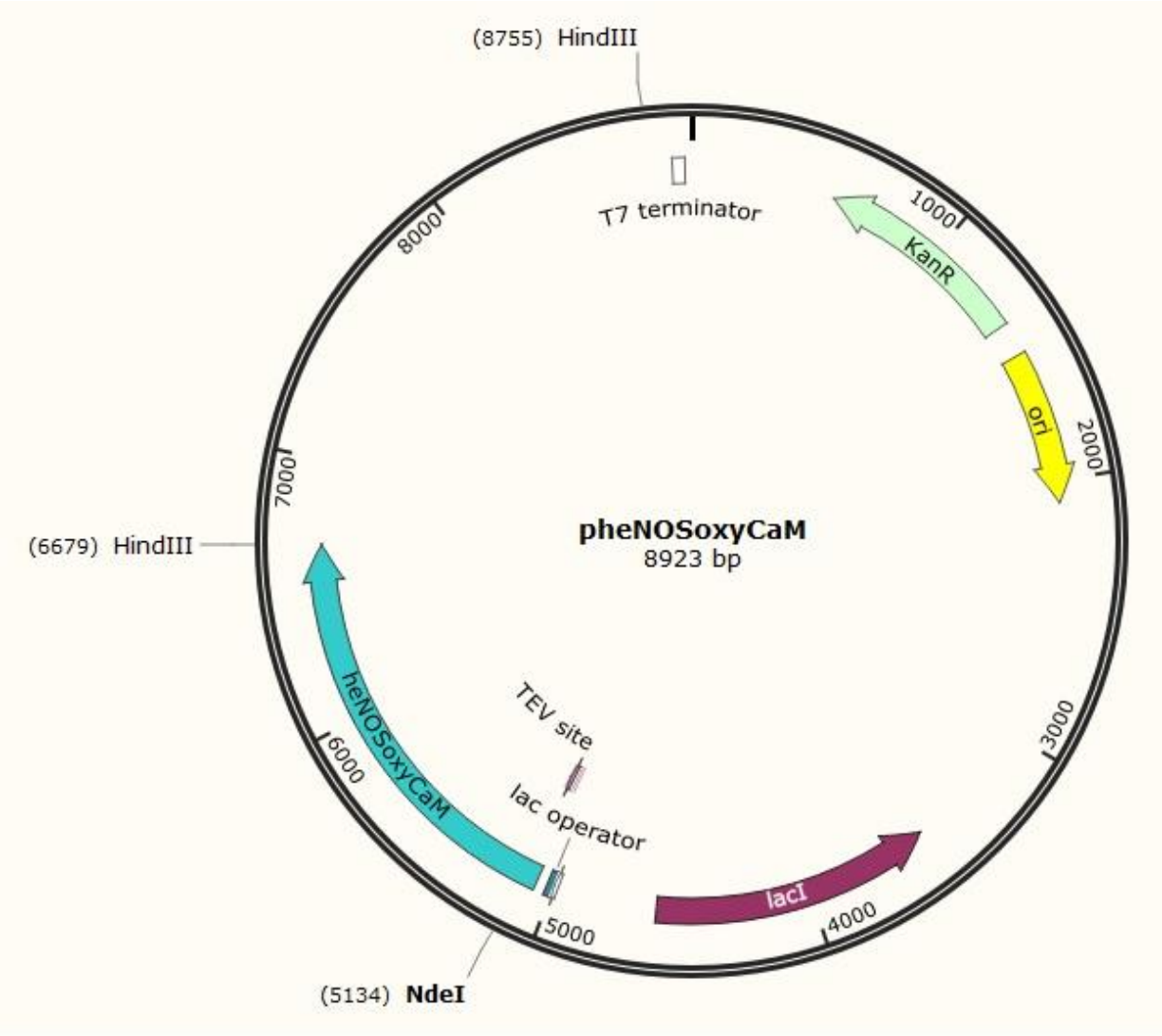

Figure 2.5 Vector map of pheNOSoxyCaM coding human eNOS oxygenase domain with CaM-binding region. Human eNOS oxygenase domain with CaM-binding region is in the kanamycin resistant pDS-78 vector. It was created by addition of a stop codon and a HindIII site downstream to CaM-binding region in full-length human eNOS.

For pCWori-hiNOSoxyCaM, the vector was digested with HindIII. As a result, a 1.8-kb and a 6.4-kb fragment were seen and the intended mutation could be identified by sequencing. From these results, it could be confirmed that the vector was mutated as planned. Most part of the oxygenase domain with CaM-binding region was sequenced except the initial part (1 – 165) that needs to be sequenced with primer pCWOri-fr.

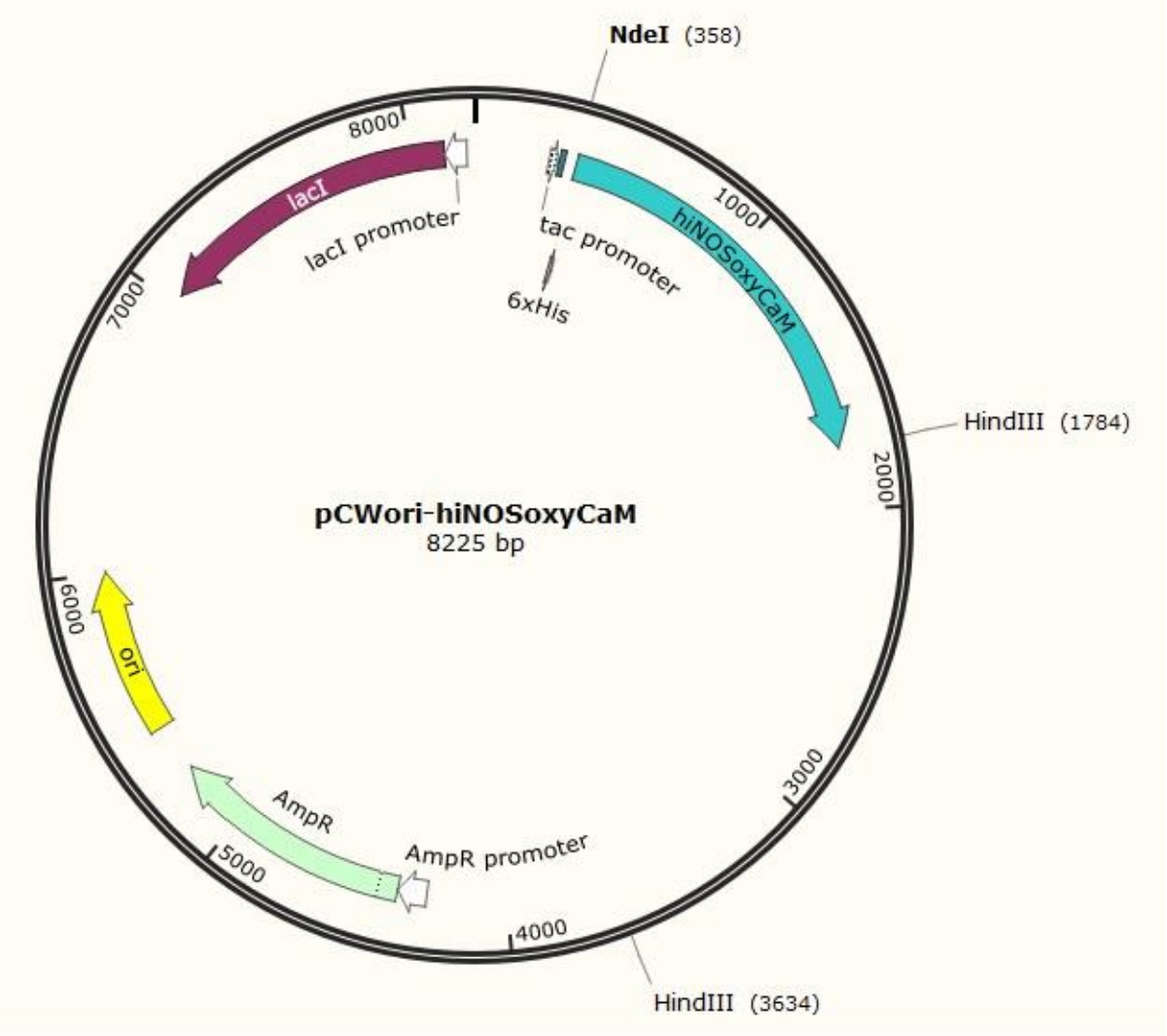

Figure 2.6 Vector map of phiNOSoxyCaM coding human Δ70iNOS oxygenase domain with CaM-binding region. Similarly to pCWori-hiNOSox (Figure 2.3), the human Δ70 iNOS oxygenase domain with CaM-binding region is present in a pCWori vector. Accordingly, the vector includes an ampicillin resistance gene. The oxygenase domain has an N-terminal hexahistidine tag but a TEV protease site is absent in between. For its construction, full-length human Δ70 iNOS in pCWori was mutated such that a stop codon and a HindIII are present downstream to CaM-binding region.

2.3.3 Expression Vectors for Human NOS Isoforms

The insertion of full-length human nNOS was confirmed by single digestions with BglII and HindIII. The expected band patterns were seen and its vector map is shown in Figure 2.7. The insert was confirmed by sequencing except DNA sequences 2392 – 2562 that needs to be sequenced by the primer hnNOSfr2600. Sequencing results showed that in comparison to UniProt sequence, mutations have occurred at E583Q, G726W, and G1355R. Nonetheless, mutation E583Q was questionable since it was not seen in the sequencing result for phnNOSoxyCaM whose original vector was phnNOS.

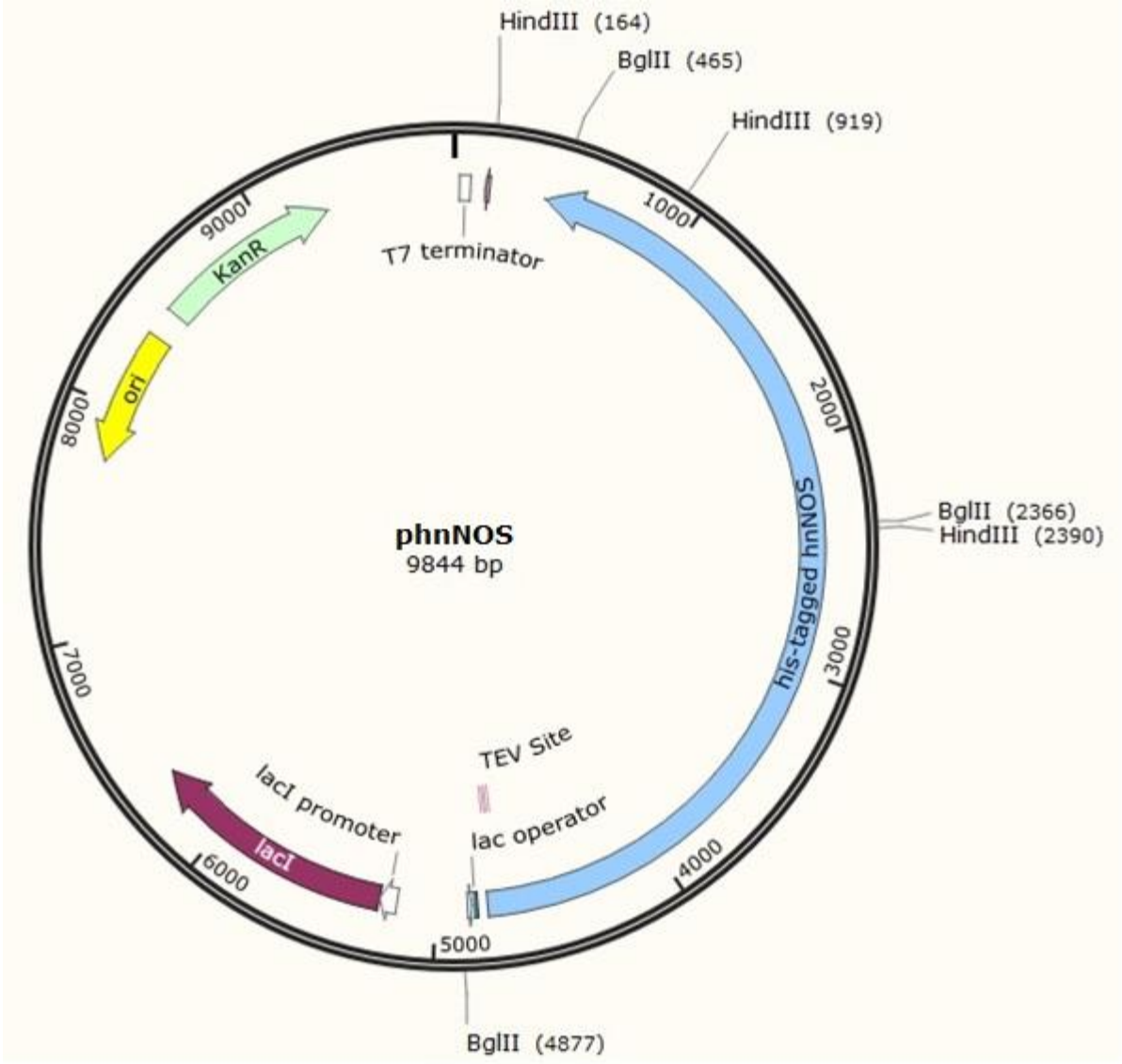

Figure 2.7 Vector map of phnNOS coding human full-length nNOS. The full-length human nNOS was inserted without the use of restriction enzymes through the one-step sequence- and ligation-independent cloning method into kanamycin resistant pDS-78 vector. The cloning into pDS-78 added an N-terminal hexahistine tag to the insert and a TEV protease site between the tag and the insert. This vector map is showing restriction enzyme sites used for confirmation of presence of the insert.

The vector map of pheNOS is shown in Figure 2.8. Single digestion with NcoI and double digestion with NdeI and EcoRI verified successful molecular cloning of the full-length human eNOS in pDS-78. NcoI digestion produced a 3.4-kb and a 5.5-kb fragment, while double digestion with NdeI and EcoRI yielded two fragments with sizes of 3.6 kb and 5.4 kb, as

expected. Sequencing of pheNOS also confirmed the presence of the holoenzyme in the vector. DNA sequences 1375 – 1524 just need to be sequenced by primer heNOS1280fr.

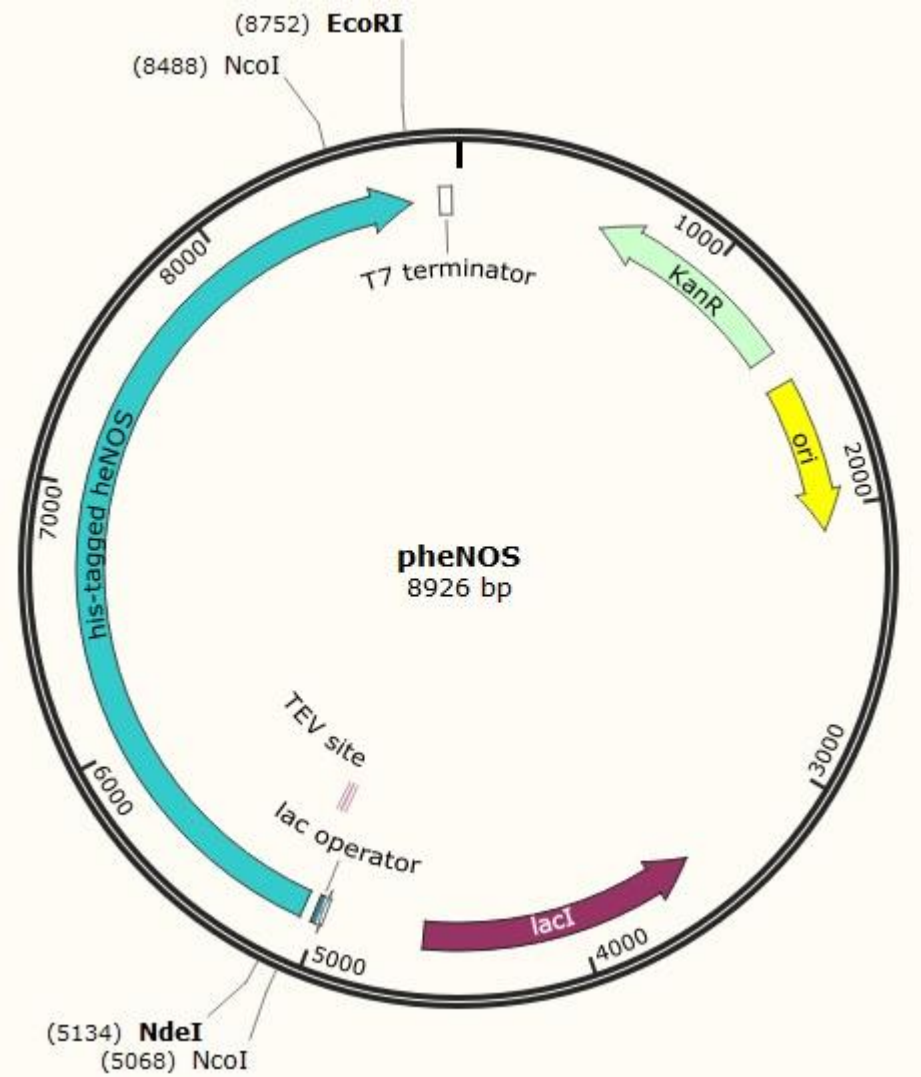

Figure 2.8 Vector map of pheNOS coding human full-length eNOS. This vector holds the full-length human eNOS in pDS-78. For its construction, the human eNOS was cloned into pDS-78 at NdeI and EcoRI sites. Upon insertion into pDS-78, same features, N-terminal histidine tag and a TEV protease site, were added to eNOS, as in phnNOS (Figure 2.7). This vector is kanamycin resistant. The insertion was also verified by digestion with NcoI.

phiNOS vector was digested with NdeI and HindIII, restriction enzymes for confirmation of the presence of the insert in the vector. Upon the double digestion, one was able to see the 3.3-kb insert and 5.3-kb vector (Figure 2.9). The presence of the insert was also verified by sequencing with primers 505iNOSfr and 3496iNOSfr, but a thorough sequencing of the whole insert was not performed.

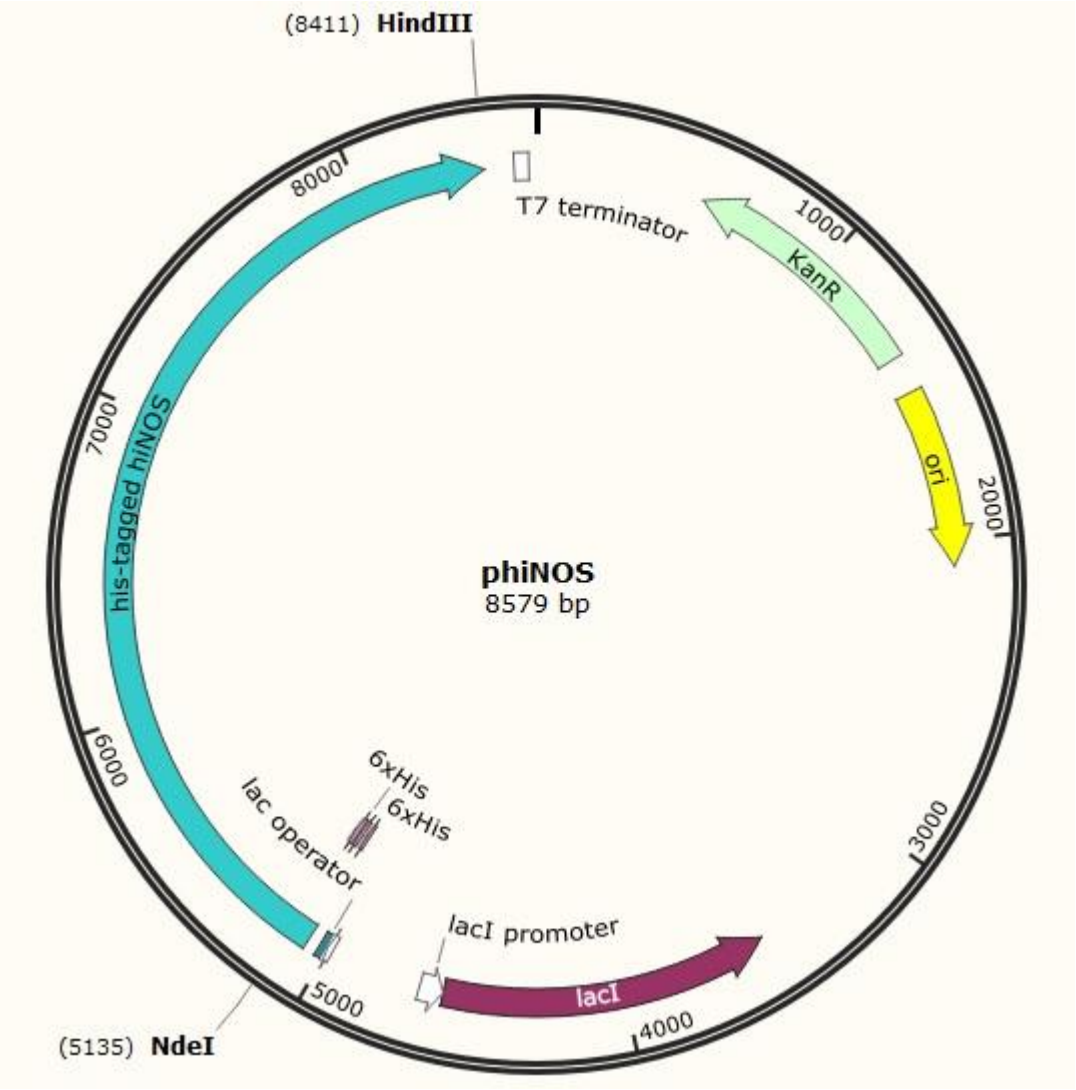

Figure 2.9 Vector map of phiNOS coding human Δ70iNOS. Human Δ70iNOS was subcloned into kanamycin resistant pDS-78. As a result, same features, as in phnNOS (Figure 2.7) were added to human Δ70iNOS. There is an additional hexahistidine tag at the N-terminus of hiNOS, which was cut out with hiNOS from its previous vector.

Table 2.1 Summary table of human NOS constructs made.

Name of Construct	NOS Form	Plasmid #	Vector	Promoter	TEV Protease Site	DNA Sequencing
phnNOSox	nNOSox	p511	pDS-78	T7	Present	Complete
pheNOSox	eNOSox	p513	pDS-78	T7	Present	Complete
pCWori-hiNOSox	Δ70 iNOSox	p508	pCWori	tac	Absent	Incomplete
phnNOSoxyCaM	nNOSoxyCaM	p525	pDS-78	T7	Present	Complete
pheNOSoxyCaM	eNOSoxyCaM	p526	pDS-78	T7	Present	Complete
pCWori-hiNOSoxyCaM	Δ70 iNOSoxyCaM	p524	pCWori	tac	Absent	Incomplete
phnNOS	nNOS	p522	pDS-78	T7	Present	Incomplete
pheNOS	eNOS	p523	pDS-78	T7	Present	Incomplete
phiNOS	Δ70 iNOS	p510	pDS-78	T7	Present	Incomplete

Constructs in pDS-78 vector are kanamycin resistant while those in pCWori vector are ampicillin resistant.

2.4 Discussion

Upon constructions of expression vectors for various forms of human NOS, different molecular cloning methods could be examined. Human NOSox constructs, phnNOSox, pheNOSox, and phiNOSox, were created by the digestion and ligation method. This method was useful in that restriction enzymes are known to be very active and specific for generation of sticky ends. However, compared to the SLIC method, the method can take longer time with both digestion and ligation reactions, since the SLIC method does not involve a ligation reaction that can take overnight. In addition, for phnNOSox and pheNOSox, their cloning method was prone to mutation, since the inserts were PCR amplified with addition of flanking restriction enzyme sites.

For human NOSoxyCaM constructs, two-stage PCR site-directed mutagenesis was used for introduction of stop codons downstream to the CaM-binding regions. An advantage of this method is that it is more efficient than the original PCR site-directed mutagenesis due to its separate forward and reverse primer PCR reactions. Although it is an additional step, upon separate single-primer reactions, there is no competition to primers for annealing sites (Wang & Malcolm, 1999). Yet, it is possible to introduce unintended mutations with this method, as the whole plasmid was PCR amplified.

Another molecular cloning method that was employed was the SLIC method for sub-cloning of the full-length nNOS into pDS-78. It was advantageous as the ligation step was omitted and instead, the vector and the insert were incubated with T4 DNA polymerase for 3.5 minutes (Jeong et al., 2012). However, this method also suffers from the disadvantage that unintended mutations can occur upon PCR amplification of the insert.

Analysis of sequencing results revealed that cloning methods involving PCR amplification introduced unintended mutations in the inserts. In heNOSoxyCaM, ATG was deleted by which the following codon was shifted to its position. This resulted in a mutation from a methionine to an alanine at amino acid position 514. This amino acid position was found to be the last amino acid in heNOSoxyCaM and to be not within any of the binding sites. However, a crystal structure that includes the amino acid position was not available. Accordingly, it was suggested that this mutation may not be a significant mutation that would interfere with enzyme activity.

Table 2.2 Mutation Table

NOS form	DNA position	Mutation	Amino acid change	Amino acid position
hnNOSoxyCaM	2242	G → T	Gly → Trp	726
heNOSoxyCaM	1606 – 1608	deletion of ATG	Met → Ala	514
hnNOS	1813	G → C	Glu → Gln	583
	2242	G → T	Gly → Trp	726
	1567	G → A	Gly → Arg	1355

In hnNOS, a guanine was mutated to a cytosine at DNA position 1813. This changed a glutamate to a glutamine at amino acid position 583. It was a mutation from a negatively charged to a neutral amino acid. Crystal structure of human nNOS oxygenase domain (PDB 4D1N) showed that the amino acid position is within a β-sheet and is distant from the binding sites (Figure 2.10 (b)). An nNOS form that could be related to this mutation was nNOS2 which is a splice variant of nNOS. nNOS2 having a deletion of residues 509 – 613 showed to have no nNOS activity but an opposing pharmacological role to wild-type nNOS (Iwasaki et al., 1999; Kolesnikov et al., 1997). This suggested that our mutant may exhibit features similar to those in nNOS2.

A common mutation was seen in both hnNOSoxyCaM and hnNOS at DNA position 2242. This made sense since construction of phnNOSoxyCaM involved introduction of a stop codon in phnNOS. This mutation changed the codon for glycine to a codon for tryptophan at amino acid position 726. This amino acid position was within none of the binding sites. Also, no structural data related to the mutation could be found.

The third mutation that was seen in hnNOS was a mutation from a guanine to an adenine at DNA position 1567. In terms of amino acids, it was a mutation from glycine to arginine at amino acid position 1355. This position was located to be within the NADPH-binding region in the reductase domain. The position was further examined in the crystal

structure of rat nNOS reductase domain (PDB 1TLL) since crystal structure of human form was not available. G1355 in hnNOS was identified to be equivalent to G1350 in the crystal structure of rat nNOS. Crystal structure revealed that the amino acid position is between the NADPH- and FAD-binding regions and is in the region that is responsible for hydride transfer from NADPH to FAD (Figure 2.10 (c)) (Garcin et al., 2004). Also, being a mutation from a small hydrophobic residue to a larger positively charged residue, it suggested that the mutation may interfere with NOS activity and may be necessary to revert it.

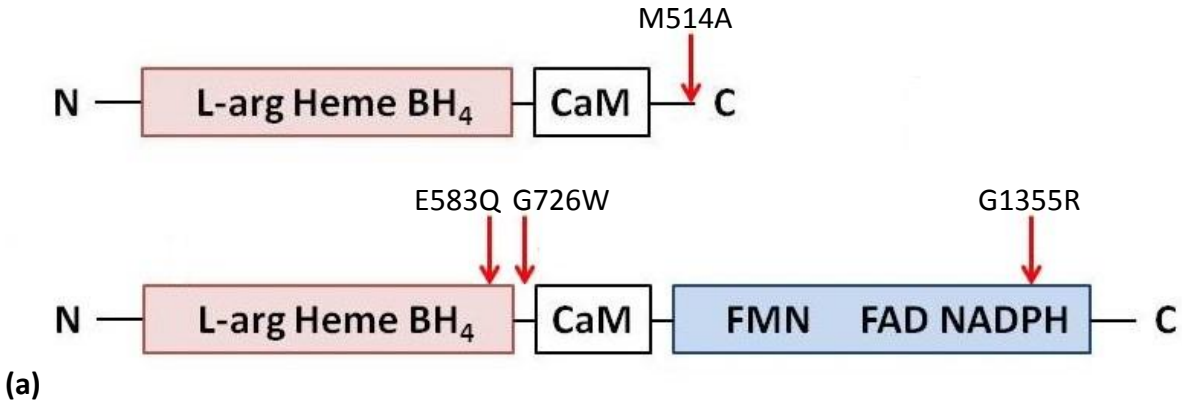

Figure 2.10 (a) NOS structures indicating mutation sites in heNOSoxyCaM (top) and hnNOS (bottom) (b) Crystal structure of human nNOS oxygenase domain (PDB 4D1N) showing E583 and cofactor binding sites (c) Crystal structure of rat nNOS reductase domain (PDB 1TLL) showing G1350 with NADPH- and FAD-binding sites (a) is showing the mutation sites that occurred in heNOSoxyCaM and hnNOS by PCR amplification of the inserts. In (b), cofactor binding sites in the oxygenase domain are shown with E583, which is not in close proximity to the binding sites. During the molecular cloning of phnNOS, E583 was mutated to a glutamine. (c) showed that G1350, equivalent to G1355 in hnNOS, is present between the NADPH- and FAD-binding sites. In phnNOS, G1355 was unintentionally mutated to an arginine.

Chapter 3

Investigation of Expression and Purification of Human NOS Oxygenase Domains

3.1 Introduction

The oxygenase domain is the catalytic domain in NOS that contains the active site. It holds the binding sites for a heme, BH_4, and L-arginine, and carries out the conversion of L-arginine into L-citrulline and NO. Previous studies have demonstrated that rat nNOS oxygenase domain expressed in *E. coli* was able to form binding sites as in the holoenzyme (McMillan & Masters, 1995). As well, in another study by Rafferty et al., 1999, a mouse iNOS oxygenase domain was expressed and purified by a simpler procedure. The study also showed that the domain forms a stable dimer. For these reasons, expression and purification of the oxygenase domains were first performed.

Expressions of human nNOS and eNOS oxygenase domains without the CaM-binding regions that are in pDS-78 were attempted at different temperatures for investigation of optimal expression temperatures. Then, small-scale purifications of the domains were carried out using nickel affinity columns. Human Δ70 iNOS oxygenase domain without the CaM-binding region that is in a pCWori vector was expressed and purified as previously described (Spratt, 2008). Lastly, human nNOS oxygenase domain with the CaM-binding region in pDS-78 was expressed. Purification of hnNOSoxyCaM was done using a nickel affinity column and then with a glutathione column. Since a CaM-binding region is present in hnNOSoxyCaM, GST-TEV-CaM was added to hnNOSoxyCaM obtained from nickel affinity purification. One then applied the protein mixture to the glutathione column in which the GST portion would bind to

the glutathione column and CaM portion would bind hnNOSoxyCaM for its further purification.

3.2 Methods

3.2.1 Expression of hnNOSox and heNOSox using pET-based vector

Initially, *E. coli* BL21 (DE3) was transformed with phnNOSox for expression of hnNOSox. For heNOSox, *E. coli* BL21 (DE3) transformation was performed with pheNOSox. Then, one inoculated a 2-mL Terrific Broth (TB) media containing kanamycin with a colony of transformants of phnNOSox or pheNOSox, and allowed cell growth at 37 ˚C, 225 rpm overnight. Then, 0.3 mL of the overnight cell culture was added to 30 mL of TB media containing kanamycin and it was incubated at 37 ˚C, 225 rpm. When the optical density at 600 nm reached 0.5, protein expression was induced by adding Isopropyl β-D-1-thiogalactopyranoside (IPTG, 500 μM). Protein induction occurred for 18 – 24 hours at three different temperatures, which were 20 ˚C, 25 ˚C, and 37 ˚C. After protein induction, the cell culture was centrifuged at 6 000 rpm for 5 minutes. His binding buffer (20 mM sodium phosphate, 500 mM NaCl, 20 mM imidazole, pH 7.4) was used for cell resuspension. Then, 0.2 mg/mL lysozyme, 1 mM $MgCl_2$, 1 mM PMSF, 3.5 μg/mL E64, 2 μg/mL aprotinin, 0.6 μg/mL pepstatin, and 4 μg/mL leupeptin were added and the samples were incubated on ice for 30 minutes. Cells were lysed by sonication and the cell lysate was centrifuged at 13 000 rpm, 4 ˚C for 10 minutes.

3.2.2 Purification of hnNOSox and heNOSox

Because of the small sample size, His SpinTrap™ column (GE Healthcare) was used and the purification carried out as instructed by the manufacturer. The column was first equilibrated with 600 μL of binding buffer, and the eluate was collected by centrifugation at

100 x g for 30 s, which was done at the end of every purification step to collect the eluate. Supernatant samples were applied, and the column was washed with 600 μL of His binding buffer. The protein was eluted twice with 200 μL of His elution buffer (20 mM sodium phosphate, 500 mM NaCl, 500 mM imidazole, pH 7.4).

3.2.3 hiNOSox Expression using pCWori-based vector

At first, *E. coli* BL21 (DE3) cells were electroporated with pCWori-hiNOSox for bacterial transformation and were plated on solid Luria-Bertani (LB) broth containing ampicillin. Then, an isolated colony was selected for inoculation of 20 mL of TB media containing ampicillin. The cell culture was incubated at 37 ˚C, 225 rpm overnight and 5 mL of the overnight cell culture was added to 500 mL of TB media. The 500-mL cell culture was cultured at 37 ˚C, 225 rpm until it reached an optical density at 600 nm of 1.0. For protein induction, IPTG (500 μM), trace metals ((9.6 mg/L $FeSO_4$•$7H_2O$, 2.4 mg/L $MnSO_4$•H_2O, 2.4 mg/L $AlCl_3$•$6H_2O$, 1.0 mg/L $CoCl_2$•$6H_2O$, 0.5 mg/L $ZnSO_4$•$7H_2O$, 2.4 mg/L Na_2MoO_4•$2H_2O$, 0.1 mg/L $CuCl_2$•$2H_2O$, and 0.5 mg/L H_3BO_3), δ-aminolevulinic acid (δ-ALA, 400 μM), and 15 μL of 45 mg/mL chloramphenicol were added to the cell culture which was then incubated at 20 ˚C, 225 rpm for 40 hours. Cells were collected by centrifugation, and were resuspended in lysis buffer (40 mM TrisHCl, pH 7.5, 10% glycerol, 150 mM NaCl, 10 μM H_4B, 3 mM ascorbic acid, 1 mM PMSF, 3.5 μg/mL E64, 2 μg/mL aprotinin, 0.6 μg/mL pepstatin, and 4 μg/mL leupeptin). Cell lysis was done by homogenization and the lysate was centrifuged at 20 000 rpm, 4 ˚C for 30 minutes.

3.2.4 hiNOSox Purification

To the sample supernatant, ammonium sulfate was added to a final concentration of 35% and the sample was stirred at 4 ˚C for 45 minutes. Afterwards, the sample was centrifuged at

20 000 rpm, 4 ˚C for 30 minutes, and the supernatant was collected. Ammonium sulfate was added to the supernatant to a final concentration of 55%. Again, the sample with ammonium sulfate was stirred for 45 minutes at 4 ˚C, and then spun at 20 000 rpm, 4 ˚C for 30 minutes. The supernatant was decanted and the pellet was resuspended in ~15 mL of pellet buffer (40 mM TrisHCl, pH 7.5, 10% glycerol, and 250 mM NaCl).

For hiNOSox purification, Ni^{2+}-chelating resin with a column volume of 10 mL was equilibrated with 5 column volumes of pellet buffer and the 15 mL of pellet sample was applied to the column. The column was washed with 10 column volumes of pellet buffer and the protein was eluted with 3 column volumes of pellet buffer containing 200 mM imidazole and collected as in 2-mL fractions. Then, elution fractions with heme absorbance peaks between 700 nm and 300 nm were pooled. The pooled samples were transferred to a dialysis bag with a MWCO 6 000 – 8 000. This dialysis bag was placed in 1 L of Dialysis buffer 1 (50 mM TrisHCl, pH 7.5, 10% glycerol, 250 mM NaCl, 1 mM DTT, 4 μM H_4B, 3 mM ascorbic acid) overnight at 4 ˚C. Then, the sample was dialysed in 1 L of Dialysis buffer 1 containing 100 mM NaCl at 4 ˚C overnight. The heme absorbance peak of the final sample was monitored between 700 nm and 300 nm.

3.2.5 hnNOSoxyCaM Expression and Purification

For expression of hnNOSoxyCaM, transformation of *E. coli* BL21 (DE3) was performed with the phnNOSoxyCaM plasmid. 20 mL of LB media containing kanamycin was inoculated with a colony of the transformants and incubated at 37 ˚C, 225 rpm overnight. 10 mL of the overnight starter culture was then used for inoculation of 1 L of TB media containing kanamycin. The cell culture was grown at 37 ˚C, 225 rpm until an optical density at 600 nm of 1.1 was reached. Protein expression was induced by addition of IPTG (500 μM),

and with it, δ-ALA (400 μM), a heme precursor, and trace metals were also added. Induction conditions were 20 °C, 225 rpm and protein expression was allowed for 40 hours. A 30 mL sample of cell culture was centrifuged at 6 000 rpm for 5 minutes. The rest of the cells were harvested by centrifugation at 6 000 rpm for 10 minutes and the cell pellets were then flash frozen on dry ice and stored at -80 °C.

The first step for purification of hnNOSoxyCaM involved the use of His SpinTrap™ column (GE Healthcare). The protocol described by the manufacturer was followed with several modifications. Initially, the cell pellet from 30 mL of cell culture was resuspended in His binding buffer (20 mM sodium phosphate, 500 mM NaCl, 20 mM imidazole, pH 7.4), and lysozyme (0.2 mg/mL), $MgCl_2$ (1 mM), and PMSF (1 mM) were added to the cell sample. It was left on ice for 30 minutes and then sonicated. The sample was then centrifuged at 13 000 rpm for 10 minutes at 4 °C. The column was first equilibrated with His binding buffer and then centrifuged at 100 x g for 30 seconds. Afterwards, the cell supernatant was applied to column which was then followed by centrifugation in a similar manner. Since the maximum volume the column can hold was 600 μL, sample application was repeated several times. The column was washed with 600 μL of His binding buffer and centrifuged. Lastly, protein was eluted by centrifugation using 200 μL of His elution buffer (20 mM sodium phosphate, 500 mM NaCl, 500 mM imidazole, pH 7.4). Addition of 200 μL of His elution buffer was repeated once more for a thorough elution of the protein.

As a second step for protein purification, purification of hnNOSoxyCaM, that was eluted from His SpinTrap™ column, was attempted with GST SpinTrap™ column (GE Healthcare) and GST-TEV-CaM. Purification was performed as described by the manufacturer along with a few modifications. GST-TEV-CaM was added to hnNOSoxyCaM sample so that

hnNOSoxyCaM-to-GST-TEV-CaM ratio would be 1:1. Also, $CaCl_2$ (5 mM) was added to the protein sample. GST SpinTrap™ column was prepared similarly to His SpinTrap™ column. The column was equilibrated with 600 μL of GST binding buffer (10 mM Na_2HPO_4, 140 mM NaCl, 2.7 mM KCl, 1.8 mM KH_2PO_4, pH 7.4) and then centrifuged at 100 x g for 30 seconds. For each sample application, one added the sample to the column and incubated on ice for 5 minutes in order to allow optimal protein binding to the resin. Next, 200 μL of GST elution buffer (50 mM TrisHCl, 20 mM glutathione, pH 8.0) was added and centrifuged for protein elution. The last elution step was repeated once more.

3.3 Results

3.3.1 hnNOSox and heNOSox Expression at Different Temperatures

Upon expression and purification of hnNOSox and heNOSox, results showed that one can obtain the proteins in higher yields at lower expression temperatures. At expression temperature of 37 ˚C, hnNOSox (amino acids 1 – 724), whose molecular weight is 83 kDa, appeared to not have expressed, as one could not observe a protein band around 83 kDa in the elution lanes (Figure 3.1., (a), lanes 7 – 8). The elution lanes are similar to the control which was obtained with pDS-78 (Figure 3.1, (d), lanes 8 – 9). In contrast, a protein band with the expected molecular weight was seen for hnNOSox that was expressed at 25 ˚C (Figure 3.1, (b), indicated in red box). The band for hnNOSox seemed to intensify at a lower expression temperature of 20 ˚C (Figure 3.1, (c), indicated in a red box). The cell sample with the vector, pDS-78, that went through the same purification steps as hnNOSox did not produce such protein band, suggesting that hnNOSox expression occurred at 25 ˚C and at 20 ˚C in Figure 3.1 (b) and (c).

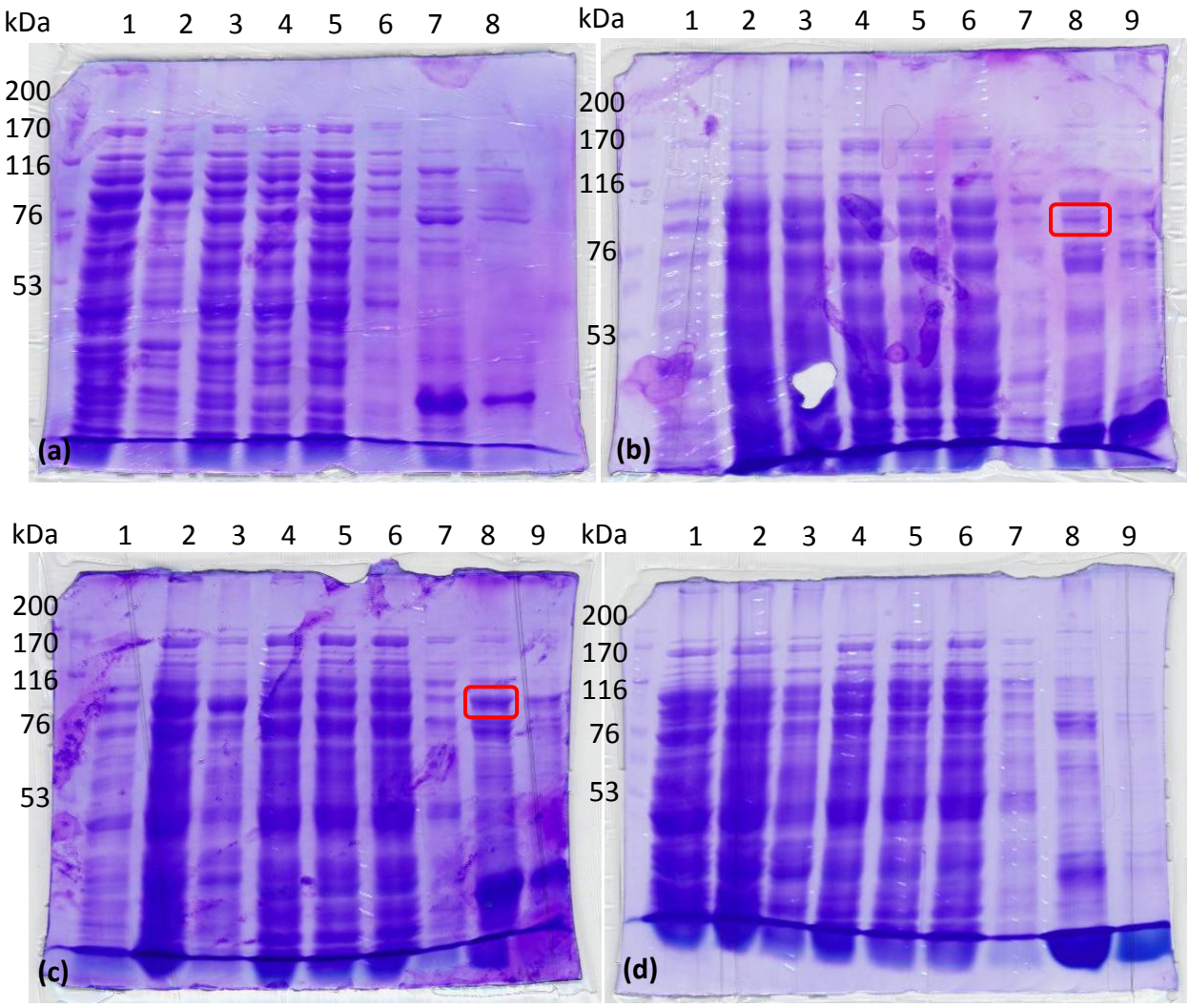

Figure 3.1 7.5% SDS-PAGEs of hnNOSox purifications with expression temperatures at 37 ˚C (a), 25 ˚C (b), and 20 ˚C (c) and of same treatment of cell sample with pDS-78 (control) and expression temperature at 20 ˚C (d). Cell samples that were subjected to different expression temperatures were applied to nickel affinity columns for hnNOSox purification. Cell sample with pDS-78 which was solely the vector without the hnNOSox insert was treated in the same manner as in hnNOSox purification for comparison. For (a), Lane 1 – cell lysate; Lane 2 – cell lysate pellet; Lane 3 – cell lysate supernatant; Lanes 4 – 5 – flowthrough; Lane 6 – wash; Lanes 7 – 8 – elutions 1 & 2. For (b), (c), and (d), Lane 1 – cell lysate; Lane 2 – cell lysate pellet; Lane 3 – cell lysate supernatant; Lanes 4 – 6 – flowthrough; Lane 7 – wash; Lanes 8 – 9 – elutions 1 & 2.

Similar results to hnNOSox were seen with expression and purification of heNOSox (amino acids 1 – 490). heNOSox with a molecular weight of 58 kDa could not be seen at expression temperature of 37 ˚C (Figure 3.2, (a), lanes 7 – 8). The elution lanes were observed

to be similar to those of the control. While it was hard to analyze the results at an expression temperature of 25 ˚C, heNOSox appeared to be visible in the results from expression temperature at 20 ˚C (Figure 3.2, (c), indicated in a red box). Such intense protein band of 58 kDa could not be seen in the purification with pDS-78 (Figure 3.2, (d), lanes 8 – 9).

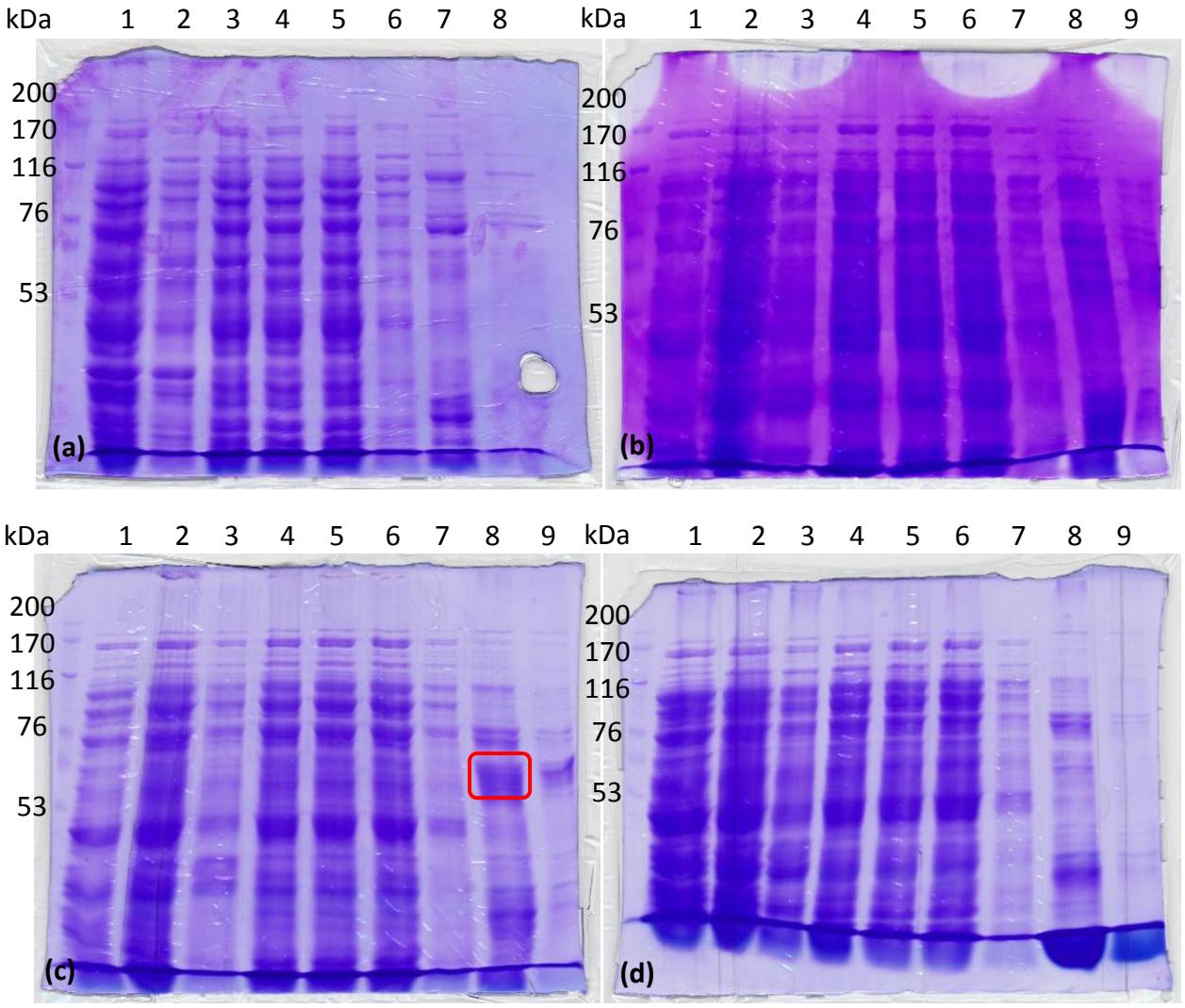

Figure 3.2 7.5% SDS-PAGEs of heNOSox purifications with expression temperatures at 37 ˚C (a), 25 ˚C (b), and 20 ˚C (c) and of same treatment of cell sample with pDS-78 (control) and expression temperature at 20 ˚C (d). Cell samples of heNOSox and pDS-78 were purified in the same manner as with hnNOSox (Figure 3.1). For (a), Lane 1 – cell lysate; Lane 2 – cell lysate pellet; Lane 3 – cell lysate supernatant; Lanes 4 – 5 – flowthrough; Lane 6 – wash; Lanes 7 – 8 – elutions 1 & 2. For (b), (c), and (d), Lane 1 – cell lysate; Lane 2 – cell lysate pellet; Lane 3 – cell lysate supernatant; Lanes 4 – 6 – flowthrough; Lane 7 – wash; Lanes 8 – 9 – elutions 1 & 2.

3.3.2 hiNOSox Expression and Purification

Purification results for hiNOSox (amino acids 71 – 508) at different expression temperatures are shown in Figure 3.3. hiNOSox, a protein with a molecular weight of 51 kDa, appeared to have expressed as one could identify protein bands with the right size in the elution lanes (lanes 14 - 16). However, lane 14 which appeared to have larger amount of hiNOSox showed to contain other contaminating protein, while lanes 15 – 16 showed a clean protein sample of hiNOSox. The fraction in lane 14 was pooled for dialysis as the highest heme absorbance peak was observed with the fraction (results not shown). Subsequently, similar protein pattern was seen in the dialysis supernatant (lane 17). Heme absorbance peaks for fractions in lane 15 and 16 were also monitored. However, their heme absorbances were lower than that of lane 14.

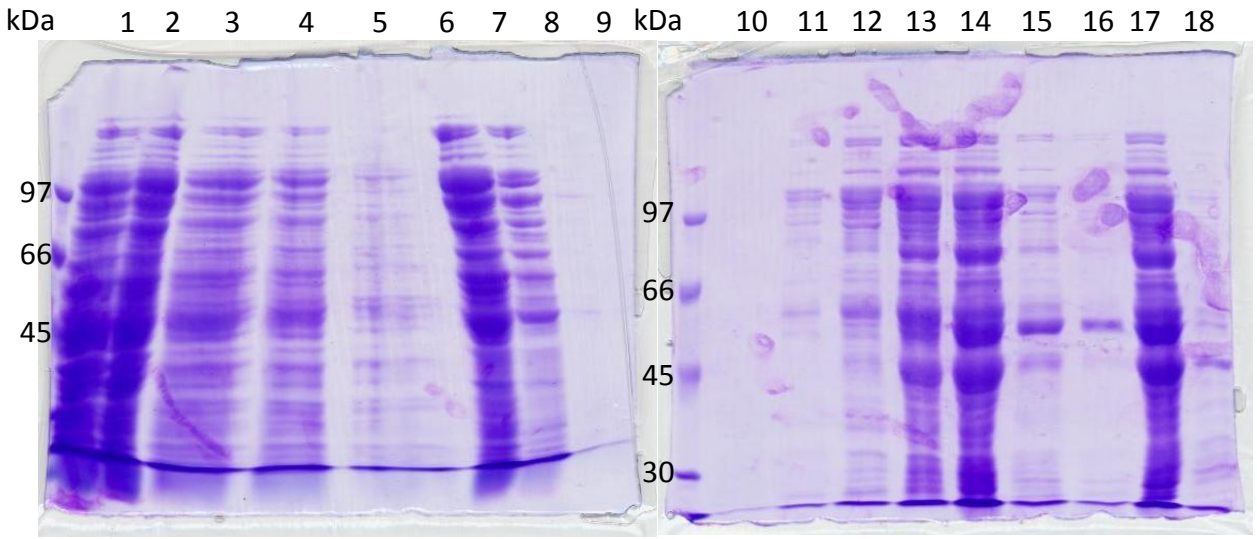

Figure 3.3 7.5% SDS-PAGE of hiNOSox purification.
Purification of hiNOSox involved precipitation by addition of ammonium sulfate and purification with a nickel affinity column. Lane 1 – cell lysate before protein induction; Lane 2 – cell lysate after 40 hours of induction; Lane 3 – cell lysate supernatant; Lane 4 – supernatant after 35% $(NH_4)_2SO_4$ precipitation; Lane 5 – supernatant after 55% $(NH_4)_2SO_4$ precipitation; Lane 6 – resuspended pellet after 55% $(NH_4)_2SO_4$ precipitation; Lane 7 – flowthrough eluted from nickel affinity column; Lane 8 – wash; Lanes 9 – 16 – elutions 1 – 8; Lane 17 – supernatant after dialysis; Lane 18 – pellet after dialysis.

3.3.3 hnNOSoxyCaM Expression and Purification

In the results from purification of hnNOSoxyCaM (amino acids 1 – 755) with a nickel affinity column, hnNOSoxyCaM could be seen in the elution lanes whose molecular weight is 84 kDa (Figure 3.3, (a), lanes 7 – 8, indicated in red box). However, one also observed an intense unknown protein band of approximately 30 kDa in the elution lanes that seems to be present in large amounts. Upon purification with a glutathione column, protein bands for hnNOSoxyCaM (84 kDa) and GST-TEV-CaM (44 kDa) were hardly seen in the elution lanes (Figure 3.3, (b), lanes 4 – 5). GST-TEV-CaM was added in order to obtain a purer sample of hnNOSoxyCaM, as GST-TEV-CaM is able to bind to both the glutathione column and CaM-binding region in hnNOSoxyCaM. The unknown protein of 30 kDa was again found in the elution fractions from the glutathione column.

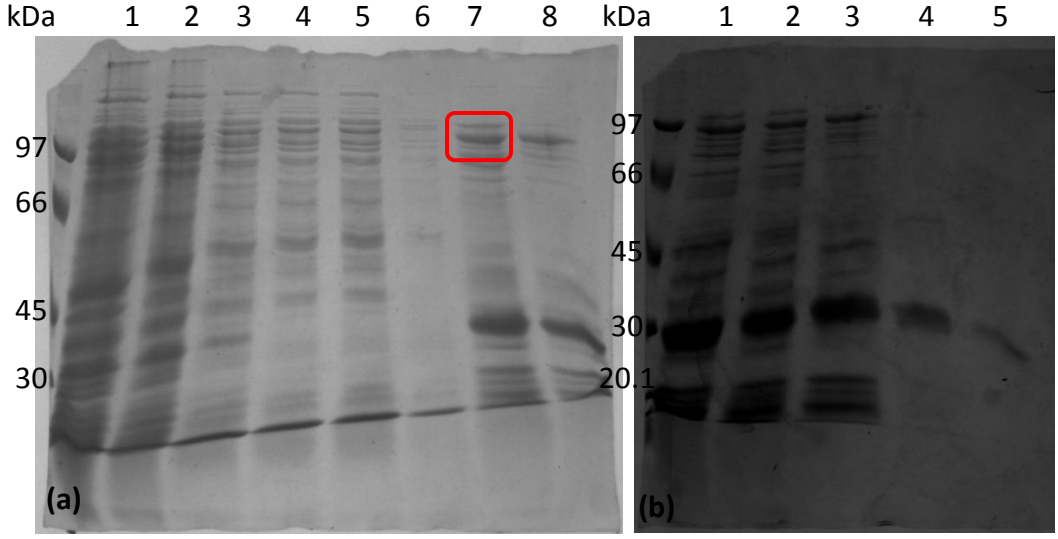

Figure 3.4 7.5% SDS-PAGE results for hnNOSoxyCaM purifications with nickel affinity column (a) and subsequent glutathione column (b). Initially, hnNOSoxyCaM was purified with a nickel affinity column and then, GST-TEV-CaM was added to the elution sample which was applied to a glutathione column. (a) Lane 1 – cell lysate; Lane 2 – cell lysate pellet; Lane 3 – cell lysate supernatant; Lanes 4 – 5 – flowthroughs 1 & 2; Lane 6 – wash; Lanes 7 – 8 – elutions 1 & 2. (b) Lane 1 – elution sample from nickel affinity column with added GST-TEV-CaM; Lanes 2 – 3 – flowthroughs; Lanes 4 – 5 – elutions 1 & 2.

3.4 Discussion

hnNOSox and heNOSox expression at different temperatures, 20°C, 25 °C, and 37 °C demonstrated that protein expression occurred best at 20 °C. This made sense since activities of some proteases are known to reduce at low temperatures which would increase the resulting amounts of proteins (Sahdev et al., 2008). As well, it was shown with protein purification that the proteins can be purified by nickel affinity columns. However, other contaminating proteins seemed to be present as well in the elution fractions. Protein purification may be improved by protein precipitation with ammonium sulfate.

Expression and purification of hiNOSox was moderately successful. One was able to acquire pure elution fractions of hiNOSox (Figre 3.2, lanes 15 – 16), although the amounts and the heme absorbance peaks were low. However, an elution fraction with a high heme absorbance peak (Figure 3.2, lane 14) was obtained. This indicated that the heme was present in the active site as in the native enzyme, and with a purer protein sample, spectroscopic studies of inhibitor binding may be carried out (Montgomery et al., 2010). Alternatively, expression and purification of hiNOSoxyCaM may be attempted which may be further purified by a glutathione column with GST-TEV-CaM.

In the experiment with hnNOSoxyCaM, expression and purification showed that the purification procedure needs improvement. hnNOSoxyCaM could be purified by nickel affinity purification. However, it was hard to observe purification with glutathione column. This might have occurred because of the small sample volume of lysate used or due to the presence of the unknown 30-kDa protein in large amounts that might have interfered with hnNOSoxyCaM binding. In the future, a large-scale protein purification as well as ammonium sulfate precipitation may be performed.

Chapter 4

Preparation of GST-TEV-CaM and Optimization of Its Cleavage Reaction by TEV Protease

4.1 Introduction

Glutathione S-transferase-tagged calmodulin or GST-TEV-CaM is a fusion protein of glutathione-S-transferase and CaM. Glutathione S-transferase is a protein that can strongly bind to glutathione. Due to its strong affinity, it is developed as an affinity tag for protein purification (Harper & Speicher, 2011). CaM is a calcium-binding protein which, upon calcium binding, undergoes a conformational change and can bind other proteins such as NOS. As such, GST-TEV-CaM with two affinity motifs was made which could be used in NOS purification. The CaM domain would be able to bind to the CaM-binding region of NOS, while GST can bind to glutathione resins and this would allow an alternate method for purifying NOS. The third feature in GST-TEV-CaM is the TEV protease cleavage site, ENLYFQG, that is present between the CaM and GST domains (Nallamsetty et al., 2004). This site would allow removal of the GST domain in sample of NOS and CaM in solution or during column purification.

In this study, GST-TEV-CaM would be useful in purification of various forms of human NOS isozymes. It may be coexpressed with hiNOS and hiNOSoxyCaM since active forms are only produced upon coexpression with CaM. GST-TEV-CaM can be used in purification of human NOS forms with CaM-binding regions, such hnNOSoxyCaM and heNOS. In this chapter, expression and purification of GST-TEV-CaM were performed, and optimal reaction conditions for GST-TEV-CaM cleavage by TEV protease were explored.

4.2 Methods

4.2.1 Expression and Purification of GST-TEV-CaM

For expression of GST-TEV-CaM, *E. coli* BL21 (DE3) was transformed with pGST-TEV-CaM. Then, a single colony of the transformants was used for inoculation in 20 mL of Super Broth (SB) media containing ampicillin. It was incubated for growth at 37 ˚C, 225 rpm overnight. 1 L of SB media containing ampicillin was inoculated with 10 mL of overnight cell culture, and cells were grown at 37 ˚C, 225 rpm. When an optical density at 600 nm of ~0.8 was reached, IPTG (500 μM) was added for GST-TEV-CaM expression. Protein was expressed at 37 ˚C, 225 rpm for 4 hours, and cells were harvested by centrifugation. Afterwards, cells were resuspended in GST binding buffer (10 mM Na_2HPO_4, 140 mM NaCl, 2.7 mM KCl, 1.8 mM KH_2PO_4, pH 7.4) and homogenized for cell lysis. The sample was then centrifuged at 20 000 rpm at 4 ˚C for 30 minutes.

For GST-TEV-CaM purification, β-mercaptoethanol was added to supernatant sample and to the buffers for final concentration of 10 mM. Then, the supernatant sample was applied to GSTrap FF column (GE Healthcare) that has been equilibrated with GST binding buffer. The purification was carried out at a flow rate of 0.3 mL/min for optimal protein binding. After sample application, the column was washed with 5 column volumes of binding buffer, and GST-TEV-CaM was eluted off with 10 column volumes of GST elution buffer (50 mM Tris-HCl, 10 mM reduced glutathione, pH 8.0) in 1-mL fractions.

4.2.2 Cleavage Reaction of GST-TEV-CaM by TEV Protease

The reaction buffer consisted of 50 mM TrisHCl, pH 8.0, 0.5 mM EDTA, and 1 mM DTT. For optimization of reaction conditions, protease-to-substrate ratio, temperature, and reaction duration were varied. Protease-to-substrate ratios tested were 1:100, 1:50, and 1:10.

These ratios were based on sample absorbances at 280 nm. TEV protease reactions were attempted at room temperature and 4 ˚C for 30 minutes, 1 hour, 1 hour and 30 minutes, 2 hours, and overnight.

4.3 Results

4.3.1 GST-TEV-CaM Expression and Purification

SDS-PAGE results of GST-TEV-CaM preparation revealed that production of GST-TEV-CaM of 44kDa, occurred well. Large amount of it was seen in the flowthrough (Figure 4.1, lanes 1 – 5). Also, small amount of it was observed in the wash fractions (Figure 4.1, lanes 6 – 11). Lastly, one could notice that large amount of it was eluted in one fraction during elution (Figure 4.1, lane 12).

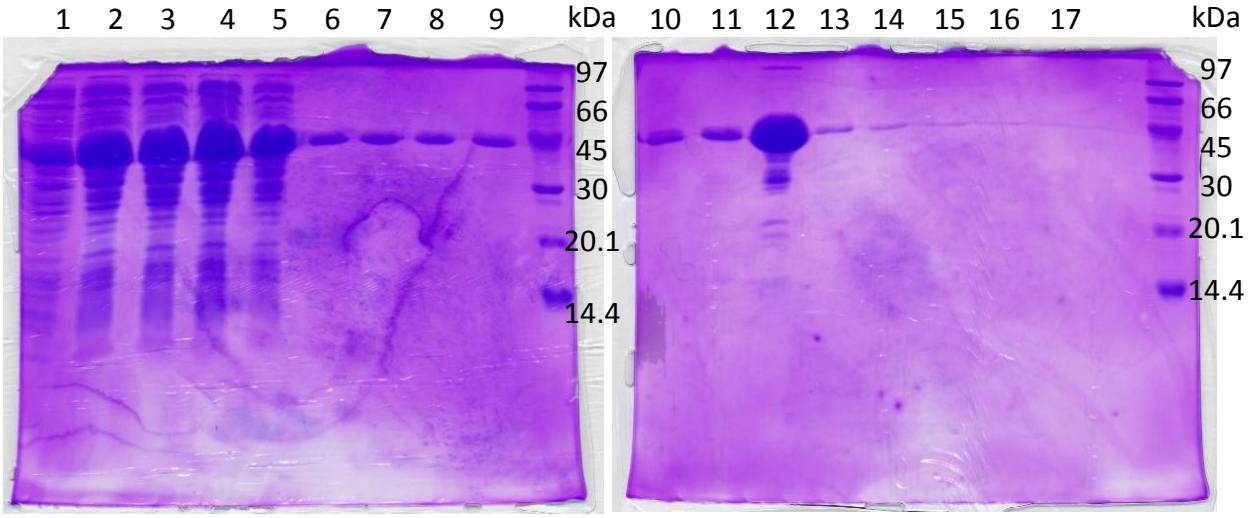

Figure 4.1 15% SDS-PAGE of GST-TEV-CaM purification with glutathione column. This figure shows the SDS-PAGE results of protein samples eluted in various stages of GST-TEV-CaM purification. Lanes 1 – 5 – flowthroughs; Lanes 6 – 11 – wash; Lanes 12 – 17 – elutions.

4.3.2 TEV reactions of GST-TEV-CaM in Different Reaction Conditions

In Figure 4.2, protein band around 45-kDa ladder represented GST-TEV-CaM whose molecular weight is 44 kDa. TEV protease and cleaved GST appeared as one protein band as they have similar molecular weights. The molecular weight of TEV protease is 27 kDa, while that of GST is 26 kDa. The smallest protein that ran down the furthest was CaM which has a molecular weight of 17 kDa. Sufficient cleavages of GST-TEV-CaM were mostly seen in TEV reactions at ratio of 1:10 for both temperatures. In particular, TEV reactions at ratio of 1:10 at room temperature showed to have little amounts of GST-TEV-CaM left. TEV reactions at ratio of 1:10 at 4 ˚C also demonstrated high cleavage activity but not as much as those at room temperature, and at 4 ˚C, the overnight reaction seemed to have most of GST-TEV-CaM cleaved.

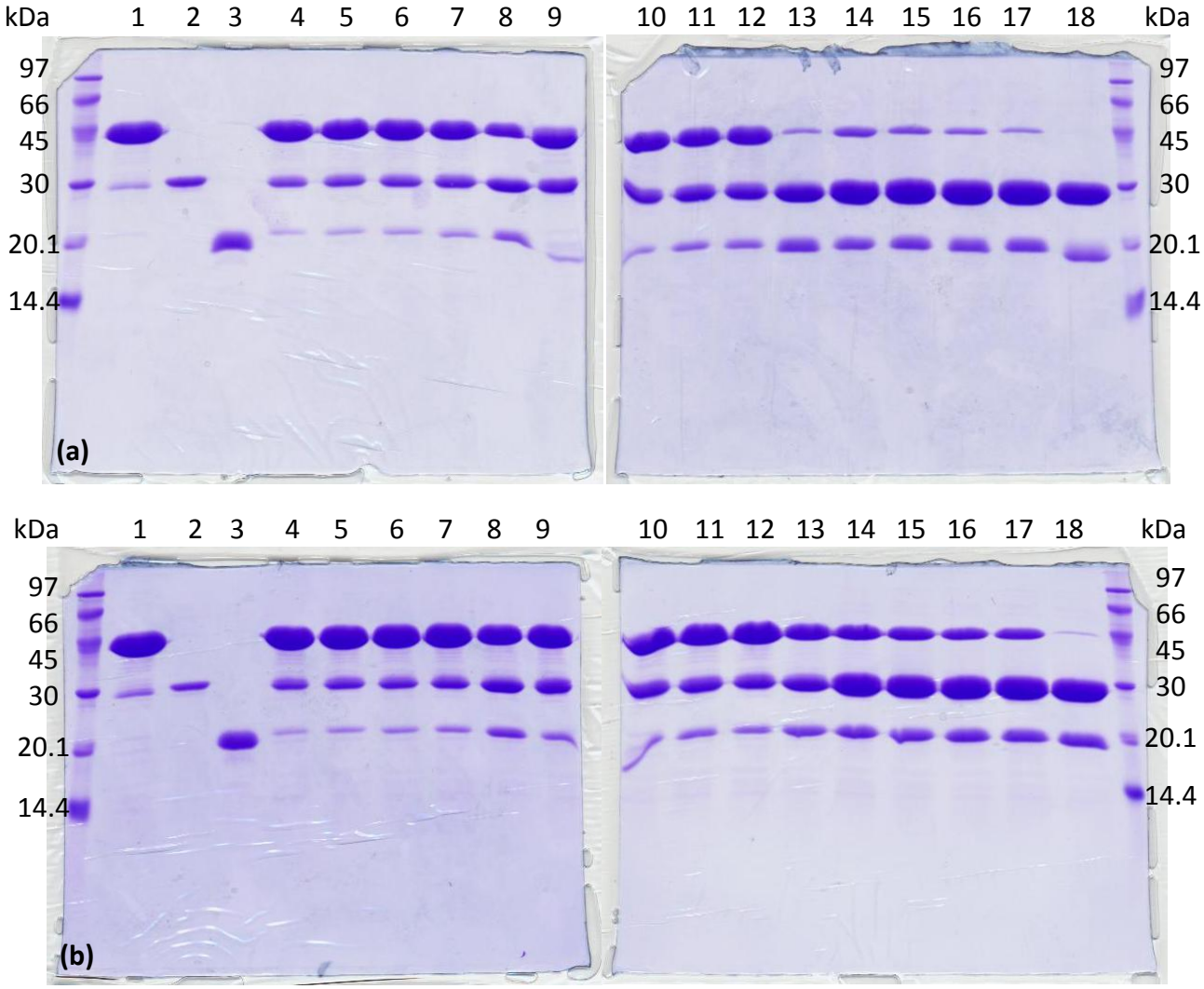

Figure 4.2 15% SDS-PAGE of TEV protease reactions of GST-TEV-CaM at room temperature (a) and at 4 ˚C (b). Cleavage reactions of GST-TEV-CaM by TEV protease were performed at room temperature and at 4 ˚C with varying protease-to-substrate ratios and durations. Lanes 1 – 3 ran undigested GST-TEV-CaM, TEV protease, and CaM, respectively, as controls. Lanes 4 – 8 contained reactions with protease-to-substrate ratio of 1:100, while lanes 9 – 12 had those of 1:50 and lanes 13 – 18 had those of 1:10. For each ratio, reaction with the shortest time was added first and the one with the next shortest time was added to the next right lane. Time durations tested were 30 minutes 1 hour, 1 hour 30 minutes, 2 hours, and overnight.

4.4 Discussion

From the results for GST-TEV-CaM expression and purification, it was shown that GST-TEV-CaM could be expressed and purified by a glutathione column in large amounts. Digestion results showed that reaction condition with protease-to-substrate ratio of 1:10 can achieve cleavage of most GST-TEV-CaM in the sample. Reaction condition at ratio of 1:10 and 4 ˚C for 2 hours seemed to be favourable for cleavage of GST-TEV-CaM in the presence of NOS. This is because TEV protease is a highly reactive protease which might also degrade NOS in an overnight reaction. Reaction conditions at ratio of 1:10 at room temperature appeared to be good but not in the presence of unstable proteins such as NOS.

Our result agreed well to studies done by Fang et al. (2007). Their results demonstrated that with increasing concentration of TEV protease at 30 ◦C, the cleavage reaction reached a plateau approximately at protease-to-substrate ratio of 1:20. Similar results could be seen in our results where the cleavage reaction at protease-to-substrate ratio of 1:10 was most efficient compared to those at 1:100 and 1:50 at both temperatures. In regards to reaction time, studies by Fang et al. (2007) presented that although longer reaction time resulted in more protein cleavage at 30 ◦C at ratio of 1:10, most of the cleavage reaction occurred in the first several hours. Similarly in our results, almost all GST-TEV-CaM was observed to be cleaved in the overnight reaction but reaction time of 2 hours also seemed to be enough for cleavage of most of GST-TEV-CaM.

With TEV protease reactions at two different temperatures, room temperature and 4 ◦C, results showed that although the protease was more active at room temperatures, it was still able to cleave at 4 ◦C. This corresponded well to published results by Nallamsetty et al. (2004). This study demonstrated that optimal temperature for TEV protease activity was 30 ◦C while

its activity decreased at low temperatures. These reaction conditions would allow cleavage reaction by TEV protease of GST-TEV-CaM in purification of NOS which is an unstable protein.

Chapter 5

Future Work

Future work with the expression systems described in Chapter 1 will include production of human forms of NOS isozymes and various oxygenase domains. As a next step for hnNOSoxyCaM purification in Chapter 2, a large-scale expression and purification of hnNOSoxyCaM with GST-TEV-CaM may be performed. Ammonium sulfate precipitation of hnNOSoxyCaM will need to be carried out prior to column application for removal of contaminating proteins which may interfere with hnNOSoxyCaM purification. Larger nickel affinity and glutathione columns with greater binding capacities could be used for purification of hnNOSoxyCaM in larger amounts. In a similar manner, expression and purification of heNOSoxyCaM can be attempted. For production of hiNOS, the protein will need to be coexpressed with GST-TEV-CaM, as iNOS expression was found to only work upon coexpression with CaM (Spratt, 2008). The cell lysate from coexpression of hiNOS and GST-TEV-CaM then could be directly applied to glutathione column without further addition of GST-TEV-CaM.

Once a NOS holoenzyme or oxygenase domain has been purified in large scale, the heme in the active site can be analyzed by ultraviolet-visible spectroscopy from which information on the state of the heme iron can be obtained. Upon addition of NOS inhibitors, the change in spectrum for the heme iron can be monitored and binding of inhibitors in the active site can be examined (Montgomery et al., 2010).

NOS Inhibitor binding may also be studied by generation of NOS biosensors, similarly to cytochrome P450 biosensors that are currently being developed. The purified NOSoxyCaM protein may be immobilized to an electrode with the CaM-binding region and NOS oxygenase

activity may be assayed by electron transfer from the electrode to the enzyme in the absence and presence of various NOS inhibitors (Schneider & Clark, 2013).

Appendix –Sequences and Sequence Analysis of Various Forms of Human NOS Isozymes

phnNOSox – human nNOS oxidase domain without calmodulin-binding region in pDS-78 (pET28a with *N*-terminal HisTEV tag)

Vector map

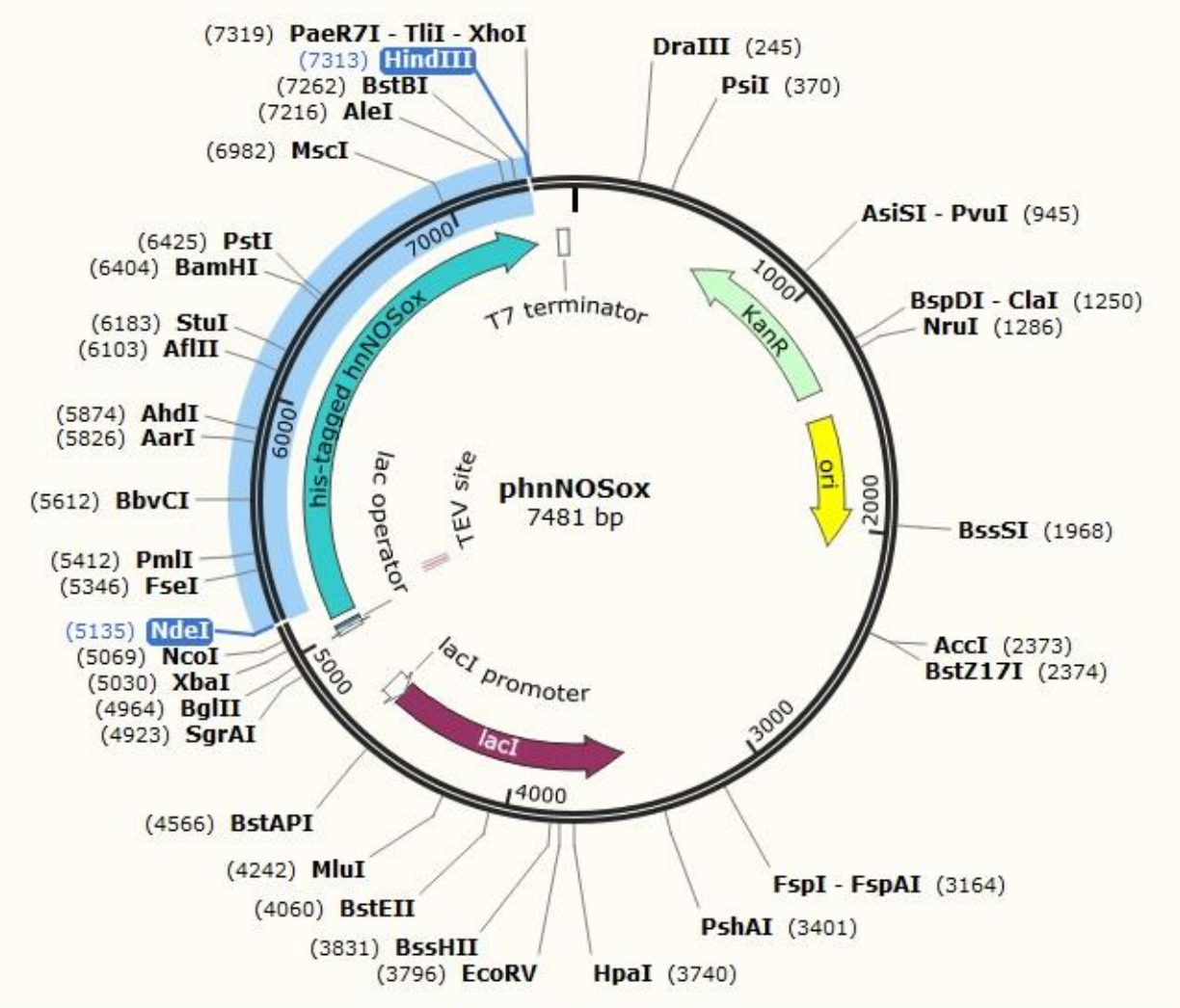

Sequence details of hnNOSox

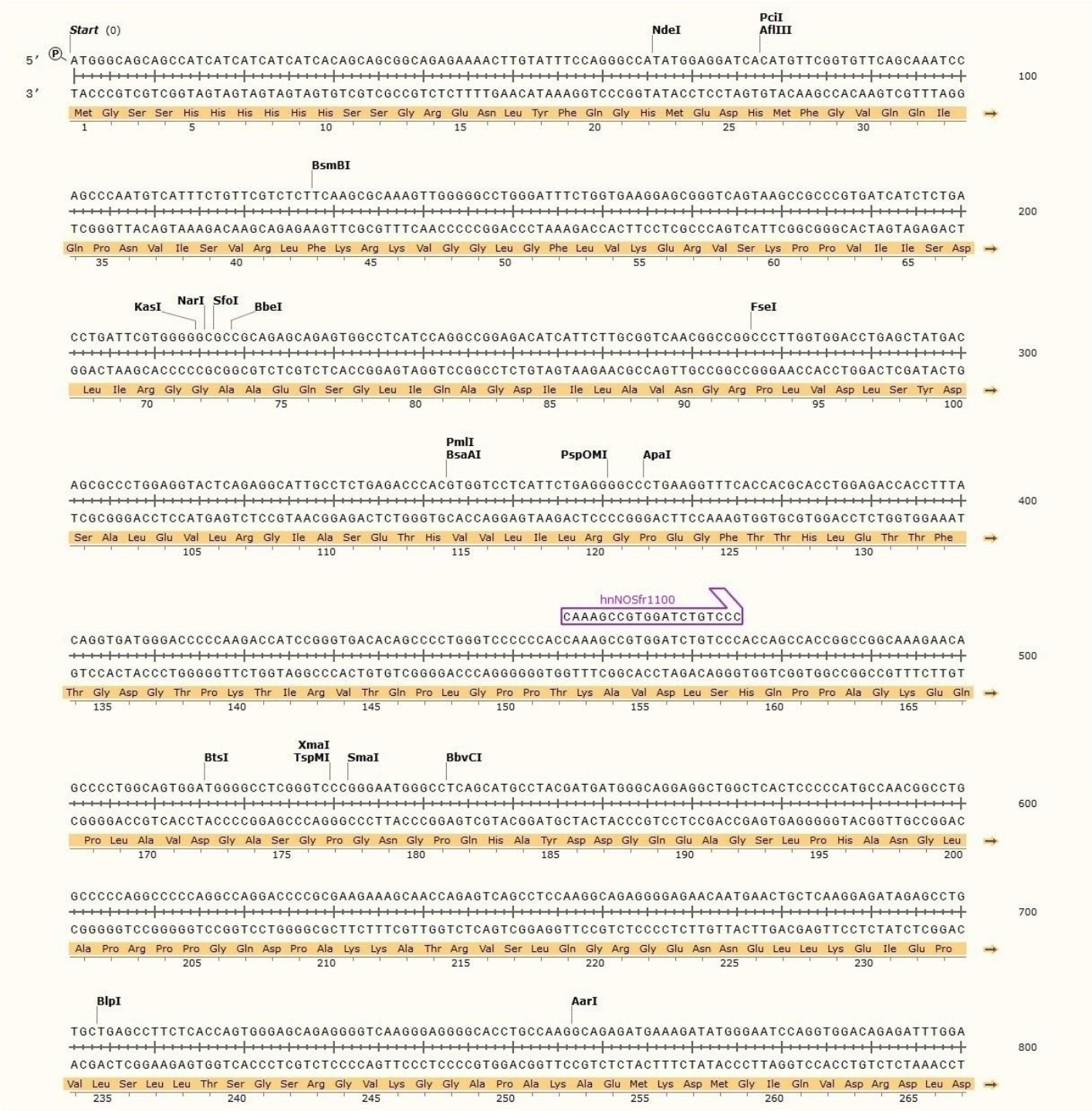

hnNOSox (cont'd – 2)

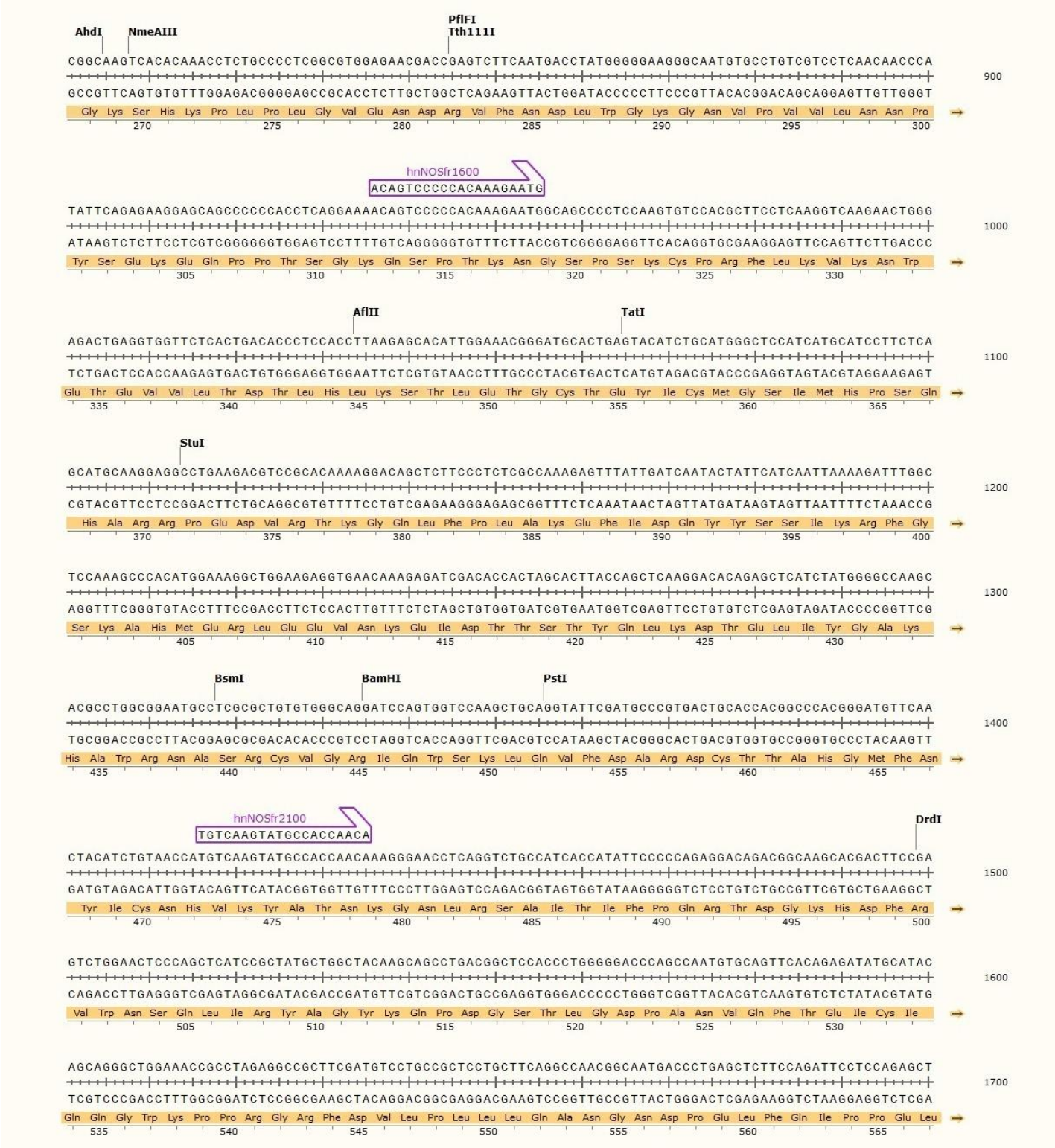

hnNOSox (cont'd – 3)

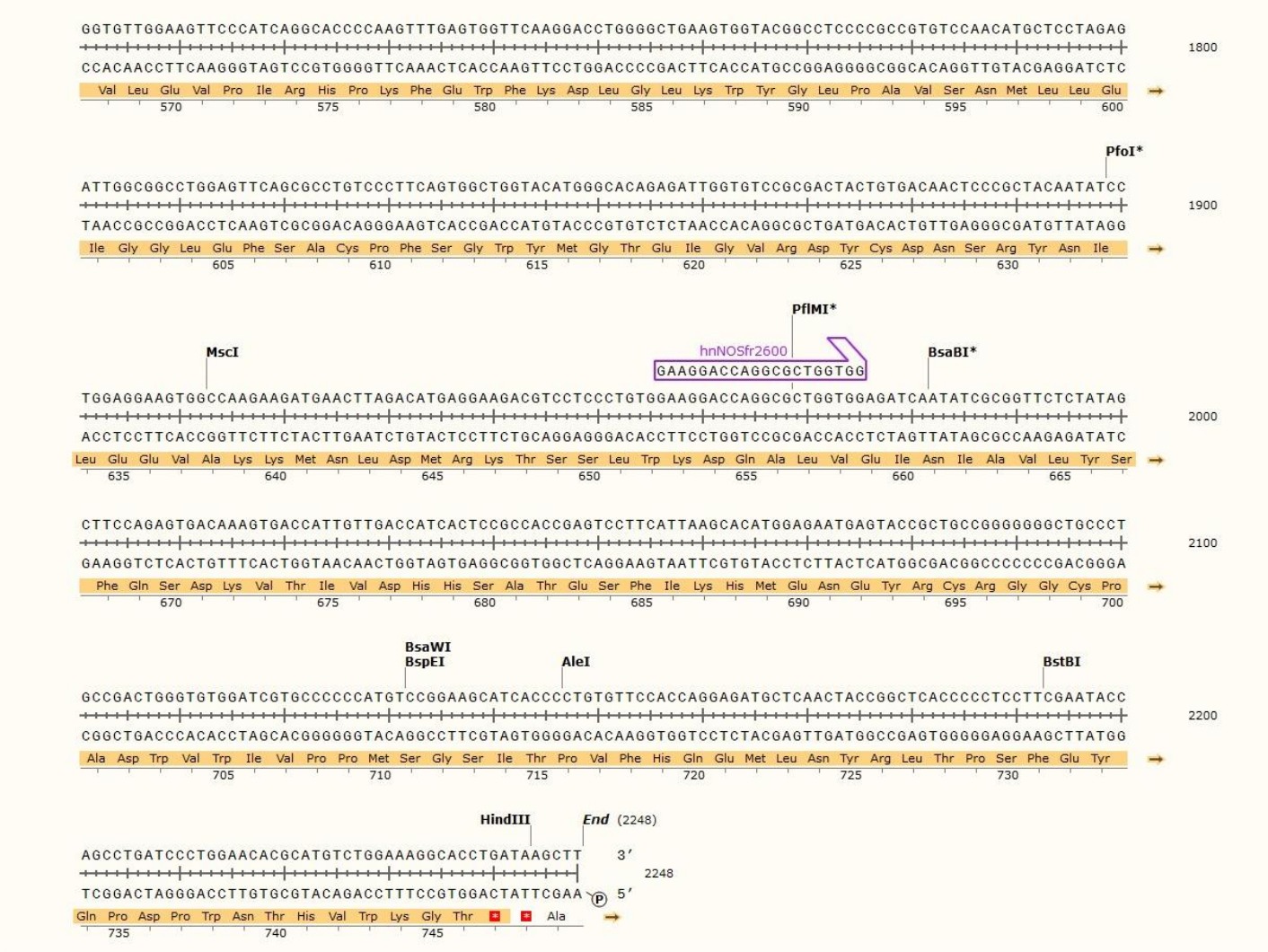

Sequencing summary of hnNOSox – sequencing complete

DNA section	DNA sequencing	Primer to be used
1 – 2248	Complete	–

No mutation was found in hnNOSox.

Sequencing data of hnNOSox

atgggcagcagccatcatcatcatcacagcagcggcagagaaaacttgtatttccagggccatatggaggatcacatgttcggtg
ttcagcaaatccagcccaatgtcatttctgttcgtctcttcaagcgcaaagttgggggcctgggatttctggtgaaggagcgggtcagta
agccgcccgtgatcatctctgacctgattcgtgggggcgccgcagagcagagtggcctcatccaggccggagacatcattcttgcggtc
aacggccggcccttggtggacctgagctatgacagcgccctggaggtactcagaggcattgcctctgagacccacgtggtcctcattct
gaggggccctgaaggtttcaccacgcacctggagaccacctttacaggtgatgggacccccaagaccatccgggtgacacagcccct
gggtccccccaccaaagccgtggatctgtcccaccagccaccggccggcaaagaacagcccctggcagtggatggggcctcgggtcc
cgggaatgggcctcagcatgcctacgatgatgggcaggaggctggctcactcccccatgccaacggcctggcccccaggcccccagg
ccaggaccccgcgaagaaagcaaccagagtcagcctccaaggcagaggggagaacaatgaactgctcaaggagatagagcctgtg
ctgagccttctcaccagtgggagcagaggggtcaagggaggggcacctgccaaggcagagatgaaagatatgggaatccaggtgga
cagagatttggacggcaagtcacacaaacctctgcccctcggcgtggagaacgaccgagtcttcaatgacctatgggggaagggcaa
tgtgcctgtcgtcctcaacaacccatattcagagaaggagcagccccccacctcaggaaaacagtcccccacaaagaatggcagccc
ctccaagtgtccacgcttcctcaaggtcaagaactgggagactgaggtggttctcactgacaccctccaccttaagagcacattggaa
acgggatgcactgagtacatctgcatgggctccatcatgcatccttctcagcatgcaaggaggcctgaagacgtccgcacaaaagga
cagctcttccctctcgccaaagagtttattgatcaatactattcatcaattaaaagatttggctccaaagcccacatggaaaggctgga
agaggtgaacaaagagatcgacaccactagcacttaccagctcaaggacacagagctcatctatggggccaagcacgcctggcgga
atgcctcgcgctgtgtgggcaggatccagtggtccaagctgcaggtattcgatgcccgtgactgcaccacggcccacgggatgttcaa
ctacatctgtaaccatgtcaagtatgccaccaacaaagggaacctcaggtctgccatcaccatattcccccagaggacagacggcaa
gcacgacttccgagtctggaactcccagctcatccgctatgctggctacaagcagcctgacggctccaccctgggggacccagccaat
gtgcagttcacagagatatgcatacagcagggctggaaaccgcctagaggccgcttcgatgtcctgccgctcctgcttcaggccaacg
gcaatgaccctgagctcttccagattcctccagagctggtgttggaagttcccatcaggcaccccaagtttgagtggttcaaggacctg
gggctgaagtggtacggcctccccgccgtgtccaacatgctcctagagattggcggcctggagttcagcgcctgtcccttcagtggctg
gtacatgggcacagagattggtgtccgcgactactgtgacaactcccgctacaatatcctggaggaagtggccaagaagatgaactta
gacatgaggaagacgtcctccctgtggaaggaccaggcgctggtggagatcaatatcgcggttctctatagcttccagagtgacaaag
tgaccattgttgaccatcactccgccaccgagtccttcattaagcacatggagaatgagtaccgctgccgggggggctgccctgccgac
tgggtgtggatcgtgccccccatgtccggaagcatcacccctgtgttccaccaggagatgctcaactaccggctcacccccctccttcga
ataccagcctgatccctggaacacgcatgtctggaaaggcacctga

Blast results of hnNOSox

Score	Expect	Method	Identities	Positives	Gaps	Frame
1518 bits(3931)	0.0	Compositional matrix adjust.	724/724(100%)	724/724(100%)	0/724(0%)	+1

```
Query  67    MEDHMFGVQQIQPNVISVRLFKRKVGGLGFLVKERVSKPPVIISDLIRGGAAEQSGLIQA  246
             MEDHMFGVQQIQPNVISVRLFKRKVGGLGFLVKERVSKPPVIISDLIRGGAAEQSGLIQA
Sbjct  1     MEDHMFGVQQIQPNVISVRLFKRKVGGLGFLVKERVSKPPVIISDLIRGGAAEQSGLIQA  60

Query  247   GDIILAVNGRPLVDLSYDSALEVLRGIASETHVVLILRGPEGFTTHLETTFTGDGTPKTI  426
             GDIILAVNGRPLVDLSYDSALEVLRGIASETHVVLILRGPEGFTTHLETTFTGDGTPKTI
Sbjct  61    GDIILAVNGRPLVDLSYDSALEVLRGIASETHVVLILRGPEGFTTHLETTFTGDGTPKTI  120

Query  427   RVTQPLGPPTKAVDLSHQPPAGKEQPLAVDGASGPGNGPQHAYDDGQEAGSLPHANGLAP  606
             RVTQPLGPPTKAVDLSHQPPAGKEQPLAVDGASGPGNGPQHAYDDGQEAGSLPHANGLAP
Sbjct  121   RVTQPLGPPTKAVDLSHQPPAGKEQPLAVDGASGPGNGPQHAYDDGQEAGSLPHANGLAP  180

Query  607   RPPGQDPAKKATRVSLQGRGENNELLKEIEPVLSLLTSGSRGVKGGAPAKAEMKDMGIQV  786
             RPPGQDPAKKATRVSLQGRGENNELLKEIEPVLSLLTSGSRGVKGGAPAKAEMKDMGIQV
Sbjct  181   RPPGQDPAKKATRVSLQGRGENNELLKEIEPVLSLLTSGSRGVKGGAPAKAEMKDMGIQV  240

Query  787   DRDLDGKSHKPLPLGVENDRVFNDLWGKGNVPVVLNNPYSEKEQPPTSGKQSPTKNGSPS  966
             DRDLDGKSHKPLPLGVENDRVFNDLWGKGNVPVVLNNPYSEKEQPPTSGKQSPTKNGSPS
Sbjct  241   DRDLDGKSHKPLPLGVENDRVFNDLWGKGNVPVVLNNPYSEKEQPPTSGKQSPTKNGSPS  300

Query  967   KCPRFLKVKNWETEVVLTDTLHLKSTLETGCTEYICMGSIMHPSQHARRPEDVRTKGQLF  1146
             KCPRFLKVKNWETEVVLTDTLHLKSTLETGCTEYICMGSIMHPSQHARRPEDVRTKGQLF
Sbjct  301   KCPRFLKVKNWETEVVLTDTLHLKSTLETGCTEYICMGSIMHPSQHARRPEDVRTKGQLF  360

Query  1147  PLAKEFIDQYYSSIKRFGSKAHMERLEEVNKEIDTTSTYQLKDTELIYGAKHAWRNASRC  1326
             PLAKEFIDQYYSSIKRFGSKAHMERLEEVNKEIDTTSTYQLKDTELIYGAKHAWRNASRC
Sbjct  361   PLAKEFIDQYYSSIKRFGSKAHMERLEEVNKEIDTTSTYQLKDTELIYGAKHAWRNASRC  420

Query  1327  VGRIQWSKLQVFDARDCTTAHGMFNYICNHVKYATNKGNLRSAITIFPQRTDGKHDFRVW  1506
             VGRIQWSKLQVFDARDCTTAHGMFNYICNHVKYATNKGNLRSAITIFPQRTDGKHDFRVW
Sbjct  421   VGRIQWSKLQVFDARDCTTAHGMFNYICNHVKYATNKGNLRSAITIFPQRTDGKHDFRVW  480

Query  1507  NSQLIRYAGYKQPDGSTLGDPANVQFTEICIQQGWKPPRGRFDVLPLLLQANGNDPELFQ  1686
             NSQLIRYAGYKQPDGSTLGDPANVQFTEICIQQGWKPPRGRFDVLPLLLQANGNDPELFQ
```

```
Sbjct  481   NSQLIRYAGYKQPDGSTLGDPANVQFTEICIQQGWKPPRGRFDVLPLLLQANGNDPELFQ  540

Query  1687  IPPELVLEVPIRHPKFEWFKDLGLKWYGLPAVSNMLLEIGGLEFSACPFSGWYMGTEIGV  1866
              IPPELVLEVPIRHPKFEWFKDLGLKWYGLPAVSNMLLEIGGLEFSACPFSGWYMGTEIGV
Sbjct  541   IPPELVLEVPIRHPKFEWFKDLGLKWYGLPAVSNMLLEIGGLEFSACPFSGWYMGTEIGV  600

Query  1867  RDYCDNSRYNILEEVAKKMNLDMRKTSSLWKDQALVEINIAVLYSFQSDKVTIVDHHSAT  2046
              RDYCDNSRYNILEEVAKKMNLDMRKTSSLWKDQALVEINIAVLYSFQSDKVTIVDHHSAT
Sbjct  601   RDYCDNSRYNILEEVAKKMNLDMRKTSSLWKDQALVEINIAVLYSFQSDKVTIVDHHSAT  660

Query  2047  ESFIKHMENEYRCRGGCPADWVWIVPPMSGSITPVFHQEMLNYRLTPSFEYQPDPWNTHV  2226
              ESFIKHMENEYRCRGGCPADWVWIVPPMSGSITPVFHQEMLNYRLTPSFEYQPDPWNTHV
Sbjct  661   ESFIKHMENEYRCRGGCPADWVWIVPPMSGSITPVFHQEMLNYRLTPSFEYQPDPWNTHV  720

Query  2227  WKGT  2238
              WKGT
Sbjct  721   WKGT  724
```

pheNOSox – human eNOS oxidase domain without calmodulin-binding region in pDS-78

Vector map

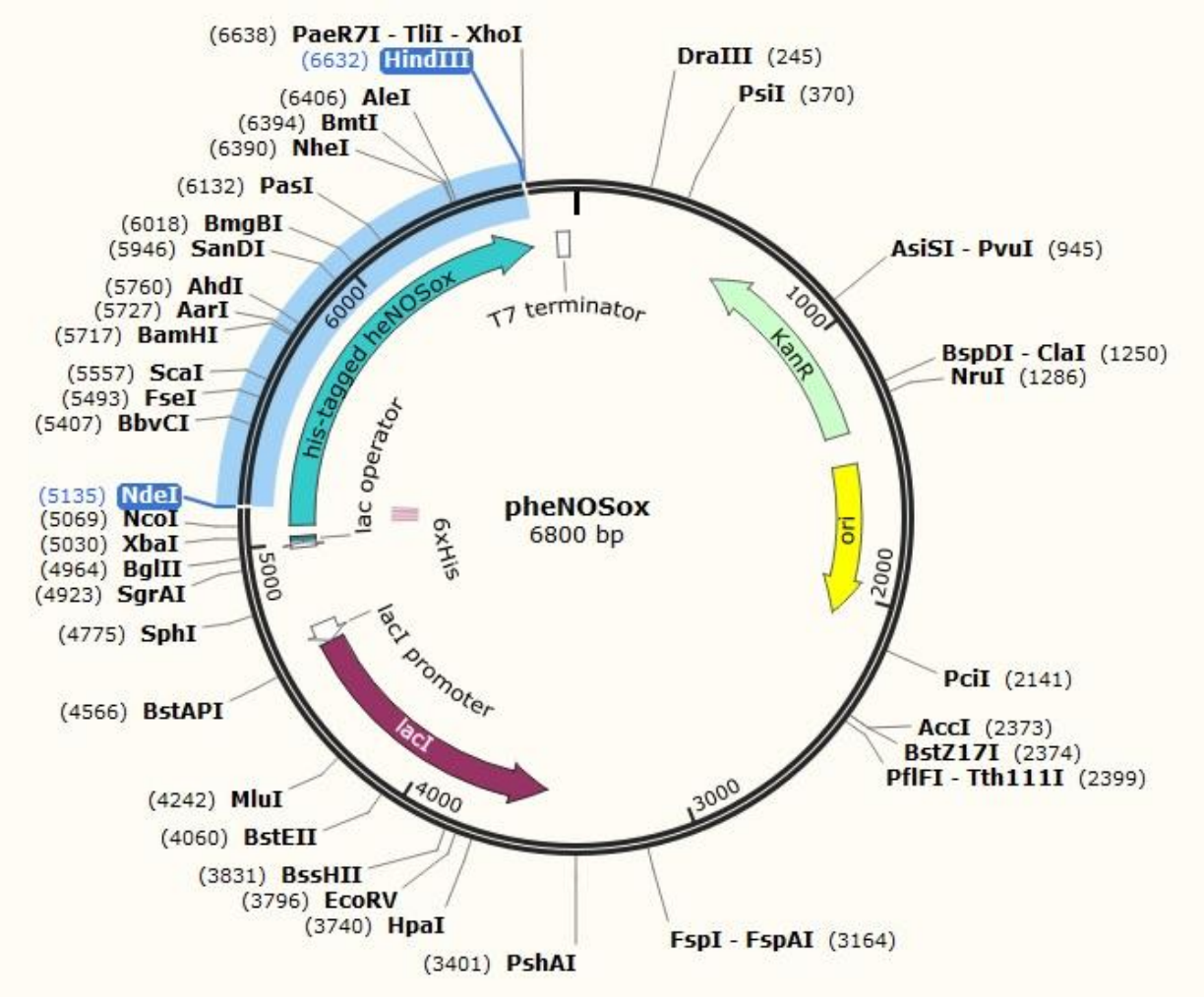

Sequence details of heNOSox

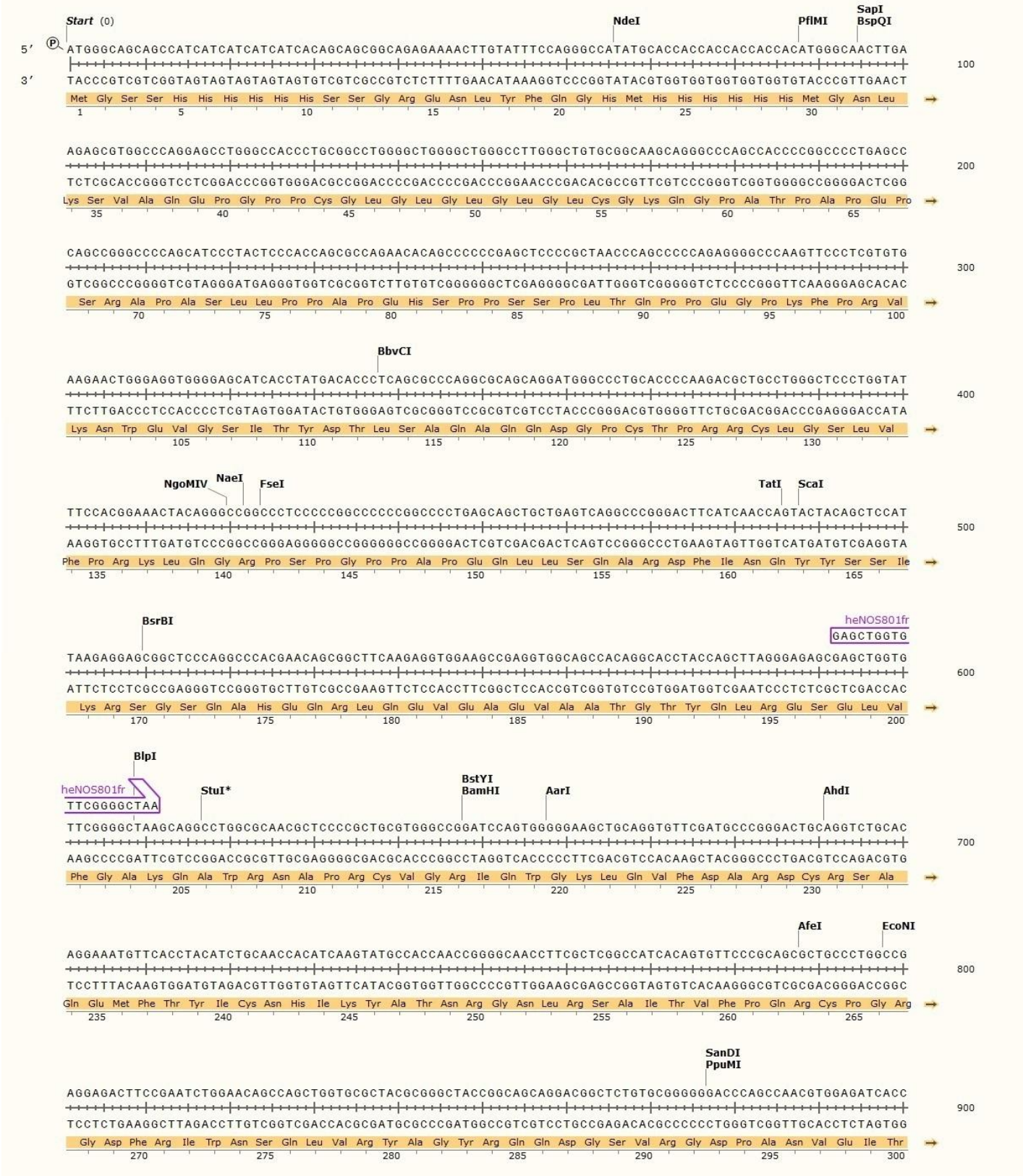

heNOSox (cont'd – 2)

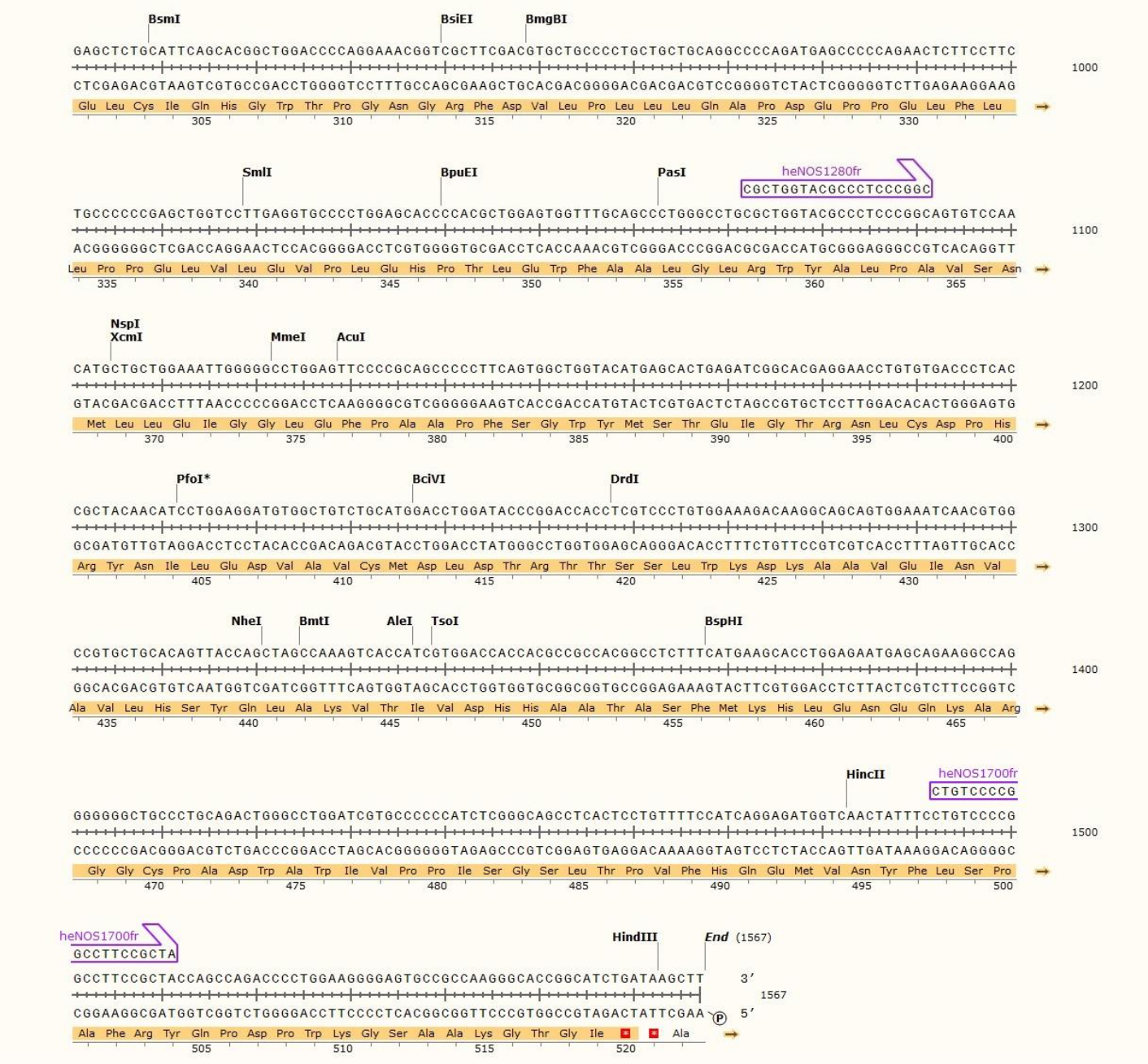

Sequencing summary of heNOSox – sequencing complete

DNA section	DNA sequencing	Primer to be used
1 – 1567	Complete	–

No mutation was found in heNOSox.

Sequencing data of heNOSox

atgggcagcagccatcatcatcatcacagcagcggcagagaaaacttgtatttccagggccatatgcaccaccaccaccaccac
atgggcaacttgaagagcgtggcccaggagcctgggccaccctgcggcctggggctggggctgggccttgggctgtgcggcaagcag
ggcccagccaccccggcccctgagcccagccgggccccagcatccctactcccaccagcgccagaacacagccccccgagctccccg
ctaacccagcccccagaggggcccaagttccctcgtgtgaagaactgggaggtggggagcatcacctatgacaccctcagcgcccag
gcgcagcaggatgggccctgcaccccaagacgctgcctgggctccctggtatttccacggaaactacagggccggccctcccccggcc
ccccggcccctgagcagctgctgagtcaggcccgggacttcatcaaccagtactacagctccattaagaggagcggctcccaggccca
cgaacagcggcttcaagaggtggaagccgaggtggcagccacaggcacctaccagcttagggagagcgagctggtgttcggggcta
agcaggcctggcgcaacgctccccgctgcgtgggccggatccagtgggggaagctgcaggtgttcgatgcccgggactgcaggtctg
cacaggaaatgttcacctacatctgcaaccacatcaagtatgccaccaaccggggcaaccttcgctcggccatcacagtgttcccgca
gcgctgccctggccgaggagacttccgaatctggaacagccagctggtgcgctacgcgggctaccggcagcaggacggctctgtgcg
gggggacccagccaacgtggagatcaccgagctctgcattcagcacggctggaccccaggaaacggtcgcttcgacgtgctgcccct
gctgctgcaggccccagatgagcccccagaactcttccttctgccccccgagctggtccttgaggtgcccctggagcaccccacgctgg
agtggtttgcagccctgggcctgcgctggtacgccctcccggcagtgtccaacatgctgctggaaattgggggcctggagttccccgca
gccccccttcagtggctggtacatgagcactgagatcggcacgaggaacctgtgtgaccctcaccgctacaacatcctggaggatgtgg
ctgtctgcatggacctggatacccggaccacctcgtccctgtggaaagacaaggcagcagtggaaatcaacgtggccgtgctgcaca
gttaccagctagccaaagtcaccatcgtggaccaccacgccgccacggcctctttcatgaagcacctggagaatgagcagaaggcca
ggggggggctgccctgcagactgggcctggatcgtgccccccatctcgggcagcctcactcctgttttccatcaggagatggtcaactatt
tcctgtccccggccttccgctaccagccagacccctggaaggggagtgccgccaagggcaccggcatctga

Blast results of heNOSox

Score	Expect	Method	Identities	Positives	Gaps	Frame
847 bits(2188)	0.0	Compositional matrix adjust.	489/489(100%)	489/489(100%)	0/489(0%)	+1

```
Query  91    GNLKSVAQEpgppcglglglglglcgKQGpatpapepsrapasllppapehsppssplTQ  270
             GNLKSVAQEPGPPCGLGLGLGLGLCGKQGPATPAPEPSRAPASLLPPAPEHSPPSSPLTQ
Sbjct  2     GNLKSVAQEPGPPCGLGLGLGLGLCGKQGPATPAPEPSRAPASLLPPAPEHSPPSSPLTQ  61

Query  271   PPEGPKFPRVKNWEVGSITYDTLSAQAQQDGPCTPRRCLGSLVFPRKLQGRPSPGPPAPE  450
             PPEGPKFPRVKNWEVGSITYDTLSAQAQQDGPCTPRRCLGSLVFPRKLQGRPSPGPPAPE
Sbjct  62    PPEGPKFPRVKNWEVGSITYDTLSAQAQQDGPCTPRRCLGSLVFPRKLQGRPSPGPPAPE  121

Query  451   QLLSQARDFINQYYSSIKRSGSQAHEQRLQEVEAEVAATGTYQLRESELVFGAKQAWRNA  630
             QLLSQARDFINQYYSSIKRSGSQAHEQRLQEVEAEVAATGTYQLRESELVFGAKQAWRNA
Sbjct  122   QLLSQARDFINQYYSSIKRSGSQAHEQRLQEVEAEVAATGTYQLRESELVFGAKQAWRNA  181

Query  631   PRCVGRIQWGKLQVFDARDCRSAQEMFTYICNHIKYATNRGNLRSAITVFPQRCPGRGDF  810
             PRCVGRIQWGKLQVFDARDCRSAQEMFTYICNHIKYATNRGNLRSAITVFPQRCPGRGDF
Sbjct  182   PRCVGRIQWGKLQVFDARDCRSAQEMFTYICNHIKYATNRGNLRSAITVFPQRCPGRGDF  241

Query  811   RIWNSQLVRYAGYRQQDGSVRGDPANVEITELCIQHGWTPGNGRFDVLPLLLQApdeppe  990
             RIWNSQLVRYAGYRQQDGSVRGDPANVEITELCIQHGWTPGNGRFDVLPLLLQAPDEPPE
Sbjct  242   RIWNSQLVRYAGYRQQDGSVRGDPANVEITELCIQHGWTPGNGRFDVLPLLLQAPDEPPE  301

Query  991   lfllppelvlevplehptleWFAALGLRWYALPAVSNMLLEIGGLEFPAAPFSGWYMSTE  1170
             LFLLPPELVLEVPLEHPTLEWFAALGLRWYALPAVSNMLLEIGGLEFPAAPFSGWYMSTE
Sbjct  302   LFLLPPELVLEVPLEHPTLEWFAALGLRWYALPAVSNMLLEIGGLEFPAAPFSGWYMSTE  361

Query  1171  IGTRNLCDPHRYNILEDVAVCMDLDTRTTSSLWKDKAAVEINVAVLHSYQLAKVTIVDHH  1350
             IGTRNLCDPHRYNILEDVAVCMDLDTRTTSSLWKDKAAVEINVAVLHSYQLAKVTIVDHH
Sbjct  362   IGTRNLCDPHRYNILEDVAVCMDLDTRTTSSLWKDKAAVEINVAVLHSYQLAKVTIVDHH  421

Query  1351  AATASFMKHLENEQKARGGCPADWAWIVPPISGSLTPVFHQEMVNYFLSPAFRYQPDPWK  1530
             AATASFMKHLENEQKARGGCPADWAWIVPPISGSLTPVFHQEMVNYFLSPAFRYQPDPWK
Sbjct  422   AATASFMKHLENEQKARGGCPADWAWIVPPISGSLTPVFHQEMVNYFLSPAFRYQPDPWK  481

Query  1531  GSAAKGTGI  1557
             GSAAKGTGI
```

```
Sbjct  482   GSAAKGTGI  490
```

Lower case grey letters represent low-complexity sequences. It is an automatic filter in BLAST to indicate that a match is likely an artifact when a user is searching for sequence homology.

pCWori-hiNOSox – human Δ70 iNOS oxidase domain without calmodulin-binding region in pCWori

Vector map

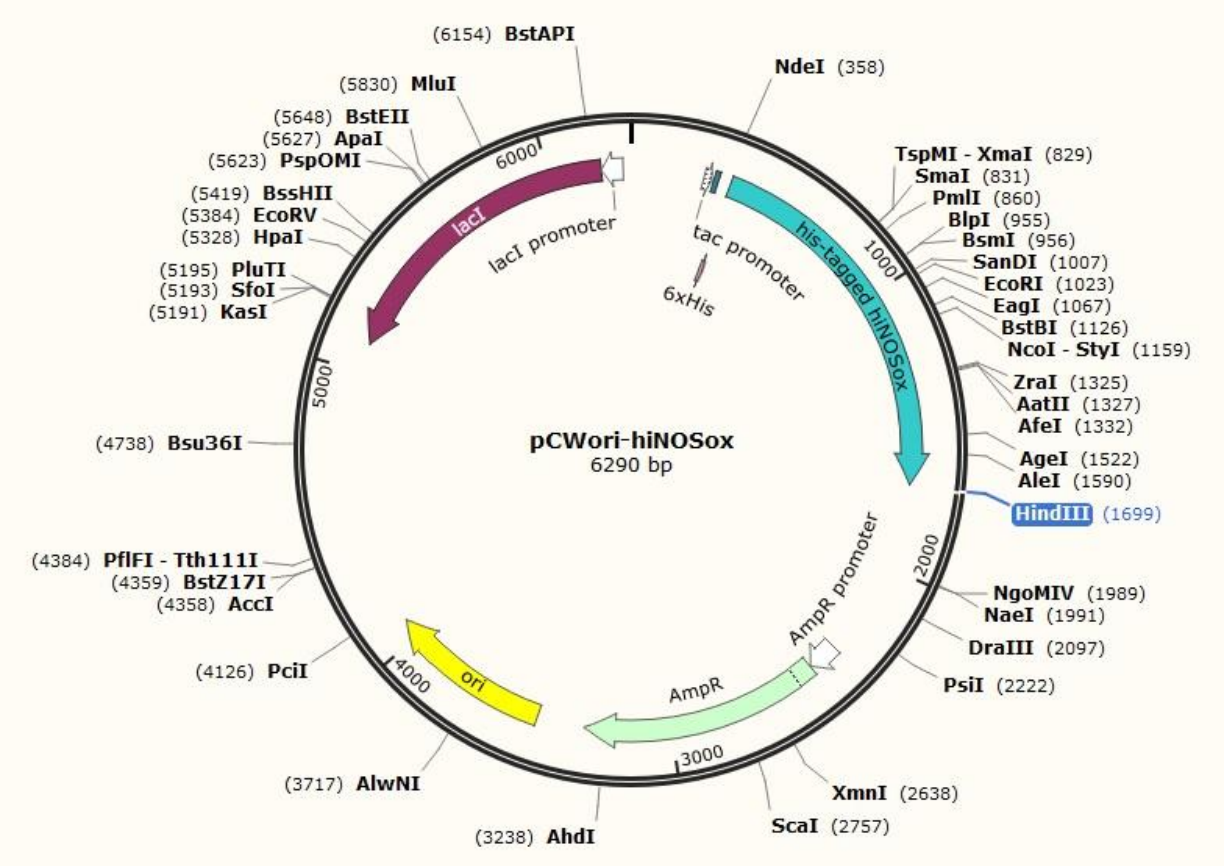

Sequence details of hiNOSox

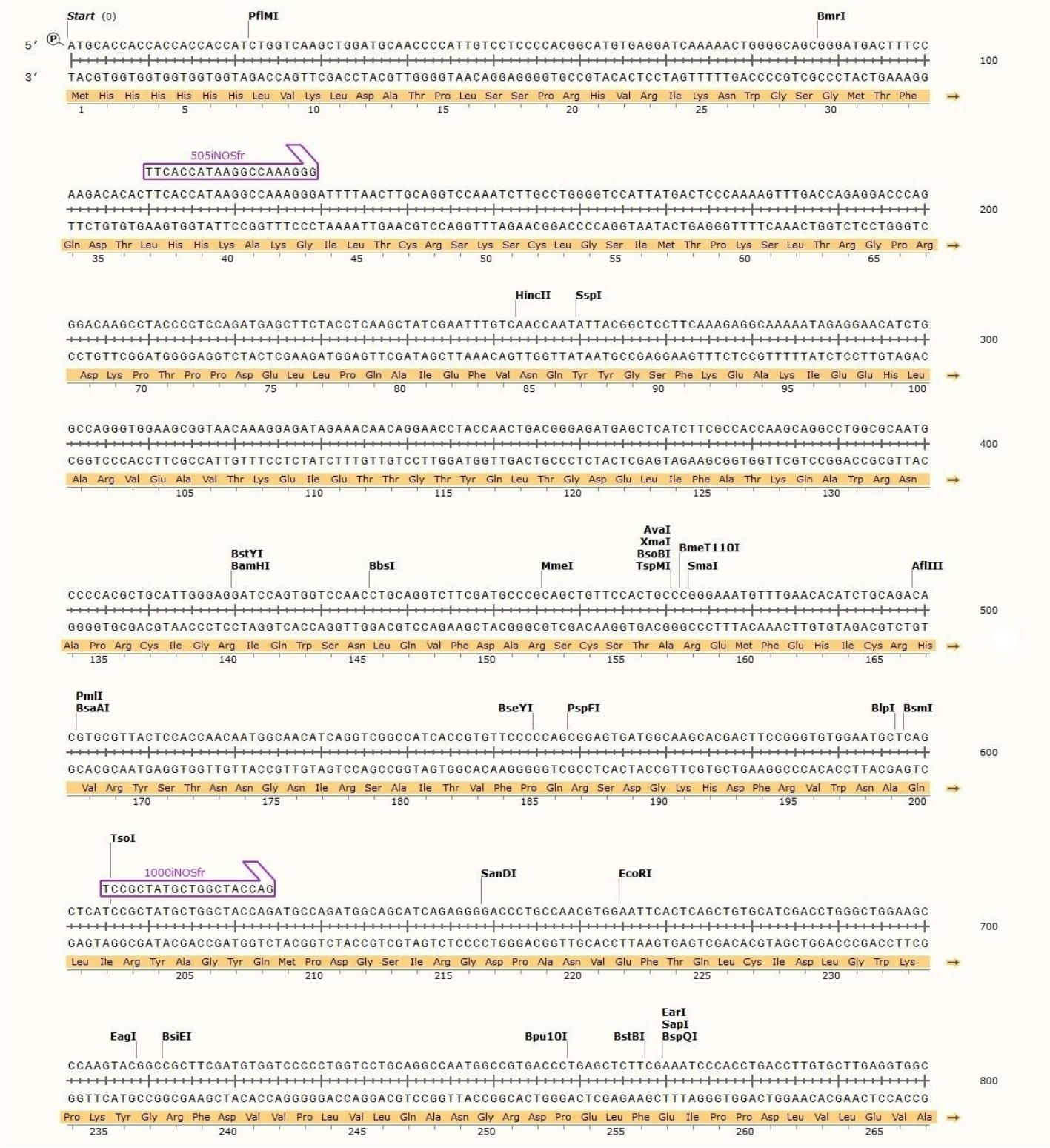

hiNOSox (cont'd – 2)

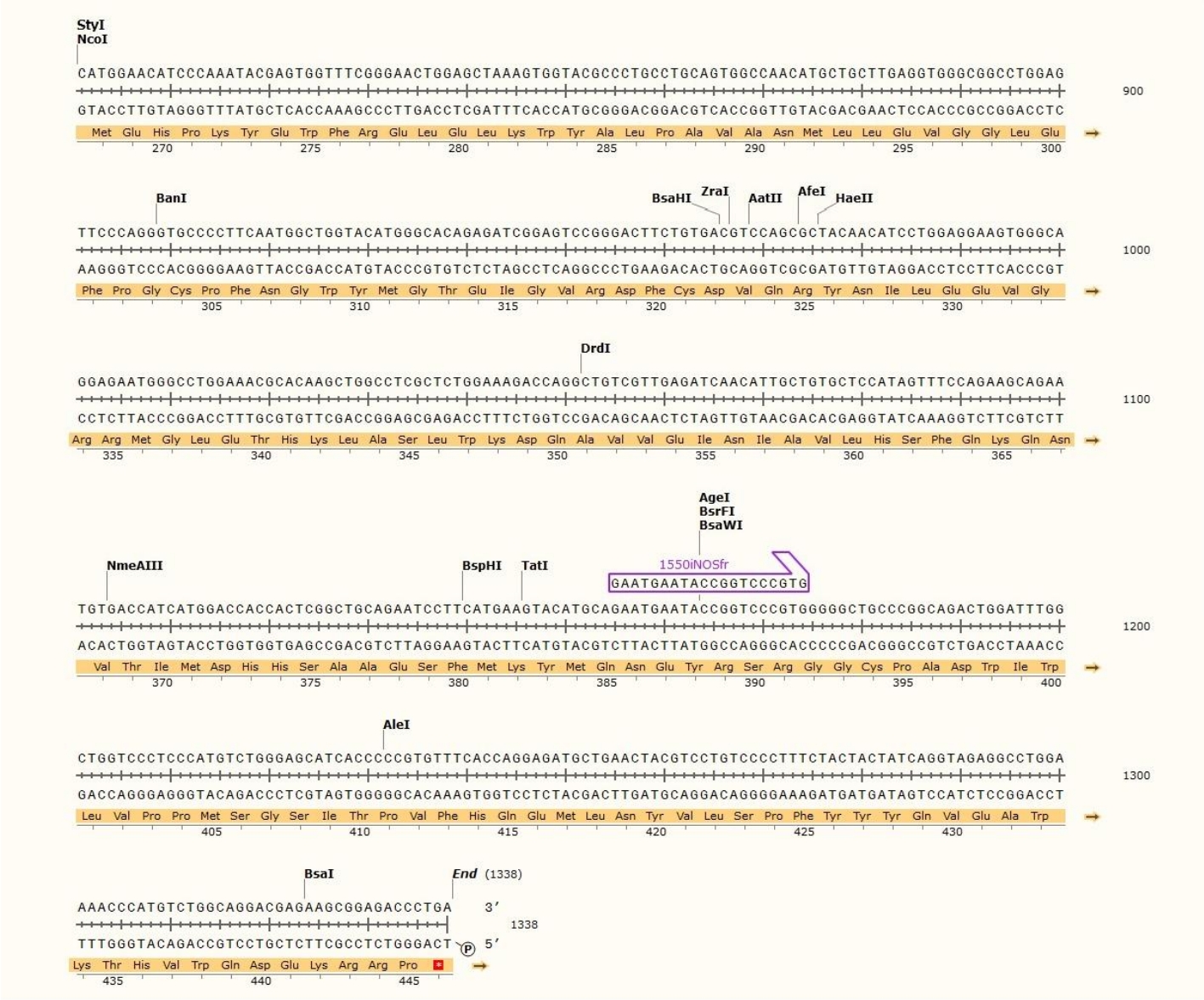

Sequencing summary of hiNOSox

DNA section	DNA sequencing	Primer to be used
1 – 165	Incomplete	pCWOri-fr
166 – 1176	Complete	–
1177 – 1206	Incomplete	1000iNOSfr
1207 – 1338	Complete	–

No mutation was found in the sequencing results of hiNOSox.

Sequencing data of hiNOSox

505iNOSfr

aattgNggtcaatcttgcctggggtcattatgactcccaaaagtttgaccagaggacccagggacaagcctacccctccagatgagct
tctacctcaagctatcgaatttgtcaaccaatattacggctccttcaaagaggcaaaaatagaggaacatctggccagggtggaagcg
gtaacaaaggagatagaaacaacaggaacctaccaactgacgggagatgagctcatcttcgccaccaagcaggcctggcgcaatgc
cccacgctgcattgggaggatccagtggtccaacctgcaggtcttcgatgcccgcagctgttccactgcccgggaaatgtttgaacaca
tctgcagacacgtgcgttactccaccaacaatggcaacatcaggtcggccatcaccgtgttcccccagcggagtgatggcaagcacga
cttccgggtgtggaatgctcagctcatccgctatgctggctaccagatgccagatggcagcatcagaggggaccctgccaacgtggaa
ttcactcagctgtgcatcgacctgggctggaagcccaagtacggccgcttcgatgtggtccccctggtcctgcaggccaatggccgtga
ccctgagctcttcgaaatcccacctgaccttgtgcttgaggtggccatggaacatcccaaatacgagtggtttcgggaactggagctaa
agtggtacgccctgcctgcagtggccaacatgctgcttgaggtgggcggcctggagttcccagggtgccccttcaatggctggtacatg
ggcacagagatcggagtccgggacttctgtgacgtccagcgctacaacatcctggaggaagtgggcaggagaatgggcctggaaac
gcacaagctggcctcgctctggaaagaccaggctgtcgttgagatcaacattgctgtgctccatagtttccagaagcagaatgtgacc
atcatggaccaccactcggctgcagaatccttcatgaagtacatgcagaatgaataccggtcccgtgggggctgcccggcagactgg
aatttggctggtccctcccatgtctgggagcatcaccccNcgtgtttcacaggagatgctgactacgtcctgtccctttctactactatca
gtaNaggctgcaaaccatgttctgcagacagaactgaatcatgatagcttatcgatgaNaggctgttcaaacattgaNgcgagaac
g

1550iNOSfr

aatggtgcNtgatggctggtcctcccatgtctgggagcatcacccccgtgtttcaccaggagatgctgaactacgtcctgtccccttttct
actactatcaggtagaggcctggaaaacccatgtctggcaggacgagaagcggagaccctgataagcttatcgatgataagctgtca
aacatgagcagatctgagcccgcctaatgagcgggctttttttttcagatctgcttgaagacgaaagggcctcgtgatacgcctatttttta
taggttaatgtcatgataataatggtttcttagacgatgcgtcaaagcaaccatagtacgcgccctgtagcggcgcattaagcgcggcg
ggtgtggtggttacgcgcagcgtgaccgctacacttgccagcgccctagcgcccgctcctttcgctttcttcccttcctttctcgccacgtt
cgccggctttccccgtcaagctctaaatcgggggctccctttagggttccgatttagagctttacggcacctcgaccccaaaaaacttga
tttgggtgatggttcacgtagtgggtcatcgccctgatagacggtttttcgccctttgacgttggagtccacgttctttaatagtggactct
tgttccaaactggaacaacactcaaccctatctcgggctattcttttgatttataagggattttgccgatttcggcctattggttaaaaaa
tgagctgatttaacaaaaatttaacgcgaattttaacaaaatattaacgtttacaatttcatcgtcaggtggcacttttcggggaaatgt
gcgcggaacccctatttgtttatttttctaaatacattcaaatatgtatccgctcatgagacaataaccctgataaatgcttcaataatat
tgaaaaaggaagagtatgagtattcaacatttccgtgtcgcccttattNccttttttgcggcattttgccttctgttttgctcaccagaacg
ctggtgaaagtaaaagatgctgaagatcagttgggtgcacgaNtgggattacatcgaactgaatctcacagccgtagatcagaagtt
ttcgcNctgaaNacgtttccaatgatNacNctttaagttNggNtNgtgccgtattatccgNgtgNccgacaagcaccgtNgccct
actattctNgattgaa

Blast results of hiNOSox

505iNOSfr

Score	Expect	Method	Identities	Positives	Gaps	Frame
728 bits(1879)	0.0	Compositional matrix adjust.	354/379(93%)	360/379(94%)	6/379(1%)	+3

```
Query  21    GVIMTPKSLTRGPRDKPTPPDELLPQAIEFVNQYYGSFKEAKIEEHLARVEAVTKEIETT  200
             G IMTPKSLTRGPRDKPTPPDELLPQAIEFVNQYYGSFKEAKIEEHLARVEAVTKEIETT
Sbjct  117   GSIMTPKSLTRGPRDKPTPPDELLPQAIEFVNQYYGSFKEAKIEEHLARVEAVTKEIETT  176

Query  201   GTYQLTGDELIFATKQAWRNAPRCIGRIQWSNLQVFDARSCSTAREMFEHICRHVRYSTN  380
             GTYQLTGDELIFATKQAWRNAPRCIGRIQWSNLQVFDARSCSTAREMFEHICRHVRYSTN
Sbjct  177   GTYQLTGDELIFATKQAWRNAPRCIGRIQWSNLQVFDARSCSTAREMFEHICRHVRYSTN  236

Query  381   NGNIRSAITVFPQRSDGKHDFRVWNAQLIRYAGYQMPDGSIRGDPANVEFTQLCIDLGWK  560
             NGNIRSAITVFPQRSDGKHDFRVWNAQLIRYAGYQMPDGSIRGDPANVEFTQLCIDLGWK
Sbjct  237   NGNIRSAITVFPQRSDGKHDFRVWNAQLIRYAGYQMPDGSIRGDPANVEFTQLCIDLGWK  296

Query  561   PKYGRFDVVPLVLQANGRDPELFEIPPDLVLEVAMEHPKYEWFRELELKWYALPAVANML  740
             PKYGRFDVVPLVLQANGRDPELFEIPPDLVLEVAMEHPKYEWFRELELKWYALPAVANML
Sbjct  297   PKYGRFDVVPLVLQANGRDPELFEIPPDLVLEVAMEHPKYEWFRELELKWYALPAVANML  356

Query  741   LEVGGLEFPGCPFNGWYMGTEIGVRDFCDVQRYNILEEVGRRMGLETHKLASLWKDQAVV  920
             LEVGGLEFPGCPFNGWYMGTEIGVRDFCDVQRYNILEEVGRRMGLETHKLASLWKDQAVV
Sbjct  357   LEVGGLEFPGCPFNGWYMGTEIGVRDFCDVQRYNILEEVGRRMGLETHKLASLWKDQAVV  416

Query  921   EINIAVLHSFQKQNVTIMDHHSAAESFMKYMQNEYRSRGGLPGRLEFGWSLPCL-GASPX  1097
             EINIAVLHSFQKQNVTIMDHHSAAESFMKYMQNEYRSRGG P   ++ W +P + G+
Sbjct  417   EINIAVLHSFQKQNVTIMDHHSAAESFMKYMQNEYRSRGGCPA--DWIWLVPPMSGSITP  474

Query  1098  VFHRRC*LRPV--PFYYYQ  1148
             VFH+   L  V  PFYYYQ
Sbjct  475   VFHQEM-LNYVLSPFYYYQ  492
```

1550iNOSfr

Score	Expect	Method	Identities	Positives	Gaps	Frame
96.3 bits(238)	2e-25	Compositional matrix adjust.	43/43(100%)	43/43(100%)	0/43(0%)	+3

```
Query  21   PPMSGSITPVFHQEMLNYVLSPFYYYQVEAWKTHVWQDEKRRP  149
            PPMSGSITPVFHQEMLNYVLSPFYYYQVEAWKTHVWQDEKRRP
Sbjct  466  PPMSGSITPVFHQEMLNYVLSPFYYYQVEAWKTHVWQDEKRRP  508
```

phnNOSoxyCaM – human nNOS oxygenase domain with calmodulin-binding region in pDS-78

Vector map

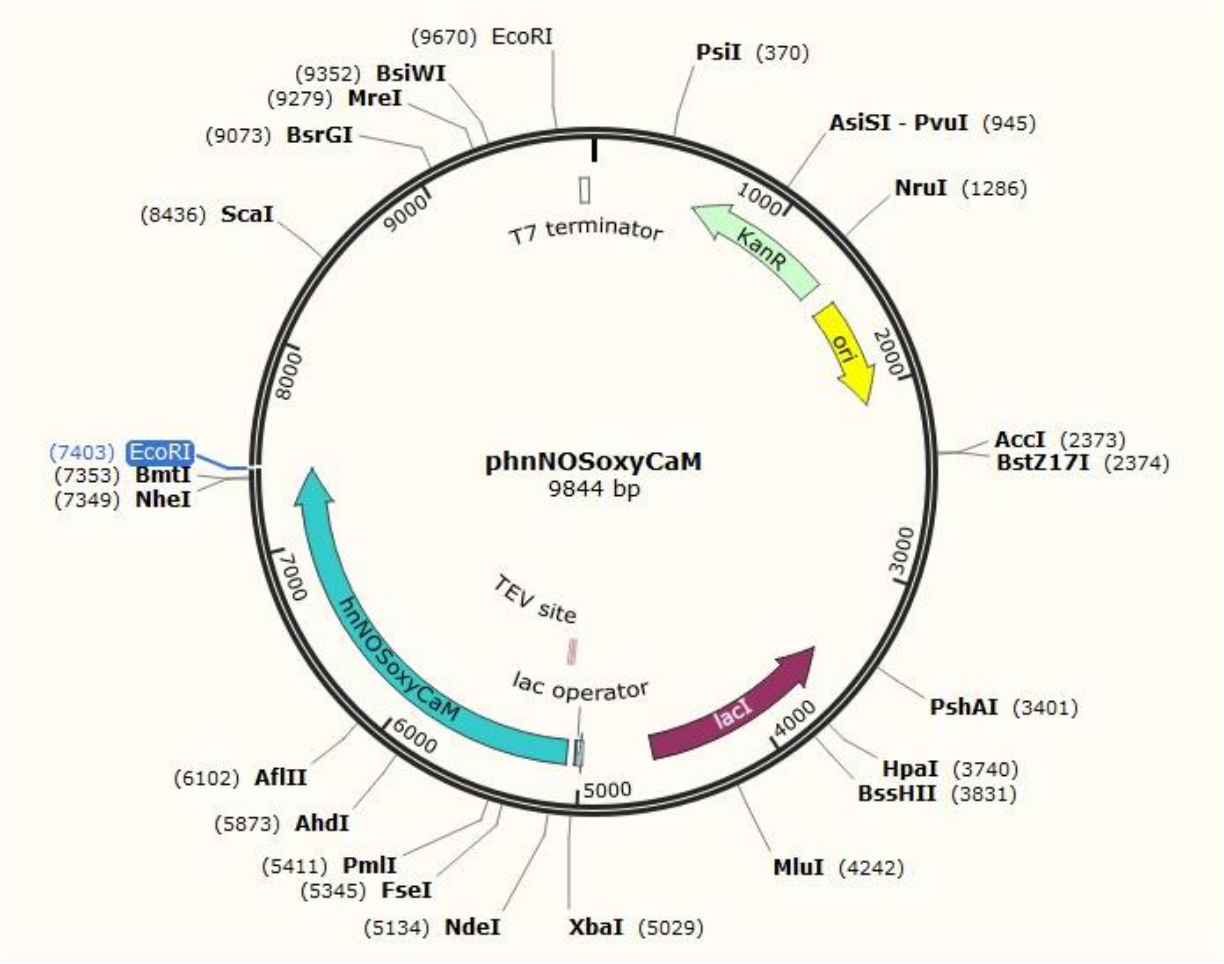

Sequence details of hnNOSoxyCaM

hnNOSoxyCaM (cont'd – 2)

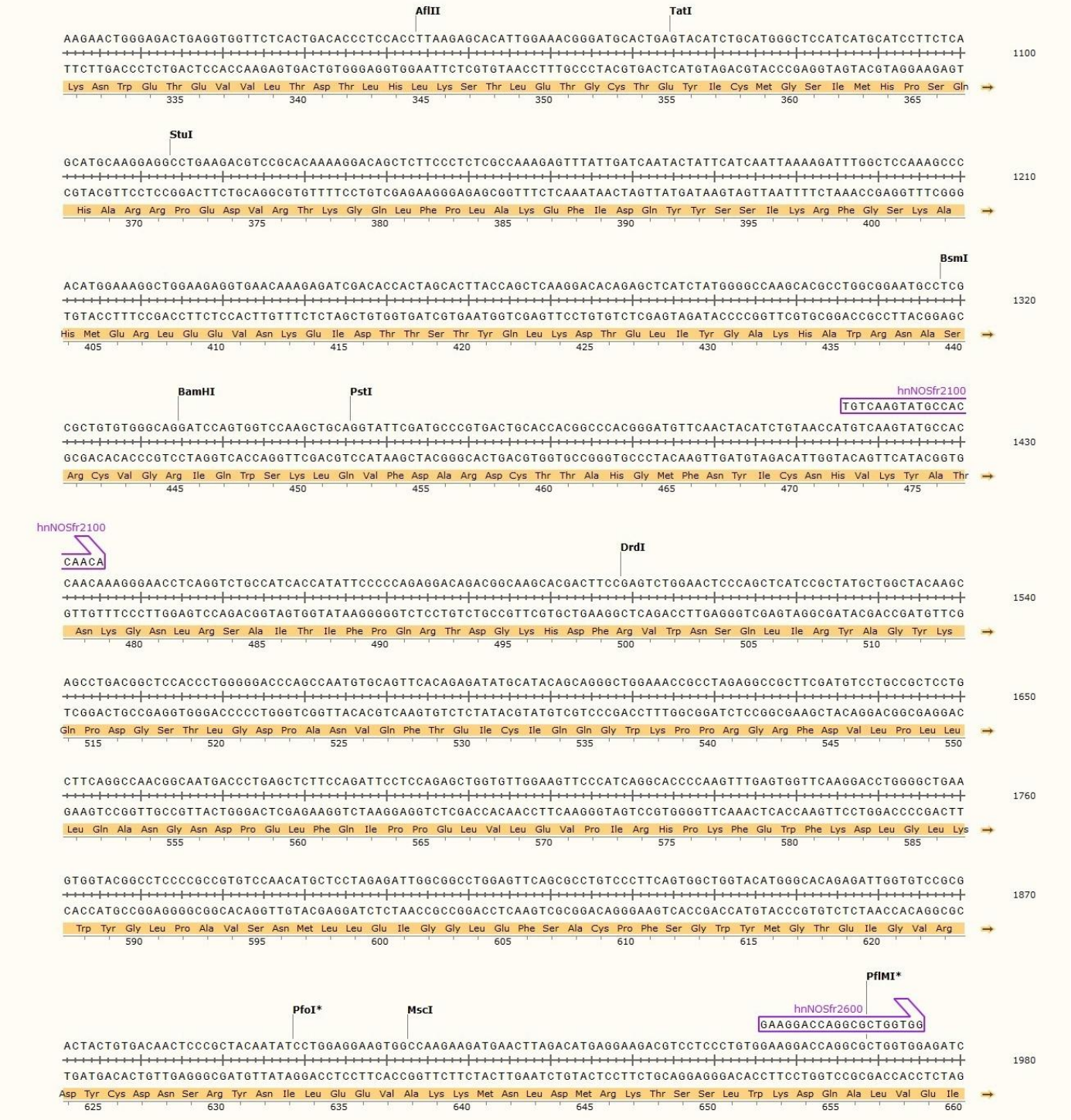

hnNOSoxyCaM (cont'd – 3)

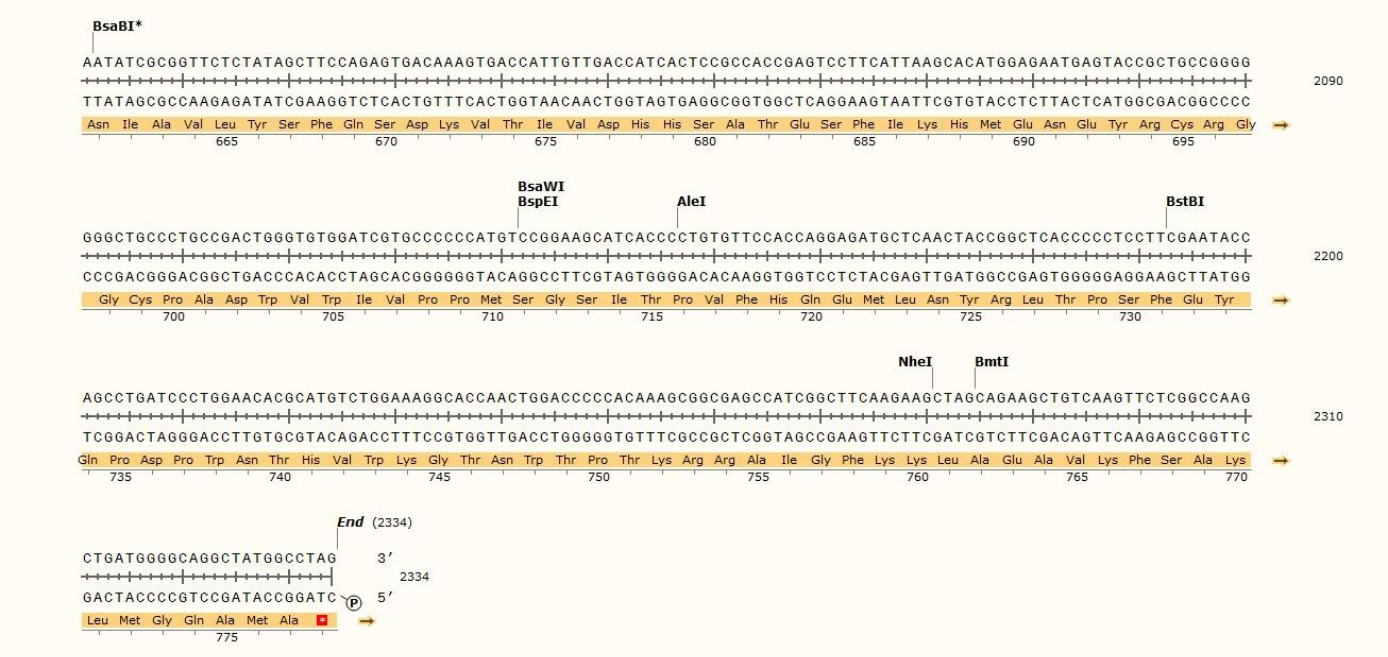

Sequencing summary of hnNOSoxyCaM – sequencing complete

DNA section	DNA sequencing	Primer to be used
1 – 2334	Complete	–

Mutation found in hnNOSoxyCaM

DNA position	Mutation	Amino acid change	Amino acid position
2242	G → T	Gly → Trp	726

Sequencing data of hnNOSoxyCaM

T7

ggggggNNattccctctagaataattttgtttaactttaagaaggagatataccatgggcagcagccatcNtNatcatcatcacag
cagcggcagagaaaacttgtatttccagggccatatggaggatcacatgttcggtgttcagcaaatccagcccaatgtcatttctgttc
gtctcttcaagcgcaaagttgggggcctgggatttctggtgaaggagcgggtcagtaagccgcccgtgatcatctctgacctgattcgt
gggggcgccgcagagcagagtggcctcatccaggccggagacatcattcttgcggtcaacggccggcccttggtggacctgagctat
gacagcgccctggaggtactcagaggcattgcctctgagacccacgtggtcctcattctgaggggccctgaaggtttcaccacgcacct
ggagaccacctttacaggtgatgggacccccaagaccatccgggtgacacagcccctgggtccccccaccaaagccgtggatctgtcc
caccagccaccggccggcaaagaacagcccctggcagtggatggggcctcgggtcccgggaatgggcctcagcatgcctacgatgat
gggcaggaggctggctcactcccccatgccaacggcctggcccccaggcccccaggccaggaccccgcgaagaaagcaaccagagt
cagcctccaaggcagaggggagaacaatgaactgctcaaggagatagagcctgtgctgagccttctcaccagtgggagcagagggg
tcaagggaggggcacctgccaaggcagagatgaaagatatgggaatccaggtggacagagatttggacggcaagtcacacaaacc
tctgcccctcggcgtgagaacgaccgagtcttcatgacctatgggggaagggcaatgtgcctgtcgtcctcaacacNcatattcagag
aaggagcagcccccacctcagaaaacagtccccNcaaagaatgcagcNcctcagtgtcacgcttctcagtcagactgggaNactga

gtgtcNNctgaNNcctccactagaNcNatgaacgatgNctgaNtaNtctgcatgtcatcatgcatcttNcacatgcagagctga
aNttcgccaaagaNgctcttcttgcaagttatggNcNaacatcatagatgtcagtcatgagNtgaaggaaggtc

nNOS1381

tttggacNaagattgggatccaggtggacagagatttggacggcaagtcacacaaacctctgcccctcggcgtggagaacgaccga
gtcttcaatgacctatgggggaagggcaatgtgcctgtcgtcctcaacaacccatattcagagaaggagcagccccccacctcaggaa
aacagtcccccacaaagaatggcagcccctccaagtgtccacgcttcctcaaggtcaagaactgggagactgaggtggttctcactga
caccctccaccttaagagcacattggaaacgggatgcactgagtacatctgcatgggctccatcatgcatccttctcagcatgcaagga
ggcctgaagacgtccgcacaaaaggacagctcttccctctcgccaaagagtttattgatcaatactattcatcaattaaaagatttggc
tccaaagcccacatggaaaggctggaagaggtgaacaaagagatcgacaccactagcacttaccagctcaaggacacagagctcat
ctatggggccaagcacgcctggcggaatgcctcgcgctgtgtgggcaggatccagtggtccaagctgcaggtattcgatgcccgtgac
tgcaccacggcccacgggatgttcaactacatctgtaaccatgtcaagtatgccaccaacaaagggaacctcaggtctgccatcacca
tattcccccagaggacagacggcaagcacgacttccgagtctggaactcccagctcatccgctatgctggctacaagcagcctgacgg
ctccaccctgggggacccagccaatgtgcagttcacagagatatgcatacagcagggctggaaaccgcctagaggccgcttcgatgt
cctgccgctctgcttcaggccaacggcaatgaccctgagctcttccagattcctccagagctgtgtgaagtcccatcagcaccccagttt
gagtgatcaggactgggctgagtgtacgcctcccgcgNgtcaacatgctctaNaNattgcgctgagtcagcgctgtccctcagtgcN
tgtaNtgccacagagatgcgtcgcgNtactggacacNtccgctacaNtctgagactgcagaaatgactgactgagaaNtctctgga
gacagctggatcaatcgtctaagctcgagtgtcaaagt

hnNOSfr1600

cccaggtttcNcgcttcctcNNgtcagaactgggagactgaggtggttctcactgacaccctccaccttaagaNcNNattggaaac
gggatgcactgagtacatctgcatgggctccatcNtgcatccttctcagcatgcaaggaggcctgaagacgtccgcacaaaaggaca
gctcttccctctcgccaaagagtttattgatcaatactattcatcaattaaaagatttggctccaaagNccacatggaaaggctggaag
aggtgaacaaagagatcgacaccactagcacttaccagctcaaggacacagagctcatctatggggccaagcacgcctggcggaat
gcctcgcgctgtgtgggcaggatccagtggtccaagctgcaggtattcgatgcccgtgactgcaccacggcccacgggatgttcaact
acatctgtaaccatgtcaagtatgccaccaacaaagggaacctcaggtctgccatcaccatattcccccagaggacagacggcaagc
acgacttccgagtctggaactcccagctcatccgctatgctggctacaagcagcctgacggctccaccctgggggacccagccaatgt
gcagttcacagagatatgcatacagcagggctggaaaccgcctagaggccgcttcgatgtcctgccgctcctgcttcaggccaacggc
aatgaccctgagctcttccagattcctccagagctggtgttggaagttcccatcagcaccccaagtttgagtggttcaaggacctgggg
ctgaagtggtacggcctccccgccgtgtccaacatgctcctagagattggcggcctgcagttcagcgcctgtcccttcagtggctggtac
atgggcacagagattggtgtccgcgactactgtgacaactcccgctacatatcctggaggaagtggccaagaagatgaacttagacat
gagaagacgtcctccctgtggaaggaccagcgctgNtggagatcatatcgcgtNtctatagcttccagagtgacaagtgacatgtga
catcNNtccgNcaNcgagtctcatagcacatgagatgagtacgctgctgggggctgcctgcgactgggNNgatcNgcNcatgtc
cgaagcatcacctNgttcNcagaaaNgcNagtNccttaccctctgatcacctgatctgaNgcaNtctggaaggacctactggaa

hnNOSfr2100

cagactgcatcaccatattcccccagaggacagacggcaagcacgacttccgagtctggaactcccagctcNtccgctatgctggcta
caagcagcctgacggctccaccctgggggacccagccaatgtgcagttcacagagatatgcatacagcagggctggaaaccgcctag
aggccgcttcgatgtcctgccgctcctgcttcaggccaacggcaatgaccctgagctcttccagattcctccagagctggtgttggaagt
tcccatcaggcaccccaagtttgagtggttcaaggacctggggctgaagtggtacggcctccccgccgtgtccaacatgctcctagag
attggcggcctggagttcagcgcctgtcccttcagtggctggtacatgggcacagagattggtgtccgcgactactgtgacaactcccg

ctacaatatcctggaggaagtggccaagaagatgaacttagacatgaggaagacgtcctccctgtggaaggaccaggcgctggtgg
agatcaatatcgcggttctctatagcttccagagtgacaaagtgaccattgttgaccatcactccgccaccgagtccttcattaagcaca
tggagaatgagtaccgctgccgggggggctgccctgccgactgggtgtggatcgtgccccccatgtccggaagcatcacccctgtgttc
caccaggagatgctcaactaccggctcacccccctccttcgaataccagcctgatccctggaacacgcatgtctggaaaggcaccaact
ggacccccacaaagcggcgagccatcggcttcaagaagctagcagaagctgtcaagttctcggccaagctgatggggcaggctatgg
cctagaattcgaaagcgaccatcctctatgccacagagacaggcaatcgcaagcttatgccagaccttgtgtgagatcttcaacacgc
cttgatgccagNgatgtccatggagatatgacatgtgcactggaacatgaactNtggtcctNNgtcNcagcactttggcatggagat
ccctggagatggggagaatcggctgNgcttgatggatgaggcacccactNtgtcagagataagctNagtcgatcNaNgtNcttct
actgattccaaatcNcagcatgcgactgaacctgaagctgacctgcatgagtcNgttggcNgccggc

Blast results of hnNOSoxyCaM

T7

Score	Expect	Method	Identities	Positives	Gaps	Frame
535 bits(1377)	0.0	Compositional matrix adjust.	277/321(86%)	283/321(88%)	5/321(1%)	+2

```
Query  122   MEDHMFGVQQIQPNVISVRLFKRKVGGLGFLVKERVSKPPVIISDLIRGGAAEQSGLIQA  301
             MEDHMFGVQQIQPNVISVRLFKRKVGGLGFLVKERVSKPPVIISDLIRGGAAEQSGLIQA
Sbjct  1     MEDHMFGVQQIQPNVISVRLFKRKVGGLGFLVKERVSKPPVIISDLIRGGAAEQSGLIQA  60

Query  302   GDIILAVNGRPLVDLSYDSALEVLRGIASETHVVLILRGPEGFTTHLETTFTGDGTPKTI  481
             GDIILAVNGRPLVDLSYDSALEVLRGIASETHVVLILRGPEGFTTHLETTFTGDGTPKTI
Sbjct  61    GDIILAVNGRPLVDLSYDSALEVLRGIASETHVVLILRGPEGFTTHLETTFTGDGTPKTI  120

Query  482   RVTQPLGPPTKAVDLSHQPPAGKEQPLAVDGASGPGNGPQHAYDDGQEAGSLPHANGLAP  661
             RVTQPLGPPTKAVDLSHQPPAGKEQPLAVDGASGPGNGPQHAYDDGQEAGSLPHANGLAP
Sbjct  121   RVTQPLGPPTKAVDLSHQPPAGKEQPLAVDGASGPGNGPQHAYDDGQEAGSLPHANGLAP  180

Query  662   RPPGQDPAKKATRVSLQGRGENNELLKEIEPVLSLLTSGSRGVKGGAPAKAEMKDMGIQV  841
             RPPGQDPAKKATRVSLQGRGENNELLKEIEPVLSLLTSGSRGVKGGAPAKAEMKDMGIQV
Sbjct  181   RPPGQDPAKKATRVSLQGRGENNELLKEIEPVLSLLTSGSRGVKGGAPAKAEMKDMGIQV  240

Query  842   DRDLDGKSHKPLPLGVRTTESS*PM-GEGQCACRPQHXYSEKEQPPPQ-KTVPXKNAAP-  1012
             DRDLDGKSHKPLPLGV        + G+G       + YSEKEQPP   K  P KN +P
Sbjct  241   DRDLDGKSHKPLPLGVENDRVFNDLWGKGNVPVVLNNPYSEKEQPPTSGKQSPTKNGSPS  300

Query  1013  QC--HASQSDWXTECXLXPPL  1069
             +C       +W TE  L   L
Sbjct  301   KCPRFLKVKNWETEVVLTDTL  321
```

hnNOSfr1100

Score	Expect	Method	Identities	Positives	Gaps	Frame
623 bits(1606)	0.0	Compositional matrix adjust.	291/295(99%)	293/295(99%)	0/295(0%)	+3

```
Query  12    IGIQVDRDLDGKSHKPLPLGVENDRVFNDLWGKGNVPVVLNNPYSEKEQPPTSGKQSPTK  191
             +GIQVDRDLDGKSHKPLPLGVENDRVFNDLWGKGNVPVVLNNPYSEKEQPPTSGKQSPTK
```

```
Sbjct  236  MGIQVDRDLDGKSHKPLPLGVENDRVFNDLWGKGNVPVVLNNPYSEKEQPPTSGKQSPTK  295

Query  192  NGSPSKCPRFLKVKNWETEVVLTDTLHLKSTLETGCTEYICMGSIMHPSQHARRPEDVRT  371
            NGSPSKCPRFLKVKNWETEVVLTDTLHLKSTLETGCTEYICMGSIMHPSQHARRPEDVRT
Sbjct  296  NGSPSKCPRFLKVKNWETEVVLTDTLHLKSTLETGCTEYICMGSIMHPSQHARRPEDVRT  355

Query  372  KGQLFPLAKEFIDQYYSSIKRFGSKAHMERLEEVNKEIDTTSTYQLKDTELIYGAKHAWR  551
            KGQLFPLAKEFIDQYYSSIKRFGSKAHMERLEEVNKEIDTTSTYQLKDTELIYGAKHAWR
Sbjct  356  KGQLFPLAKEFIDQYYSSIKRFGSKAHMERLEEVNKEIDTTSTYQLKDTELIYGAKHAWR  415

Query  552  NASRCVGRIQWSKLQVFDARDCTTAHGMFNYICNHVKYATNKGNLRSAITIFPQRTDGKH  731
            NASRCVGRIQWSKLQVFDARDCTTAHGMFNYICNHVKYATNKGNLRSAITIFPQRTDGKH
Sbjct  416  NASRCVGRIQWSKLQVFDARDCTTAHGMFNYICNHVKYATNKGNLRSAITIFPQRTDGKH  475

Query  732  DFRVWNSQLIRYAGYKQPDGSTLGDPANVQFTEICIQQGWKPPRGRFDVLPLCFR  896
            DFRVWNSQLIRYAGYKQPDGSTLGDPANVQFTEICIQQGWKPPRGRFDVLPL  +
Sbjct  476  DFRVWNSQLIRYAGYKQPDGSTLGDPANVQFTEICIQQGWKPPRGRFDVLPLLLQ  530
```

hnNOSfr1600

Score	Expect	Method	Identities	Positives	Gaps	Frame
512 bits(1319)	0.0	Compositional matrix adjust.	242/256(95%)	243/256(94%)	2/256(0%)	+1

```
Query  1    PRFXASSXQNWETEVVLTDTLHLKXXLETGCTEYICMGSIXHPSQHARRPEDVRTKGQLF  180
            PRF     +NWETEVVLTDTLHLK  LETGCTEYICMGSI HPSQHARRPEDVRTKGQLF
Sbjct  303  PRFL--KVKNWETEVVLTDTLHLKSTLETGCTEYICMGSIMHPSQHARRPEDVRTKGQLF  360

Query  181  PLAKEFIDQYYSSIKRFGSKXHMERLEEVNKEIDTTSTYQLKDTELIYGAKHAWRNASRC  360
            PLAKEFIDQYYSSIKRFGSK HMERLEEVNKEIDTTSTYQLKDTELIYGAKHAWRNASRC
Sbjct  361  PLAKEFIDQYYSSIKRFGSKAHMERLEEVNKEIDTTSTYQLKDTELIYGAKHAWRNASRC  420

Query  361  VGRIQWSKLQVFDARDCTTAHGMFNYICNHVKYATNKGNLRSAITIFPQRTDGKHDFRVW  540
            VGRIQWSKLQVFDARDCTTAHGMFNYICNHVKYATNKGNLRSAITIFPQRTDGKHDFRVW
Sbjct  421  VGRIQWSKLQVFDARDCTTAHGMFNYICNHVKYATNKGNLRSAITIFPQRTDGKHDFRVW  480

Query  541  NSQLIRYAGYKQPDGSTLGDPANVQFTEICIQQGWKPPRGRFDVLPLLLQANGNDPELFQ  720
            NSQLIRYAGYKQPDGSTLGDPANVQFTEICIQQGWKPPRGRFDVLPLLLQANGNDPELFQ
Sbjct  481  NSQLIRYAGYKQPDGSTLGDPANVQFTEICIQQGWKPPRGRFDVLPLLLQANGNDPELFQ  540
```

```
Query  721  IPPELVLEVPISTPSL  768
            IPPELVLEVPI  P
Sbjct  541  IPPELVLEVPIRHPKF  556
```

hnNOSfr2100

Score	Expect	Method	Identities	Positives	Gaps	Frame
641 bits(1654)	0.0	Compositional matrix adjust.	307/332(92%)	312/332(93%)	2/332(0%)	+3

```
Query  6    CITIFPQRTDGKHDFRVWNSQLXRYAGYKQPDGSTLGDPANVQFTEICIQQGWKPPRGRF  185
            ITIFPQRTDGKHDFRVWNSQL RYAGYKQPDGSTLGDPANVQFTEICIQQGWKPPRGRF
Sbjct  463  AITIFPQRTDGKHDFRVWNSQLIRYAGYKQPDGSTLGDPANVQFTEICIQQGWKPPRGRF  522

Query  186  DVLPLLLQANGNDPELFQIPPELVLEVPIRHPKFEWFKDLGLKWYGLPAVSNMLLEIGGL  365
            DVLPLLLQANGNDPELFQIPPELVLEVPIRHPKFEWFKDLGLKWYGLPAVSNMLLEIGGL
Sbjct  523  DVLPLLLQANGNDPELFQIPPELVLEVPIRHPKFEWFKDLGLKWYGLPAVSNMLLEIGGL  582

Query  366  EFSACPFSGWYMGTEIGVRDYCDNSRYNILEEVAKKMNLDMRKTSSLWKDQALVEINIAV  545
            EFSACPFSGWYMGTEIGVRDYCDNSRYNILEEVAKKMNLDMRKTSSLWKDQALVEINIAV
Sbjct  583  EFSACPFSGWYMGTEIGVRDYCDNSRYNILEEVAKKMNLDMRKTSSLWKDQALVEINIAV  642

Query  546  LYSFQSDKVTIVDHHSATESFIKHMENEYRCRGGCPADWVWIVPPMSGSITPVFHQEMLN  725
            LYSFQSDKVTIVDHHSATESFIKHMENEYRCRGGCPADWVWIVPPMSGSITPVFHQEMLN
Sbjct  643  LYSFQSDKVTIVDHHSATESFIKHMENEYRCRGGCPADWVWIVPPMSGSITPVFHQEMLN  702

Query  726  YRLTPSFEYQPDPWNTHVWKGTNWTPTKRRAIGFKKLAEAVKFSAKLMGQAMA*NSKATI  905
            YRLTPSFEYQPDPWNTHVWKGTN TPTKRRAIGFKKLAEAVKFSAKLMGQAMA   KATI
Sbjct  703  YRLTPSFEYQPDPWNTHVWKGTNGTPTKRRAIGFKKLAEAVKFSAKLMGQAMAKRVKATI  762

Query  906  LYATETGNRKLMPDLV*DL-QHAL-MPXMSME  995
            LYATETG  +     + ++ +HA     MSME
Sbjct  763  LYATETGKSQAYAKTLCEIFKHAFDAKVMSME  794
```

pheNOSoxyCaM – human eNOS oxygenase domain with calmodulin-binding region in pDS-78

Vector map

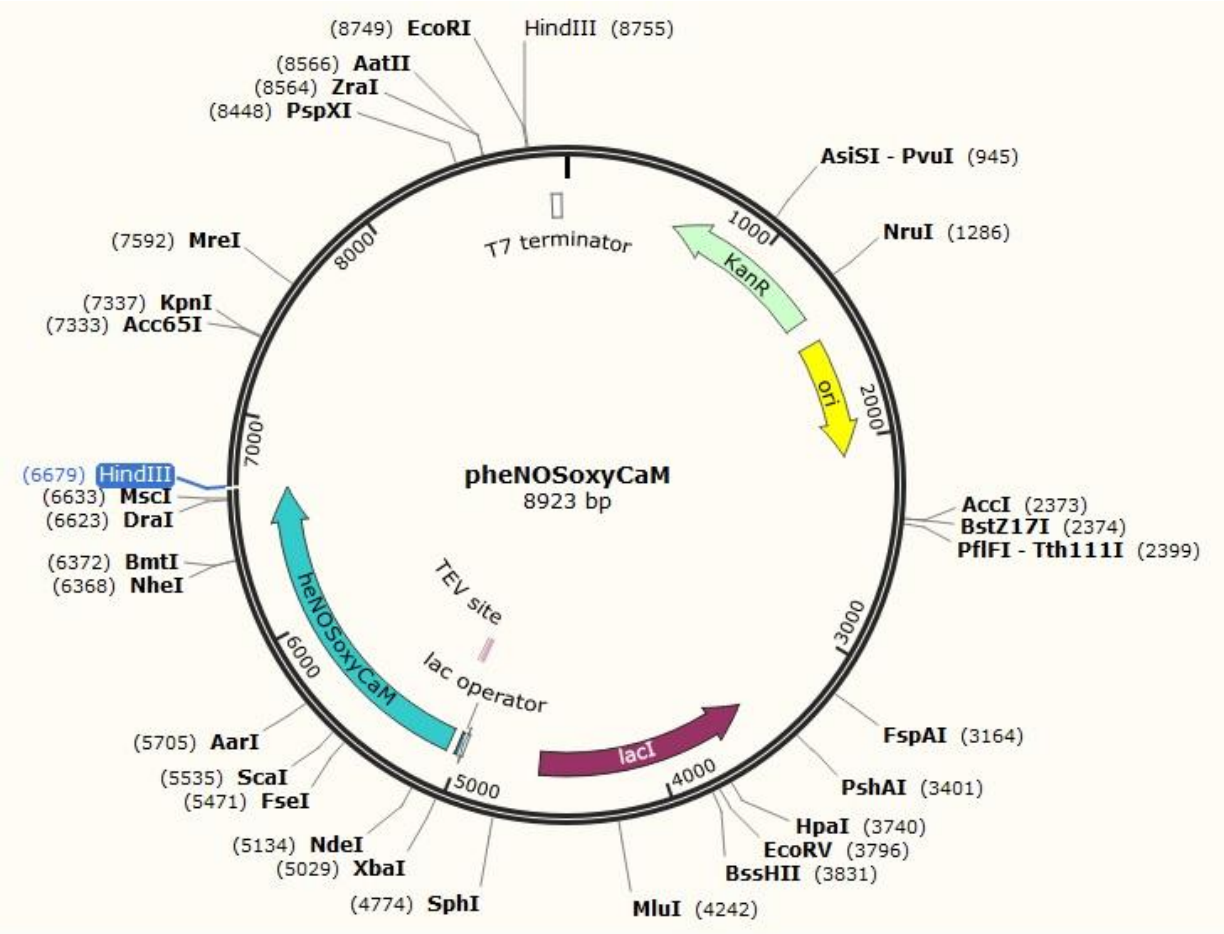

Sequence details of heNOSoxyCaM

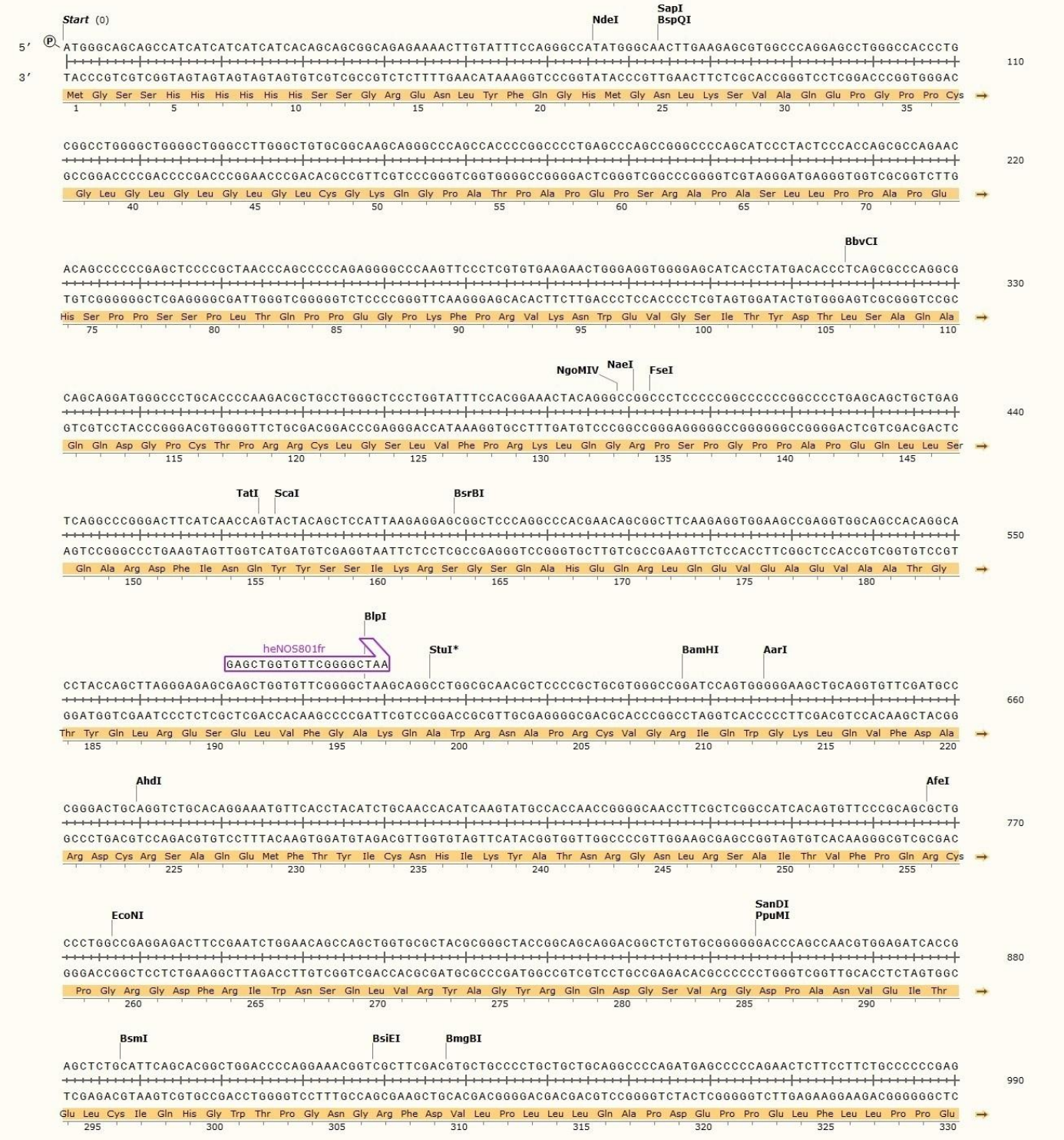

heNOSoxyCaM (cont'd – 2)

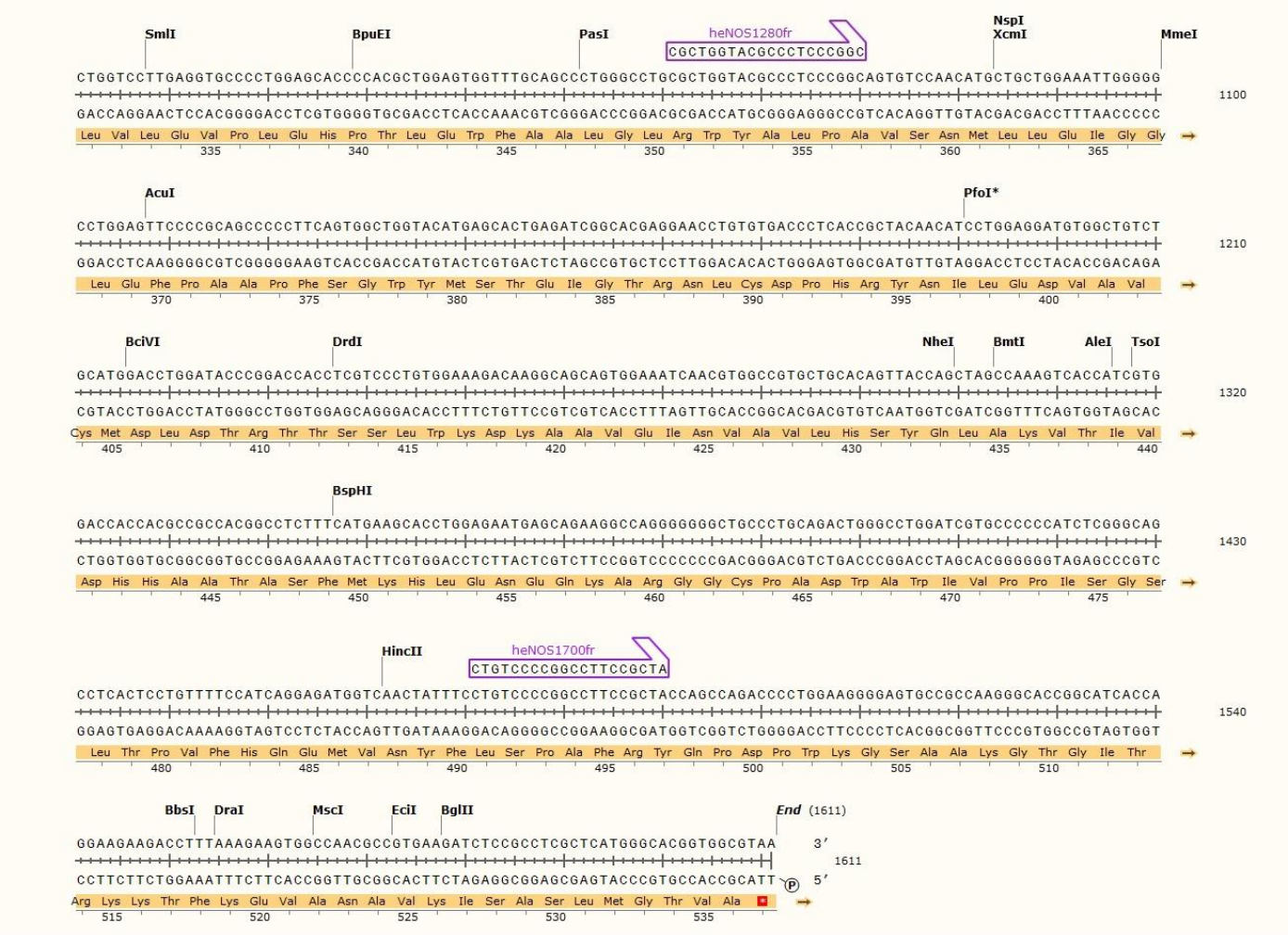

Sequencing summary of heNOSoxyCaM – sequencing complete

DNA section	DNA sequencing	Primer to be used
1 – 1611	Complete	–

Mutation found in heNOSoxyCaM

DNA position	Mutation	Amino acid change	Amino acid position
1606 – 1608	deletion of ATG	Met → Ala	514

Sequencing data of heNOSoxyCaM

T7

gaccNNNNNNNggtaattccccctctagaataattttgtttaactttaagaaggagatataccatgggcagcagccatcatcatcat
catcacagcagcggcagagaaaacttgtatttccagggccatatgggcaacttgaagagcgtggcccaggagcctgggccaccctgc
ggcctggggctggggctgggccttgggctgtgcggcaagcagggcccagccaccccggcccctgagcccagccgggccccagcatcc
ctactcccaccagcgccagaacacagccccccgagctccccgctaacccagcccccagaggggcccaagttccctcgtgtgaagaac
tgggaggtggggagcatcacctatgacaccctcagcgcccaggcgcagcaggatgggccctgcaccccaagacgctgcctgggctcc
ctggtatttccacggaaactacagggccggccctcccccggcccccccggcccctgagcagctgctgagtcaggcccgggacttcatca
accagtactacagctccattaagaggagcggctcccaggcccacgaacagcggcttcaagaggtggaagccgaggtggcagccaca
ggcacctaccagcttagggagagcgagctggtgttcggggctaagcaggcctggcgcaacgctccccgctgcgtgggccggatccag
tgggggaagctgcaggtgttcgatgcccgggactgcaggtctgcacaggaaatgttcacctacatctgcaaccacatcaagtatgcca
ccaaccggggcaaccttcgctcggccatcacagtgttcccgcagcgctgccctggccgaggagacttccNaatctggaacagccagc
tggtgcgctacgcggcNtaccggcagcaggacggctctgNgcgggggNccagccacgtgaagatcaccgaNNtNtgcattcag
cacggctggaccccaggaacgtcgcttcgacNtgctgccctgctgNtgcaggcccaNatgagcccagaacNttcttctgcccccga
NctggtcttgaggtgccctgtagcNNcccaNgctgaNNNgattgcagcctggctNtgcctggtacgccctccgcagNtcNaatgc
NNgNgaattgcgctgcaattcacgagcccNttcatggctgNtaca

heNOS801fr

gggggctgcNaatNagctccgctgcgtggccggatccagtgggggaagctgcaggtgttcgatgcccgggactgcaggtctgcaca
ggaaatgttcacctacatctgcaaccacatcaagtatgccaccaaccggggcaaccttcgctcggccatcacagtgttcccgcagcgct
gccctggccgaggagacttccgaatctggaacagccagctggtgcgctacgcgggctaccggcagcaggacggctctgtgcgggggg
acccagccaacgtggagatcaccgagctctgcattcagcacggctggaccccaggaaacggtcgcttcgacgtgctgcccctgctgct
gcaggccccagatgagcccccagaactcttccttctgcccccgagctggtccttgaggtgcccctggagcaccccacgctggagtggt
ttgcagccctgggcctgcgctggtacgccctcccggcagtgtccaacatgctgctggaaattgggggcctggagttccccgcagccccc
ttcagtggctggtacatgagcactgagatcggcacgaggaacctgtgtgaccctcaccgctacaacatcctggaggatgtggctgtctg
catggacctggatacccggaccacctcgtccctgtggaaagacaaggcagcagtggaaatcaacgtggccgtgctgcacagttacca
gctagccaaagtcaccatcgtggaccaccacgccgccacggcctctttcatgaagcacctgcagaatgagcagaaggccaggggggg
gctgccctgcagactgggcctggatcgtgcccccatctcgggcagcctcactcctgttttccatcaggagatggtcaactatttcctgtcc
ccggccttccgctaccagccagaccctggaaggggagtgccgcaagggcacggcatcacaggaagaagactttaagaagtgcacgc
gtgaNatctccgcctcgctcatggcacggtggcgtagctttgaagNgacaatctgtatgctcgaNacgcggccagagctacgcNag
cagctgggNactctcgagcttgatcccgtcNggtNgatgaatgacNggtcNgaacgaagctggNctgNgtacNcattgaatggg
atccgaatgagctgacgtcctgatgaaaNtcggcctaaccaggtc

heNOS1280fr

gttggaatgctgctggattgggggctggagttcccgcagccccccttcagtggctggtacatgagcactgagaNcNgcacgaggaacc
tgtgtgaccctcaccgctacaacatcctggaggatgtggctgtctgcatggacctggatacccggaccacctcgtccctgtggaaagac
aaggcagcagtggaaatcaacgtggccgtgctgcacagttaccagctagccaaagtcaccatcgtggaccaccacgccgccacggcc
tctttcatgaagcacctggagaatgagcagaaggccaggggggggctgccctgcagactgggcctggatcgtgccccccatctcgggc
agcctcactcctgttttccatcaggagatggtcaactatttcctgtccccggccttccgctaccagccagaccccctggaaggggagtgcc
gccaagggcaccggcatcaccaggaagaagacctttaaagaagtggccaacgccgtgaagatctccgcctcgctcatgggcacggt

ggcgtaagctttgaaggcgacaatcctgtatggctccgagaccggccgggcccagagctacgcacagcagctggggagactcttccg
gaaggcttttgatccccgggtcctgtgtatggatgagtatgacgtggtgtccctcgaacacgagacgctggtgctggtggtaaccagca
catttgggaatggggatcccccggagaatggagagagctttgcagctgccctgatggagatgtccggcccctacaacagctcccctcg
gccggaacagcacaagagttataagatccgcttcaacagcatctcctgctcagacccactggtgtcctcttggcggcggaagaggaag
gagtccagtaacacagacagtgcaggggNcctgNgcaccctcaggttctgtgtgttcgggctcggctccgggcataccccccacttctg
cgcctttgctcgtgccgtgaNNcacggctggaggaactgNgcNgggagcNctgctgcNgctgggccagggNgacgagctgtgcg
ccagagagcttccgagcctgggcccaggctgccttccagcNcctggtgaNacctNNgNgtggaagaNgatgccaagtccNcNc
NcgagaaNNNttcagacccaacNggactggagcgctNagatcgctgacctcagcNgatgcctNaatgctgcagtctgatcNcgt
gccatgcgtaaNNttccNagctNtaaatNtcNgcttacaa

Blast results of heNOSoxyCaM

T7

Score	Expect	Method	Identities	Positives	Gaps	Frame
424 bits(1090)	4e-141	Compositional matrix adjust.	260/263(99%)	260/263(98%)	0/263(0%)	+3

```
Query  129  MGNLKSVAQEpgppcglglglglglcgKQGpatpapepsrapasllppapehsppssplT  308
            MGNLKSVAQEPGPPCGLGLGLGLGLCGKQGPATPAPEPSRAPASLLPPAPEHSPPSSPLT
Sbjct  1    MGNLKSVAQEPGPPCGLGLGLGLGLCGKQGPATPAPEPSRAPASLLPPAPEHSPPSSPLT  60

Query  309  QPPEGPKFPRVKNWEVGSITYDTLSAQAQQDGPCTPRRCLGSLVFPRKLQGRPSPGPPAP  488
            QPPEGPKFPRVKNWEVGSITYDTLSAQAQQDGPCTPRRCLGSLVFPRKLQGRPSPGPPAP
Sbjct  61   QPPEGPKFPRVKNWEVGSITYDTLSAQAQQDGPCTPRRCLGSLVFPRKLQGRPSPGPPAP  120

Query  489  EQLLSQARDFINQYYSSIKRSGSQAHEQRLQEVEAEVAATGTYQLRESELVFGAKQAWRN  668
            EQLLSQARDFINQYYSSIKRSGSQAHEQRLQEVEAEVAATGTYQLRESELVFGAKQAWRN
Sbjct  121  EQLLSQARDFINQYYSSIKRSGSQAHEQRLQEVEAEVAATGTYQLRESELVFGAKQAWRN  180

Query  669  APRCVGRIQWGKLQVFDARDCRSAQEMFTYICNHIKYATNRGNLRSAITVFPQRCPGRGD  848
            APRCVGRIQWGKLQVFDARDCRSAQEMFTYICNHIKYATNRGNLRSAITVFPQRCPGRGD
Sbjct  181  APRCVGRIQWGKLQVFDARDCRSAQEMFTYICNHIKYATNRGNLRSAITVFPQRCPGRGD  240

Query  849  FXIWNSQLVRYAAYRQQDGSXRG  917
            F IWNSQLVRYA YRQQDGS RG
Sbjct  241  FRIWNSQLVRYAGYRQQDGSVRG  263
```

heNOS801fr

Score	Expect	Method	Identities	Positives	Gaps	Frame
508 bits(1309)	4e-173	Compositional matrix adjust.	280/326(86%)	291/326(89%)	4/326(1%)	+1

```
Query  28   GRIQWGKLQVFDARDCRSAQEMFTYICNHIKYATNRGNLRSAITVFPQRCPGRGDFRIWN  207
            GRIQWGKLQVFDARDCRSAQEMFTYICNHIKYATNRGNLRSAITVFPQRCPGRGDFRIWN
Sbjct  186  GRIQWGKLQVFDARDCRSAQEMFTYICNHIKYATNRGNLRSAITVFPQRCPGRGDFRIWN  245

Query  208  SQLVRYAGYRQQDGSVRGDPANVEITELCIQHGWTPGNGRFDVLPLLLQApdeppelfll  387
            SQLVRYAGYRQQDGSVRGDPANVEITELCIQHGWTPGNGRFDVLPLLLQAPDEPPELFLL
```

```
Sbjct  246  SQLVRYAGYRQQDGSVRGDPANVEITELCIQHGWTPGNGRFDVLPLLLQAPDEPPELFLL  305

Query  388  ppelvlevplehptleWFAALGLRWYALPAVSNMLLEIGGLEFPAAPFSGWYMSTEIGTR  567
            PPELVLEVPLEHPTLEWFAALGLRWYALPAVSNMLLEIGGLEFPAAPFSGWYMSTEIGTR
Sbjct  306  PPELVLEVPLEHPTLEWFAALGLRWYALPAVSNMLLEIGGLEFPAAPFSGWYMSTEIGTR  365

Query  568  NLCDPHRYNILEDVAVCMDLDTRTTSSLWKDKAAVEINVAVLHSYQLAKVTIVDHHAATA  747
            NLCDPHRYNILEDVAVCMDLDTRTTSSLWKDKAAVEINVAVLHSYQLAKVTIVDHHAATA
Sbjct  366  NLCDPHRYNILEDVAVCMDLDTRTTSSLWKDKAAVEINVAVLHSYQLAKVTIVDHHAATA  425

Query  748  SFMKHLQNEQKARGGCPADWAWIVPP-SRAASLLFSIRRWSTISCPRPSATSQTLEGECR  924
            SFMKHL+NEQKARGGCPADWAWIVPP S + + +F     +    P          +G
Sbjct  426  SFMKHLENEQKARGGCPADWAWIVPPISGSLTPVFHQEMVNYFLSPAFRYQPDPWKGSAA  485

Query  925  KGTA-SQEEDFKKCTR--XISASLMA  993
            KGT  ++++ FK+      ISASLM
Sbjct  486  KGTGITRKKTFKEVANAVKISASLMG  511
```

heNOS1280fr

Score	Expect	Method	Identities	Positives	Gaps	Frame
616 bits(1588)	0.0	Compositional matrix adjust.	308/340(91%)	310/340(91%)	2/340(0%)	+3

```
Query  45    FSGWYMSTEXXTRNLCDPHRYNILEDVAVCMDLDTRTTSSLWKDKAAVEINVAVLHSYQL  224
            FSGWYMSTE  TRNLCDPHRYNILEDVAVCMDLDTRTTSSLWKDKAAVEINVAVLHSYQL
Sbjct  353   FSGWYMSTEIGTRNLCDPHRYNILEDVAVCMDLDTRTTSSLWKDKAAVEINVAVLHSYQL  412

Query  225   AKVTIVDHHAATASFMKHLENEQKARGGCPADWAWIVPPISGSLTPVFHQEMVNYFLSPA  404
            AKVTIVDHHAATASFMKHLENEQKARGGCPADWAWIVPPISGSLTPVFHQEMVNYFLSPA
Sbjct  413   AKVTIVDHHAATASFMKHLENEQKARGGCPADWAWIVPPISGSLTPVFHQEMVNYFLSPA  472

Query  405   FRYQPDPWKGSAAKGTGITRKKTFKEVANAVKISASLMGTV-A*ALKATILYGSETGRAQ  581
            FRYQPDPWKGSAAKGTGITRKKTFKEVANAVKISASLMGTV A  +KATILYGSETGRAQ
Sbjct  473   FRYQPDPWKGSAAKGTGITRKKTFKEVANAVKISASLMGTVMAKRVKATILYGSETGRAQ  532

Query  582   SYAQQLGRLFRKAFDPRVLCMDEYDVVSLEHETLVLVVTSTFGNGDPPENGESFAAALME  761
            SYAQQLGRLFRKAFDPRVLCMDEYDVVSLEHETLVLVVTSTFGNGDPPENGESFAAALME
Sbjct  533   SYAQQLGRLFRKAFDPRVLCMDEYDVVSLEHETLVLVVTSTFGNGDPPENGESFAAALME  592
```

```
Query  762   MSGPYNSSPRPEQHKSYKIRFNSISCSDPLVSSWRRKRKESSNTDSAGXLXTLRFCVFGL  941
             MSGPYNSSPRPEQHKSYKIRFNSISCSDPLVSSWRRKRKESSNTDSAG L TLRFCVFGL
Sbjct  593   MSGPYNSSPRPEQHKSYKIRFNSISCSDPLVSSWRRKRKESSNTDSAGALGTLRFCVFGL  652

Query  942   GSGHTPTSAPLLVP*XTAGGTXXGA-LLXLGQGDELCARE  1058
             GS   P          T      G  LL LGQGDELC +E
Sbjct  653   GSRAYPHFCAFARAVDTRLEELGGERLLQLGQGDELCGQE  692
```

pCWori-hiNOSoxyCaM – human Δ70 iNOS oxygenase domain with calmodulin-binding region in pCWori

Vector map

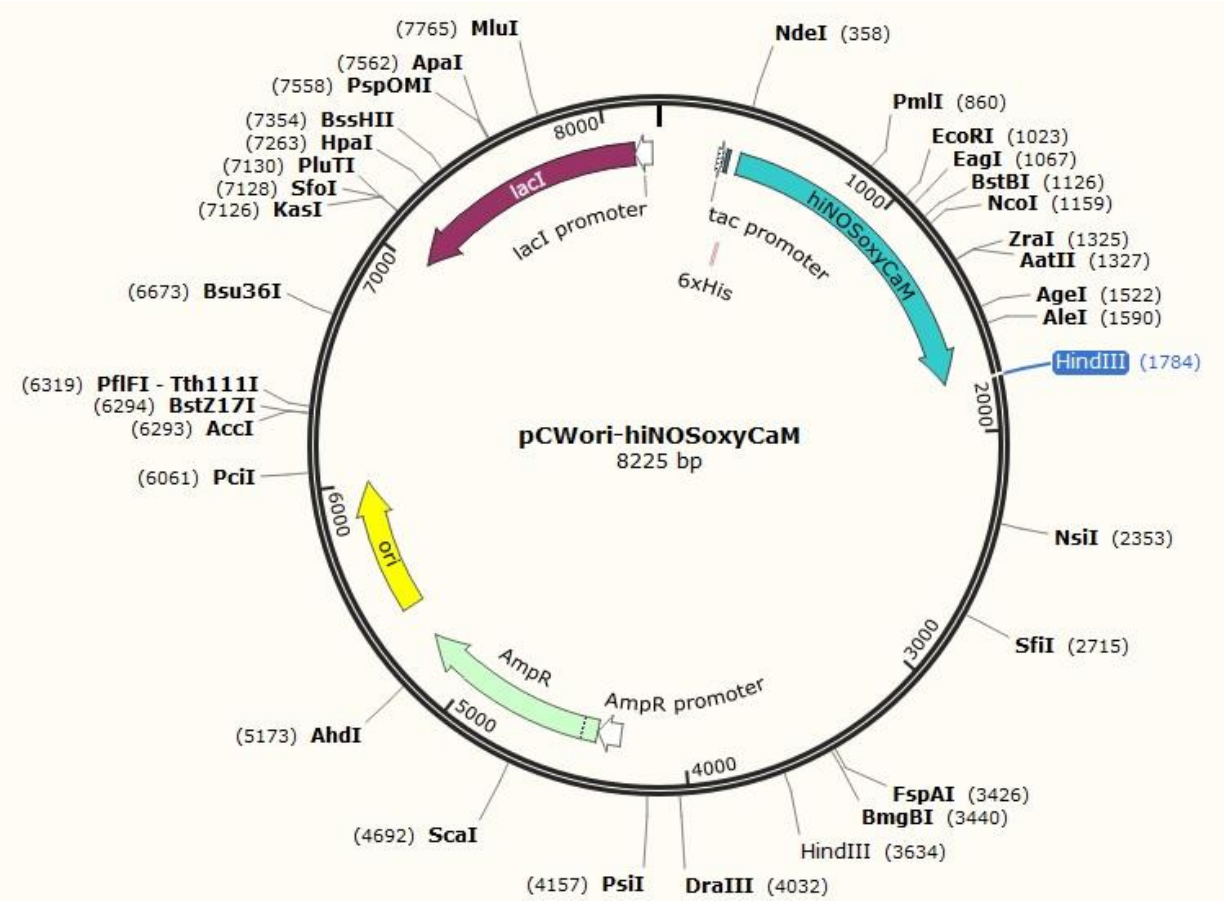

Sequence details of hiNOSoxyCaM

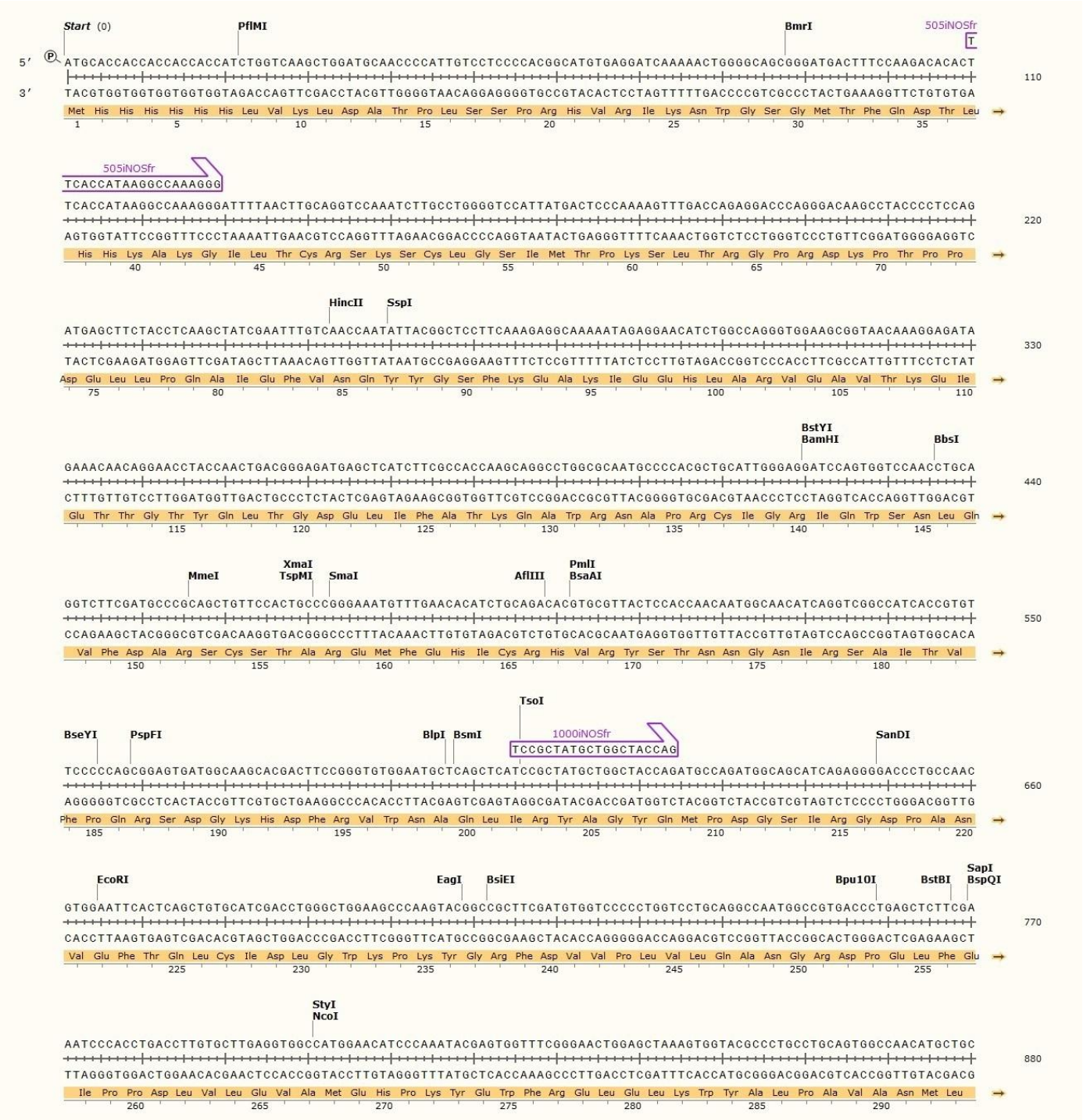

hiNOSoxyCaM (cont'd – 2)

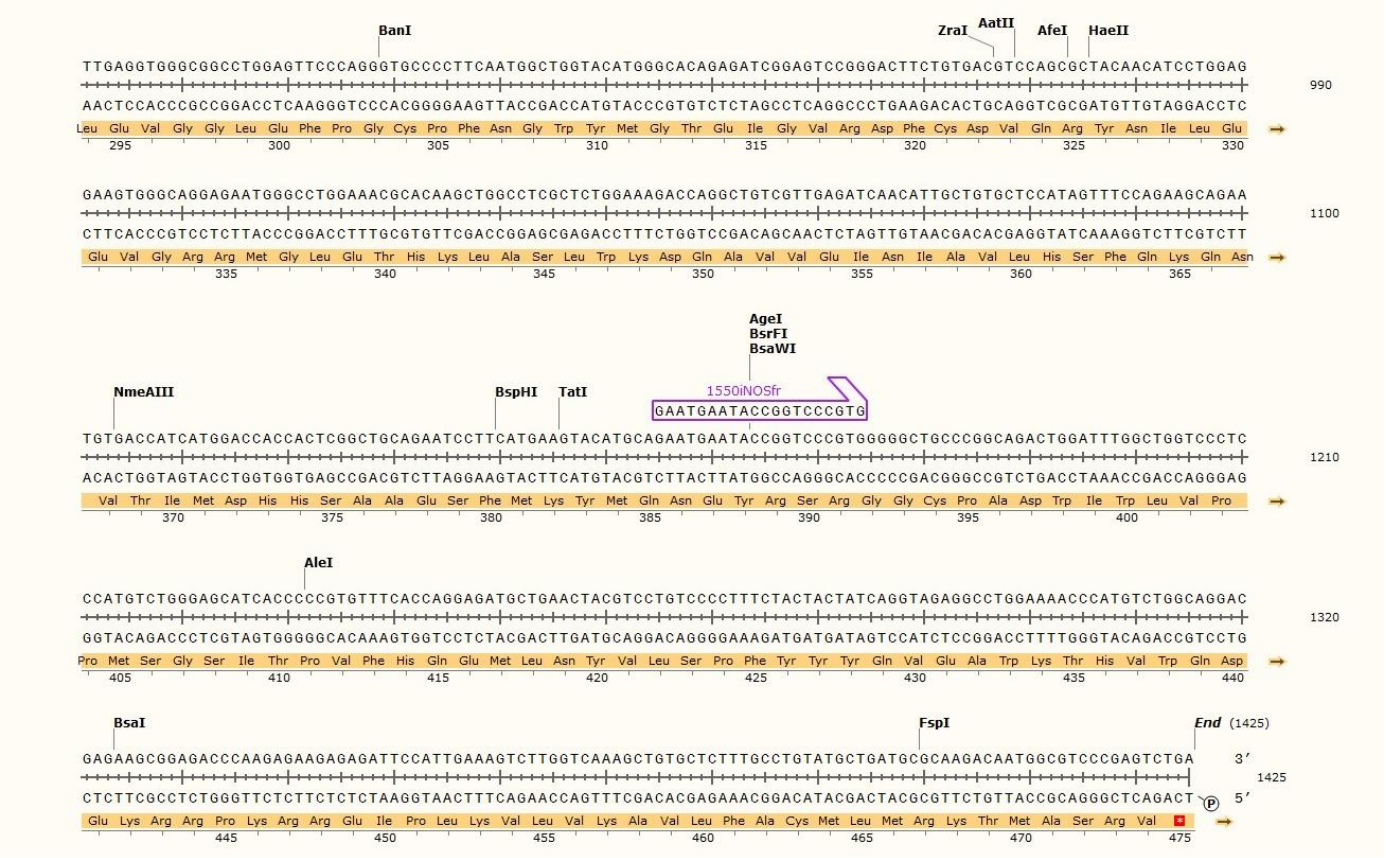

Sequencing summary of hiNOSoxyCaM

DNA section	DNA sequencing	Primer to be used
1 – 165	Incomplete	pCWOri-fr
166 – 1425	Complete	–

No mutation was found in the sequencing results of hiNOSoxyCaM.

Sequencing data of hiNOSoxyCaM

505iNOSfr

aNNggNggNcNatcttgcctggggtcattatgactcccaaaagtttgaccagaggacccagggacaagcctacccctccagatga
gcttctacctcaagctatcgaatttgtcaaccaatattacggctccttcaaagaggcaaaaatagaggaacatctggccagggtggaa
gcggtaacaaaggagatagaaacaacaggaacctaccaactgacgggagatgagctcatcttcgccaccaagcaggcctggcgca
atgccccacgctgcattgggaggatccagtggtccaacctgcaggtcttcgatgcccgcagctgttccactgcccgggaaatgtttgaa
cacatctgcagacacgtgcgttactccaccaacaatggcaacatcaggtcggccatcaccgtgttcccccagcggagtgatggcaagc
acgacttccgggtgtggaatgctcagctcatccgctatgctggctaccagatgccagatggcagcatcagaggggaccctgccaacgt

ggaattcactcagctgtgcatcgacctgggctggaagcccaagtacggccgcttcgatgtggtccccctggtcctgcaggccaatggcc
gtgaccctgagctcttcgaa

1000iNOSfr

atcccacctgaccttgtgcttgaggtggccatggaacatcccaaatacgagtggtttcgggaactggagctaaagtggtacgccctgcc
tgcagtggccaacatgctgcttgaggtgggcggcctggagttcccagggtgccccttcaatggctggtacatgggcacagagatcgga
gtccgggacttctgtgacgtccagcgctacaacatcctggaggaagtgggcaggagaatgggcctggaaacgcacaagctggcctcg
ctctggaaagaccaggctgtcgttgagatcaacattgctgtgctccatagtttccagaagcagaatgtgaccatcatggaccaccactc
ggctgcagaatccttcatgaagtacatgcagaatgaataccggtcccgtgggggctgcccggcagactggatttggctggtccctccc
atgtctgggagc

1550iNOSfr

atcacccccgtgtttcaccaggagatgctgaactacgtcctgtccccttctactactatcaggtagaggcctggaaaacccatgtctgg
caggacgagaagcggagacccaagagaagagagattccattgaaagtcttggtcaaagctgtgctctttgcctgtatgctgatgcgca
agacaatggcgtcccgagtctga

Blast results of hiNOSoxyCaM

505iNOSfr

Score	Expect	Method	Identities	Positives	Gaps	Frame
431 bits(1108)	4e-147	Compositional matrix adjust.	203/204(99%)	203/204(99%)	0/204(0%)	+3

```
Query  21   GVIMTPKSLTRGPRDKPTPPDELLPQAIEFVNQYYGSFKEAKIEEHLARVEAVTKEIETT  200
            G IMTPKSLTRGPRDKPTPPDELLPQAIEFVNQYYGSFKEAKIEEHLARVEAVTKEIETT
Sbjct  117  GSIMTPKSLTRGPRDKPTPPDELLPQAIEFVNQYYGSFKEAKIEEHLARVEAVTKEIETT  176

Query  201  GTYQLTGDELIFATKQAWRNAPRCIGRIQWSNLQVFDARSCSTAREMFEHICRHVRYSTN  380
            GTYQLTGDELIFATKQAWRNAPRCIGRIQWSNLQVFDARSCSTAREMFEHICRHVRYSTN
Sbjct  177  GTYQLTGDELIFATKQAWRNAPRCIGRIQWSNLQVFDARSCSTAREMFEHICRHVRYSTN  236

Query  381  NGNIRSAITVFPQRSDGKHDFRVWNAQLIRYAGYQMPDGSIRGDPANVEFTQLCIDLGWK  560
            NGNIRSAITVFPQRSDGKHDFRVWNAQLIRYAGYQMPDGSIRGDPANVEFTQLCIDLGWK
Sbjct  237  NGNIRSAITVFPQRSDGKHDFRVWNAQLIRYAGYQMPDGSIRGDPANVEFTQLCIDLGWK  296

Query  561  PKYGRFDVVPLVLQANGRDPELFE  632
            PKYGRFDVVPLVLQANGRDPELFE
Sbjct  297  PKYGRFDVVPLVLQANGRDPELFE  320
```

1000iNOSfr

Score	Expect	Method	Identities	Positives	Gaps	Frame
325 bits(832)	4e-108	Compositional matrix adjust.	151/151(100%)	151/151(100%)	0/151(0%)	+1

```
Query  1    IPPDLVLEVAMEHPKYEWFRELELKWYALPAVANMLLEVGGLEFPGCPFNGWYMGTEIGV  180
            IPPDLVLEVAMEHPKYEWFRELELKWYALPAVANMLLEVGGLEFPGCPFNGWYMGTEIGV
Sbjct  321  IPPDLVLEVAMEHPKYEWFRELELKWYALPAVANMLLEVGGLEFPGCPFNGWYMGTEIGV  380

Query  181  RDFCDVQRYNILEEVGRRMGLETHKLASLWKDQAVVEINIAVLHSFQKQNVTIMDHHSAA  360
            RDFCDVQRYNILEEVGRRMGLETHKLASLWKDQAVVEINIAVLHSFQKQNVTIMDHHSAA
Sbjct  381  RDFCDVQRYNILEEVGRRMGLETHKLASLWKDQAVVEINIAVLHSFQKQNVTIMDHHSAA  440

Query  361  ESFMKYMQNEYRSRGGCPADWIWLVPPMSGS  453
            ESFMKYMQNEYRSRGGCPADWIWLVPPMSGS
```

```
Sbjct  441  ESFMKYMQNEYRSRGGCPADWIWLVPPMSGS  471
```

1550iNOSfr

Score	Expect	Method	Identities	Positives	Gaps	Frame
140 bits(354)	7e-44	Compositional matrix adjust.	66/66(100%)	66/66(100%)	0/66(0%)	+1

```
Query  1    ITPVFHQEMLNYVLSPFYYYQVEAWKTHVWQDEKRRPKRREIPLKVLVKAVLFACMLMRK  180
            ITPVFHQEMLNYVLSPFYYYQVEAWKTHVWQDEKRRPKRREIPLKVLVKAVLFACMLMRK
Sbjct  472  ITPVFHQEMLNYVLSPFYYYQVEAWKTHVWQDEKRRPKRREIPLKVLVKAVLFACMLMRK  531

Query  181  TMASRV  198
            TMASRV
Sbjct  532  TMASRV  537
```

phnNOS – human full-length nNOS in pDS-78

Vector map

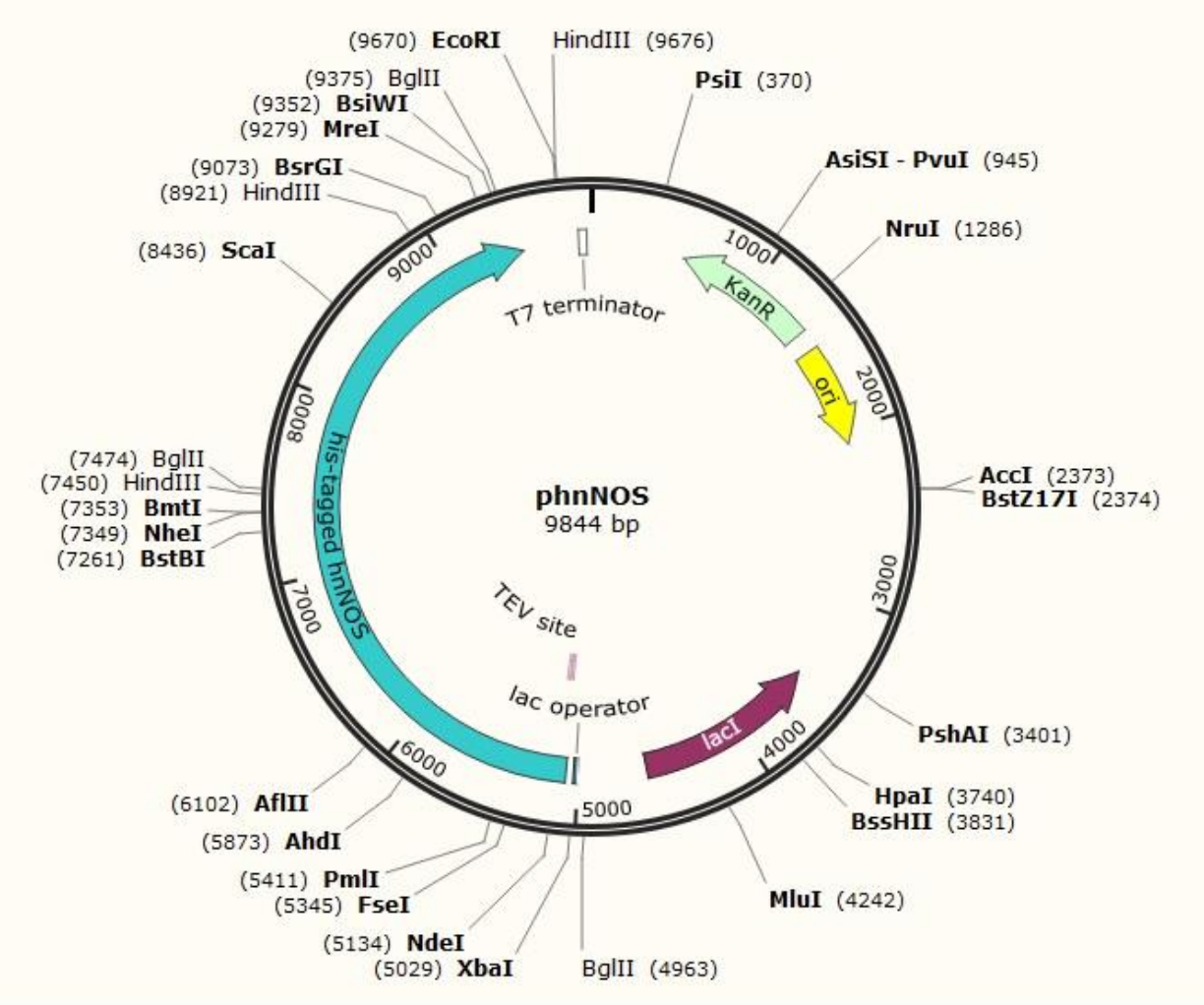

Sequence details of hnNOS

hnNOS (cont'd – 2)

hnNOS (cont'd – 3)

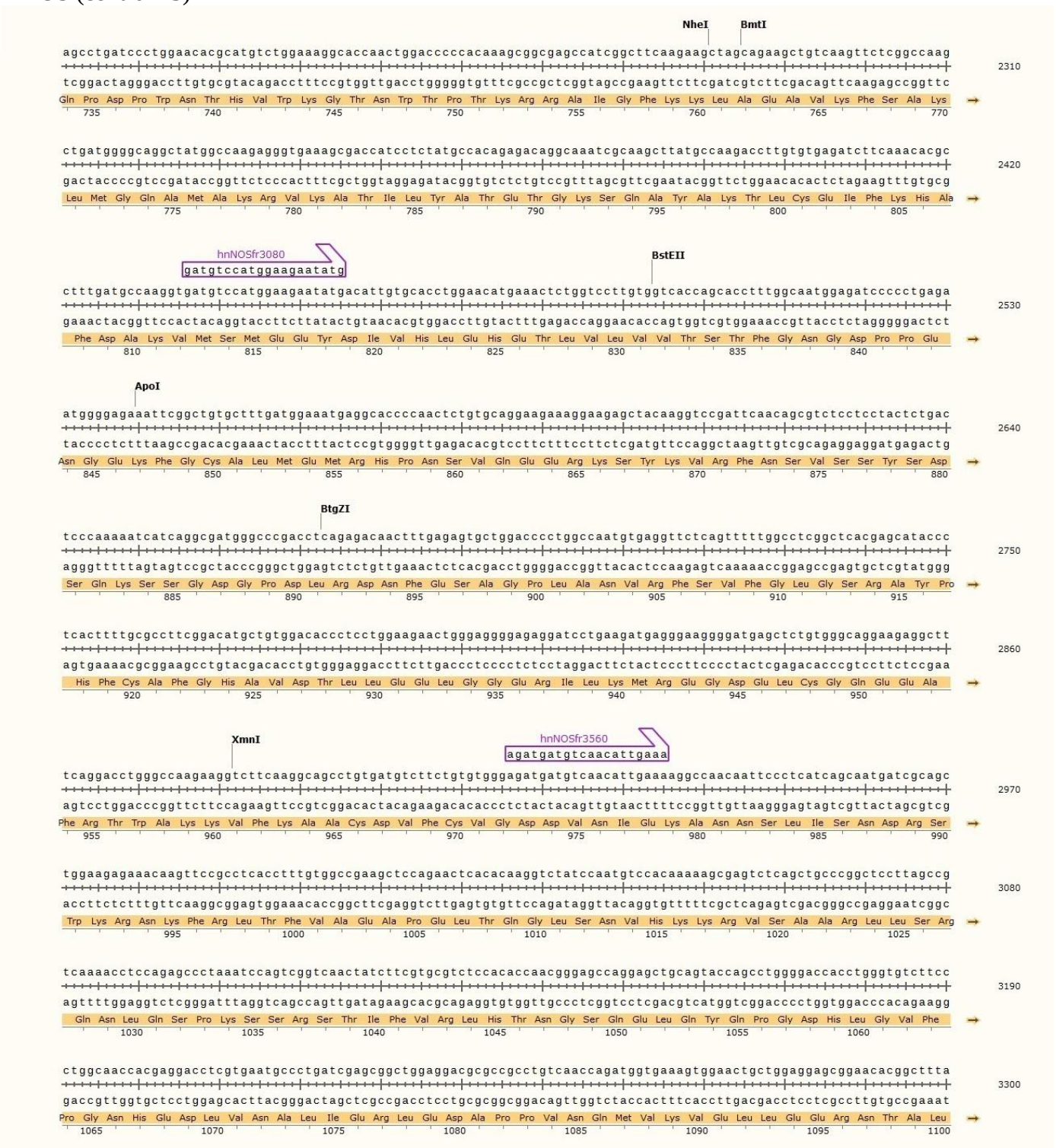

hnNOS (cont'd – 4)

hnNOS (cont'd – 5)

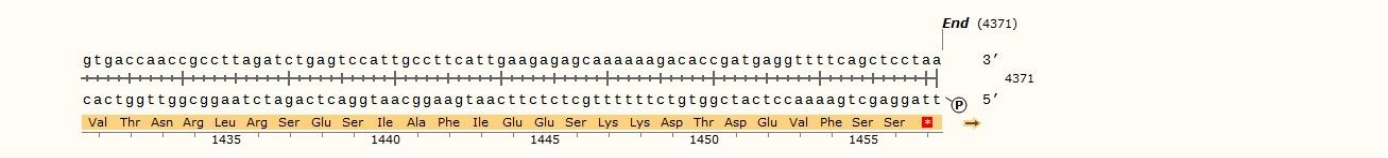

Sequencing summary of hnNOS

DNA section	DNA sequencing	Primer to be used
1 – 2391	Complete	–
2392 – 2562	Incomplete	hnNOSfr2600
2563 – 4371	Complete	–

Mutations found in hnNOS

DNA position	Mutation	Amino acid change	Amino acid position
1813	G → C	Glu → Gln	583
2242	G → T	Gly → Trp	726
1567	G → A	Gly → Arg	1355

Sequencing data of hnNOS

T7

ggggNacattcccgtctagaataattttgtttaactttaagaaggagatataccatgggcagcagccatcatcatcatcacagca
gcggcagagaaaacttgtatttccagggccatatggaggatcacatgttcggtgttcagcaaatccagcccaatgtcatttctgttcgtc
tcttcaagcgcaaagttgggggcctgggatttctggtgaaggagcgggtcagtaagccgcccgtgatcatctctgacctgattcgtggg
ggcgccgcagagcagagtggcctcatccaggccggagacatcattcttgcggtcaacggccggcccttggtggacctgagctatgaca
gcgccctggaggtactcagaggcattgcctctgagacccacgtggtcctcattctgaggggccctgaaggtttcaccacgcacctggag
accacctttacaggtgatgggacccccaagaccatccgggtgacacagcccctgggtccccccaccaaagccgtggatctgtcccacc
agccaccggccggcaaagaacagcccctggcagtggatggggcctcgggtcccgggaatgggcctcagcatgcctacgatgatggg
caggaggctggctcactcccccatgccaacggcctggcccccaggcccccaggccaggaccccgcgaagaaagcaaccagagtcag
cctccaaggcagaggggagaacaatgaactgctcaaggagatagagcctgtgctgagccttctcaccagtgggagcagaggggtca
agggaggggcacctgccaaggcagagatgaaagatatgggaatccaggtggacagagatttggacggcaagtcacacaaacctct
gcccctcggcgtggagaacgaccgagtcttcaatgacctatgggggaagggcaatgtgcctgtcgtcctcaacaacccatattcagag
aaggagcagcccccacctcaggaaaacagtcccccacaaagaatggcagcccctcagtgtcacgcttctcaaggtcagaactggga
gactgagtgtctcactgacaNcctccacttagagcacatgaaacgggatgcactgagtacatctgcatggctcatcatgcatctcNag
catgcagagctgagacgtccgNNaaagaNgctctcctctcNcaaNagtaatgatcatcNttcatcataagattgaNcagccatgg
caagctgaaaggggacaNgatNgatcNtagacttNcggctcagg

nNOS1381

gagaaggagcagccccccacctcaggaaaacagtcccccacaaagaatggcagcccctccaagtgtccacgcttcctcaag

hnNOSfr1600

aNgtagcgtcacgcttctcaggtcaagaactgggagactgaggtggttctcactgacaccctccaccttaagagcacattggaaacgg
gatgcactgagtacatctgcatgggctccatcatgcatccttctcagcatgcaaggaggcctgaagacgtccgcacaaaaggacagct
cttccctctcgccaaagagtttattgatcaatactattcatcaattaaaagatttggctccaaagcccacatggaaaggctggaagagg
tgaacaaagagatcgacaccactagcacttaccagctcaaggacacagagctcatctatggggccaagcacgcctggcggaatgcct
cgcgctgtgtgggcaggatccagtggtccaagctgcaggtattcgatgcccgtgactgcaccacggcccacgggatgttcaactacat
ctgtaaccatgtcaagtatgccaccaacaaagggaacctcaggtctgccatcaccatattcccccagaggacagacggcaagcacga
cttccgagtctggaactcccagctcatccgctatgctggctacaagcagcctgacggctccaccctgggggacccagccaatgtgcagt
tcacagagatatgcatacagcagggctggaaaccgcctagaggccgcttcgatgtcctgccgctcctgcttcaggccaacggcaatga
ccctgagctcttccagattcctccagagctggtgttggaagttcccatcaggcacccccaagtttgagtggttcaaggacctggggctga
agtggtacggcctccccgccgtgtccaacatgctcctagagattggcggcctgcagttcagcgcctgtcccttcagtggctggtacatgg
gcacagagattggtgtccgcgactactgtgacaactcccgctacaatatcctggaggaagtggccaagaagatgaacttagacatga
gg

hnNOSfr2100

tNggatNtgcatcaccatattcccccagaggacagacggcaagcacgacttccgagtctggaactcccagctcatccgctatgctggc
tacaagcagcctgacggctccaccctgggggacccagccaatgtgcagttcacagagatatgcatacagcagggctggaaaccgcct
agaggccgcttcgatgtcctgccgctcctgcttcaggccaacggcaatgaccctgagctcttccagattcctccagagctggtgttgga
agttcccatcaggcacccccaagtttgagtggttcaaggacctggggctgaagtggtacggcctccccgccgtgtccaacatgctcctag
agattggcggcctggagttcagcgcctgtcccttcagtggctggtacatgggcacagagattggtgtccgcgactactgtgacaactcc
cgctacaatatcctggaggaagtggccaagaagatgaacttagacatgaggaagacgtcctccctgtggaaggaccaggcgctggtg
gagatcaatatcgcggttctctatagcttccagagtgacaaagtgaccattgttgaccatcactccgccaccgagtccttcattaagcac
atggagaatgagtaccgctgccgggggggctgccctgccgactgggtgtggatcgtgccccccatgtccggaagcatcacccctgtgt
tccaccaggagatgctcaactaccggctcacccccctccttcgaataccagcctgatccctggaacacgcatgtctggaaaggcaccaa
ctggacccccacaaagcggcgagccatcggcttcaagaagctagcagaagctgtcaagttctcggccaagctgatggggcaggctat
ggccaagagggtgaaagcgaccatcctctatgccacagagacaggcaaatcgcaagcttatgccagaccttgtgtgagatcttcaac
acgcctttgatgcaaggtgatgtcatggagatatgacattgtgcactggacatgaactctggtcctgtgtcacagcactttgcatgagat
ccctgagatggagatcgctgtgcttgatgaatgagcacccactctgtgcagagagagagctacagtcgatcacaggtctctctatNtg
actcgaaatctcagcatgcgaacNtaaNacactgagagtgctgacccNtgcaNgtagg

hnNOSfr3080

aggNNggNgtatggaactNtggtccNtgtggtcacNagNaccttNggcNatggagagcccNctgagaatggggagaaattcg
gctgNgctttgatggNaatgaggcaccccaactctgtgcaggaagaaaggaagagctacaaggtccgattcaacagcgtctcctcct
actctgactcccaaaaatcatcaggcgatgggcccgacctcagagacaactttgagagtgctggacccctggccaatgtgaggttctc
agtttttggcctcggctcacgagcataccctcacttttgcgccttcggacatgctgtggacaccctcctggaagaactgggaggggaga
ggatcctgaagatgagggaaggggatgagctctgtgggcaggaagaggctttcaggacctgggccaagaaggtcttcaaggcagcc
tgtgatgtcttctgtgtgggagatgatgtcaacattgaaaaggccaacaattccctcatcagcaatgatcgcagctggaagagaaaca
agttccgcctcacctttgtggccgaagctccagaactcacacaaggtctatccaatgtccacaaaaagcgagtctcagctgcccggctc
cttagccgtcaaaacctccagagccctaaatccagtcggtcaactatcttcgtgcgtctccacaccaacgggagccaggagctgcagt
accagcctggggaccacctgggtgtcttccctggcaaccacgaggacctcgtgaatgccctgatcgagcggctggaggacgcgccgc
ctgtcaaccagatggtgaaagtggaactgctggaggagcggaacacggctttaggtgtcatcagtaactggacagatgagctccgcc

tcccgccctgcaccatcttccaggccttcaagtactacctggacatcaccacgccaccaacgcctctgcagctgcagcagtttgcctccc
tagctaccagcgagaaggagaagcagcgtctgctggtcctcagcaagggtttgcaggagtacgaggaatggaaatggggcaagaac
ccc

hnNOSfr3560

accatcgtggaggtgctggaggagttcccatctatccagatgccggccaccctgctcctgacccagctgtccctgctgcagccccgcta
ctattccatcagctcctccccagacatgtaccctgatgaagtgcacctcactgtggccatcgtttcctaccgcactcgagatggagaagg
accaattcaccacggcgtatgctcctcctggctcaaccggatacaggctgacgaactggtcccctgtttcgtgagaggagcacccagct
tccacctg

hnNOSfr4040

ccccggaacccccaagtcccctgcatcctcgttggaccaggcaccggcattgccccttccgaagcttctggcaacagcggcaatttga
tatccaacacaaaggaatgaacccctgccccatggtcctggtcttcgggtgccggcaatccaagatagatcatatctacagggaagag
accctgcaggccaagaacaaggggtcttcagagagctgtacacggcttactcccgggagccagacaaaccaaagaagtacgtgca
ggacatcctgcaggagcagctggcggagtctgtgtaccgagccctgaaggagcaaggggccacatatacgtctgtagggacgtcac
catggctgctgatgtcctcaaagccatccagcgcatcatgacccagcaggggaagctctcggcagaggacgccggcgtattcatc

hnNOSfr4540

gNNNNNgggNgggcatccagatagatcatatctacagggaagagaccctgcaggccaagaacaaggggtcttcagagagctg
tacacggcttactcccgggagccagacaaaccaaagaagtacgtgcaggacatcctgcaggagcagctggcggagtctgtgtaccga
gccctgaaggagcaaggggccacatatacgtctgtagggacgtcaccatggctgctgatgtcctcaaagccatccagcgcatcatga
cccagcaggggaagctctcggcagaggacgccggcgtattcatcagccggatgagggatgacaaccgataccatgaggatatttttg
gagtcaccctgcgaacgtacgaagtgaccaaccgccttagatctgagtccattgccttcattgaagagagcaaaaaagacaccgatg
aggttttcagctcctaatatggaagaagatcgtaagctgctgatccaggcggctatcgtgcgcattatgaaaatgcgcaaggttctgaa
acaccaacagctgctgggtgaggtcctgacccagctgagcagccgttttaagccgcgtgtcccggttatcaaaaagtgcatcgatattc
tgattgaaaaagaatacctggagcgcgtggacggcgaaaaagatacctactcgtacctggcataataggaattcaagcttctcgagc
accaccaccaccaccactgagatccggctgctaacaaagcccgaaaggaagctgagttggctgctgccaccgctgagcaataactag
cataaccccttggggcctctaaacgggtcttgaggggttttttgctgaaaggaggaactatatccggattggcgaatgggacgcgccct
gtagcggcgcattaagcgcggcgggtgtggtggttacgcgcagcgtgaccgctacacttgccagcgccctagcgcccgctcctttcgct
ttcttcccttcctttctcgccacgttcgcggctttcccgtcaagctctaatcggggctccctttagggttccgattagtgcttacggcactcg
acccaaaactgataggtgatgctcacgtagNggcatcgcctgaNgacgtttcgcttgacgtgagtcNgttcttatagNgactcttgtc
actgacaNctcagcNNNcgctatcttgattaagaattgcgatcgcatgctaaatgcgtatacaNttaNgaattacaattaggct

Blast results of hnNOS

T7

Score	Expect	Method	Identities	Positives	Gaps	Frame
579 bits(1493)	0.0	Compositional matrix adjust.	308/352(88%)	316/352(89%)	8/352(2%)	+1

```
Query  121   MEDHMFGVQQIQPNVISVRLFKRKVGGLGFLVKERVSKPPVIISDLIRGGAAEQSGLIQA  300
             MEDHMFGVQQIQPNVISVRLFKRKVGGLGFLVKERVSKPPVIISDLIRGGAAEQSGLIQA
Sbjct  1     MEDHMFGVQQIQPNVISVRLFKRKVGGLGFLVKERVSKPPVIISDLIRGGAAEQSGLIQA  60

Query  301   GDIILAVNGRPLVDLSYDSALEVLRGIASETHVVLILRGPEGFTTHLETTFTGDGTPKTI  480
             GDIILAVNGRPLVDLSYDSALEVLRGIASETHVVLILRGPEGFTTHLETTFTGDGTPKTI
Sbjct  61    GDIILAVNGRPLVDLSYDSALEVLRGIASETHVVLILRGPEGFTTHLETTFTGDGTPKTI  120

Query  481   RVTQPLGPPTKAVDLSHQPPAGKEQPLAVDGASGPGNGPQHAYDDGQEAGSLPHANGLAP  660
             RVTQPLGPPTKAVDLSHQPPAGKEQPLAVDGASGPGNGPQHAYDDGQEAGSLPHANGLAP
Sbjct  121   RVTQPLGPPTKAVDLSHQPPAGKEQPLAVDGASGPGNGPQHAYDDGQEAGSLPHANGLAP  180

Query  661   RPPGQDPAKKATRVSLQGRGENNELLKEIEPVLSLLTSGSRGVKGGAPAKAEMKDMGIQV  840
             RPPGQDPAKKATRVSLQGRGENNELLKEIEPVLSLLTSGSRGVKGGAPAKAEMKDMGIQV
Sbjct  181   RPPGQDPAKKATRVSLQGRGENNELLKEIEPVLSLLTSGSRGVKGGAPAKAEMKDMGIQV  240

Query  841   DRDLDGKSHKPLPLGVENDRVFNDLWGKGNVPVVLNNPYSekeqpppqensppqRMAAP-  1017
             DRDLDGKSHKPLPLGVENDRVFNDLWGKGNVPVVLNNPYSEKEQPP      P +  +P
Sbjct  241   DRDLDGKSHKPLPLGVENDRVFNDLWGKGNVPVVLNNPYSEKEQPPTSGKQSPTKNGSPS  300

Query  1018  QC-HASQGQNWETE-CLTDXLHLEHMKRDALSTSAWL--IMH-LXHAELRRP  1158
             +C    + +NWETE  LTD LHL+       +    +  IMH   HA  RRP
Sbjct  301   KCPRFLKVKNWETEVVLTDTLHLKSTLETGCTEYICMGSIMHPSQHA--RRP  350
```

nNOS1381

Score	Expect	Method	Identities	Positives	Gaps	Frame
58.2 bits(139)	2e-15	Compositional matrix adjust.	27/27(100%)	27/27(100%)	0/27(0%)	+1

```
Query  1    EKEQPPTSGKQSPTKNGSPSKCPRFLK  81
            EKEQPPTSGKQSPTKNGSPSKCPRFLK
Sbjct  281  EKEQPPTSGKQSPTKNGSPSKCPRFLK  307
```

hnNOSfr1600

Score	Expect	Method	Identities	Positives	Gaps	Frame
678 bits(1750)	0.0	Compositional matrix adjust.	316/318(99%)	318/318(100%)	0/318(0%)	+1

```
Query  19   QVKNWETEVVLTDTLHLKSTLETGCTEYICMGSIMHPSQHARRPEDVRTKGQLFPLAKEF  198
            +VKNWETEVVLTDTLHLKSTLETGCTEYICMGSIMHPSQHARRPEDVRTKGQLFPLAKEF
Sbjct  307  KVKNWETEVVLTDTLHLKSTLETGCTEYICMGSIMHPSQHARRPEDVRTKGQLFPLAKEF  366

Query  199  IDQYYSSIKRFGSKAHMERLEEVNKEIDTTSTYQLKDTELIYGAKHAWRNASRCVGRIQW  378
            IDQYYSSIKRFGSKAHMERLEEVNKEIDTTSTYQLKDTELIYGAKHAWRNASRCVGRIQW
Sbjct  367  IDQYYSSIKRFGSKAHMERLEEVNKEIDTTSTYQLKDTELIYGAKHAWRNASRCVGRIQW  426

Query  379  SKLQVFDARDCTTAHGMFNYICNHVKYATNKGNLRSAITIFPQRTDGKHDFRVWNSQLIR  558
            SKLQVFDARDCTTAHGMFNYICNHVKYATNKGNLRSAITIFPQRTDGKHDFRVWNSQLIR
Sbjct  427  SKLQVFDARDCTTAHGMFNYICNHVKYATNKGNLRSAITIFPQRTDGKHDFRVWNSQLIR  486

Query  559  YAGYKQPDGSTLGDPANVQFTEICIQQGWKPPRGRFDVLPLLLQANGNDPELFQIPPELV  738
            YAGYKQPDGSTLGDPANVQFTEICIQQGWKPPRGRFDVLPLLLQANGNDPELFQIPPELV
Sbjct  487  YAGYKQPDGSTLGDPANVQFTEICIQQGWKPPRGRFDVLPLLLQANGNDPELFQIPPELV  546

Query  739  LEVPIRHPKFEWFKDLGLKWYGLPAVSNMLLEIGGLQFSACPFSGWYMGTEIGVRDYCDN  918
            LEVPIRHPKFEWFKDLGLKWYGLPAVSNMLLEIGGL+FSACPFSGWYMGTEIGVRDYCDN
Sbjct  547  LEVPIRHPKFEWFKDLGLKWYGLPAVSNMLLEIGGLEFSACPFSGWYMGTEIGVRDYCDN  606

Query  919  SRYNILEEVAKKMNLDMR  972
            SRYNILEEVAKKMNLDMR
Sbjct  607  SRYNILEEVAKKMNLDMR  624
```

hnNOSfr2100

Score	Expect	Method	Identities	Positives	Gaps	Frame
669 bits(1727)	0.0	Compositional matrix adjust.	325/350(93%)	326/350(93%)	8/350(2%)	+2

```
Query  8     CITIFPQRTDGKHDFRVWNSQLIRYAGYKQPDGSTLGDPANVQFTEICIQQGWKPPRGRF  187
             ITIFPQRTDGKHDFRVWNSQLIRYAGYKQPDGSTLGDPANVQFTEICIQQGWKPPRGRF
Sbjct  463   AITIFPQRTDGKHDFRVWNSQLIRYAGYKQPDGSTLGDPANVQFTEICIQQGWKPPRGRF  522

Query  188   DVLPLLLQANGNDPELFQIPPELVLEVPIRHPKFEWFKDLGLKWYGLPAVSNMLLEIGGL  367
             DVLPLLLQANGNDPELFQIPPELVLEVPIRHPKFEWFKDLGLKWYGLPAVSNMLLEIGGL
Sbjct  523   DVLPLLLQANGNDPELFQIPPELVLEVPIRHPKFEWFKDLGLKWYGLPAVSNMLLEIGGL  582

Query  368   EFSACPFSGWYMGTEIGVRDYCDNSRYNILEEVAKKMNLDMRKTSSLWKDQALVEINIAV  547
             EFSACPFSGWYMGTEIGVRDYCDNSRYNILEEVAKKMNLDMRKTSSLWKDQALVEINIAV
Sbjct  583   EFSACPFSGWYMGTEIGVRDYCDNSRYNILEEVAKKMNLDMRKTSSLWKDQALVEINIAV  642

Query  548   LYSFQSDKVTIVDHHSATESFIKHMENEYRCRGGCPADWVWIVPPMSGSITPVFHQEMLN  727
             LYSFQSDKVTIVDHHSATESFIKHMENEYRCRGGCPADWVWIVPPMSGSITPVFHQEMLN
Sbjct  643   LYSFQSDKVTIVDHHSATESFIKHMENEYRCRGGCPADWVWIVPPMSGSITPVFHQEMLN  702

Query  728   YRLTPSFEYQPDPWNTHVWKGTNWTPTKRRAIGFKKLAEAVKFSAKLMGQAMAKRVKATI  907
             YRLTPSFEYQPDPWNTHVWKGTN TPTKRRAIGFKKLAEAVKFSAKLMGQAMAKRVKATI
Sbjct  703   YRLTPSFEYQPDPWNTHVWKGTNGTPTKRRAIGFKKLAEAVKFSAKLMGQAMAKRVKATI  762

Query  908   LYATETGKSQAYARP-CVRSSTRL*CKVMSW-RYDIVHWT*TLVLCHSTL  1051
             LYATETGKSQAYA+  C         KVMS   YDIVH      L H TL
Sbjct  763   LYATETGKSQAYAKTLCEIFKHAFDAKVMSMEEYDIVH------LEHETL  806
```

hnNOSfr3080

Score	Expect	Method	Identities	Positives	Gaps	Frame
499 bits(1284)	7e-170	Compositional matrix adjust.	240/240(100%)	240/240(100%)	0/240(0%)	+1

```
Query  1     ELGGERILKMREGDELCGQEEAFRTWAKKVFKAACDVFCVGDDVNIEKANNSLISNDRSW  180
             ELGGERILKMREGDELCGQEEAFRTWAKKVFKAACDVFCVGDDVNIEKANNSLISNDRSW
Sbjct  910   ELGGERILKMREGDELCGQEEAFRTWAKKVFKAACDVFCVGDDVNIEKANNSLISNDRSW  969
```

```
Query  181   KRNKFRLTFVAEAPELTQGLSNVHKKRVSAARLLSRQNLQSPKSSRSTIFVRLHTNGSQE  360
             KRNKFRLTFVAEAPELTQGLSNVHKKRVSAARLLSRQNLQSPKSSRSTIFVRLHTNGSQE
Sbjct  970   KRNKFRLTFVAEAPELTQGLSNVHKKRVSAARLLSRQNLQSPKSSRSTIFVRLHTNGSQE  1029

Query  361   LQYQPGDHLGVFPGNHEDLVNALIERLEDAPPVNQMVKVELLEERNTALGVISNWTDELR  540
             LQYQPGDHLGVFPGNHEDLVNALIERLEDAPPVNQMVKVELLEERNTALGVISNWTDELR
Sbjct  1030  LQYQPGDHLGVFPGNHEDLVNALIERLEDAPPVNQMVKVELLEERNTALGVISNWTDELR  1089

Query  541   LPPCTIFQAFKYYLDITTPPTPLQLQQFASLATSEKEKQRLLVLSKGLQEYEEWKWGKNP  720
             LPPCTIFQAFKYYLDITTPPTPLQLQQFASLATSEKEKQRLLVLSKGLQEYEEWKWGKNP
Sbjct  1090  LPPCTIFQAFKYYLDITTPPTPLQLQQFASLATSEKEKQRLLVLSKGLQEYEEWKWGKNP  1149
```

hnNOSfr3560

Score	Expect	Method	Identities	Positives	Gaps	Frame
172 bits(437)	2e-54	Composition-based stats.	92/92(100%)	92/92(100%)	0/92(0%)	+1

```
Query  1     TIVEVLEEFPSIQMPAtllltqlsllqPRYYSISSSPDMYPDEVHLTVAIVSYRTRDGEG  180
             TIVEVLEEFPSIQMPATLLLTQLSLLQPRYYSISSSPDMYPDEVHLTVAIVSYRTRDGEG
Sbjct  1150  TIVEVLEEFPSIQMPATLLLTQLSLLQPRYYSISSSPDMYPDEVHLTVAIVSYRTRDGEG  1209

Query  181   PIHHGVCSSWLNRIQADELVPCFVRGAPSFHL  276
             PIHHGVCSSWLNRIQADELVPCFVRGAPSFHL
Sbjct  1210  PIHHGVCSSWLNRIQADELVPCFVRGAPSFHL  1241
```

hnNOSfr4040

Score	Expect	Method	Identities	Positives	Gaps	Frame
304 bits(779)	3e-100	Compositional matrix adjust.	144/145(99%)	144/145(99%)	0/145(0%)	+1

```
Query  1     PRNPQVPCILVGPGTGIAPFRSFWQQRQFDIQHKGMNPCPMVLVFGCRQSKIDHIYREET  180
             PRNPQVPCILVGPGTGIAPFRSFWQQRQFDIQHKGMNPCPMVLVFGCRQSKIDHIYREET
Sbjct  1242  PRNPQVPCILVGPGTGIAPFRSFWQQRQFDIQHKGMNPCPMVLVFGCRQSKIDHIYREET  1301

Query  181   LQAKNKGVFRELYTAYSREPDKPKKYVQDILQEQLAESVYRALKEQGGHIYVCRDVTMAA  360
             LQAKNKGVFRELYTAYSREPDKPKKYVQDILQEQLAESVYRALKEQGGHIYVC DVTMAA
Sbjct  1302  LQAKNKGVFRELYTAYSREPDKPKKYVQDILQEQLAESVYRALKEQGGHIYVCGDVTMAA  1361
```

```
Query  361   DVLKAIQRIMTQQGKLSAEDAGVFI  435
             DVLKAIQRIMTQQGKLSAEDAGVFI
Sbjct  1362  DVLKAIQRIMTQQGKLSAEDAGVFI  1386
```

hnNOSfr4540

Score	Expect	Method	Identities	Positives	Gaps	Frame
291 bits(746)	2e-91	Composition-based stats.	141/143(99%)	142/143(99%)	0/143(0%)	+3

```
Query  18    QIDHIYREETLQAKNKGVFRELYTAYSREPDKPKKYVQDILQEQLAESVYRALKEQGGHI  197
             +IDHIYREETLQAKNKGVFRELYTAYSREPDKPKKYVQDILQEQLAESVYRALKEQGGHI
Sbjct  1292  KIDHIYREETLQAKNKGVFRELYTAYSREPDKPKKYVQDILQEQLAESVYRALKEQGGHI  1351

Query  198   YVCRDVTMAADVLKAIQRIMTQQGKLSAEDAGVFISRMRDDNRYHEDIFGVTLRTYEVTN  377
             YVC DVTMAADVLKAIQRIMTQQGKLSAEDAGVFISRMRDDNRYHEDIFGVTLRTYEVTN
Sbjct  1352  YVCGDVTMAADVLKAIQRIMTQQGKLSAEDAGVFISRMRDDNRYHEDIFGVTLRTYEVTN  1411

Query  378   RLRSESIAFIEESKKDTDEVFSS  446
             RLRSESIAFIEESKKDTDEVFSS
Sbjct  1412  RLRSESIAFIEESKKDTDEVFSS  1434
```

pheNOS – human full-length eNOS in pDS-78

Vector map

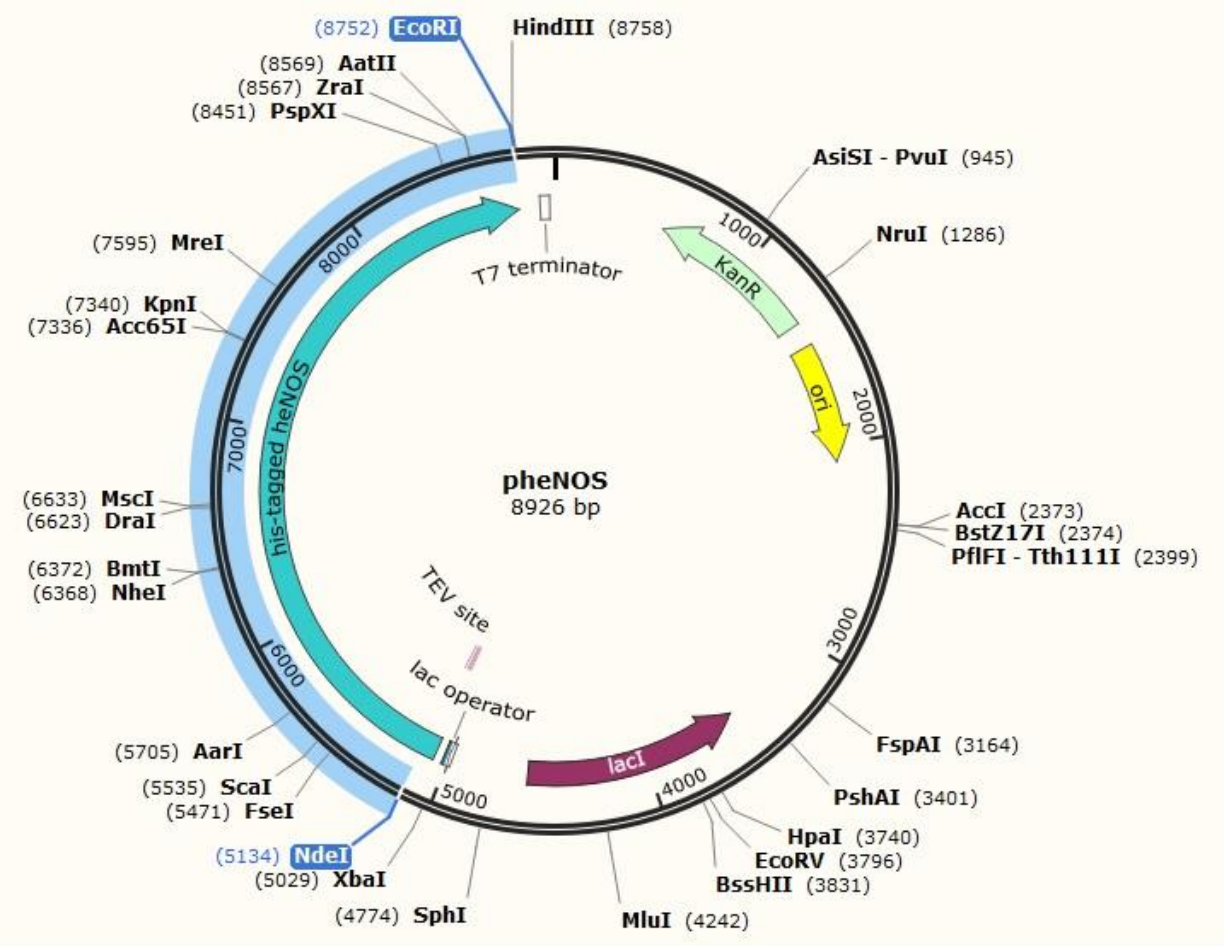

Sequence details of heNOS

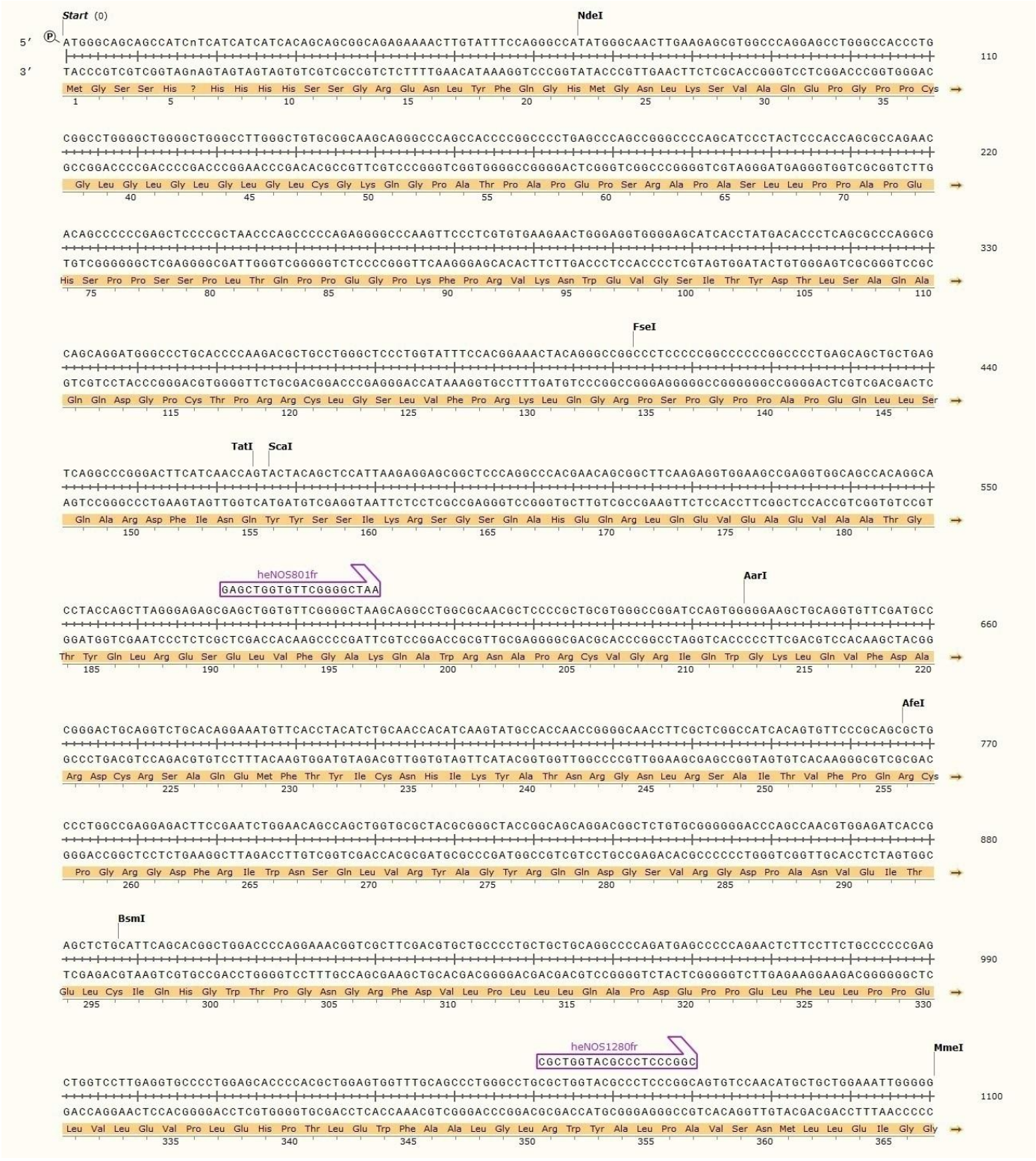

heNOS (cont'd – 2)

heNOS (cont'd – 3)

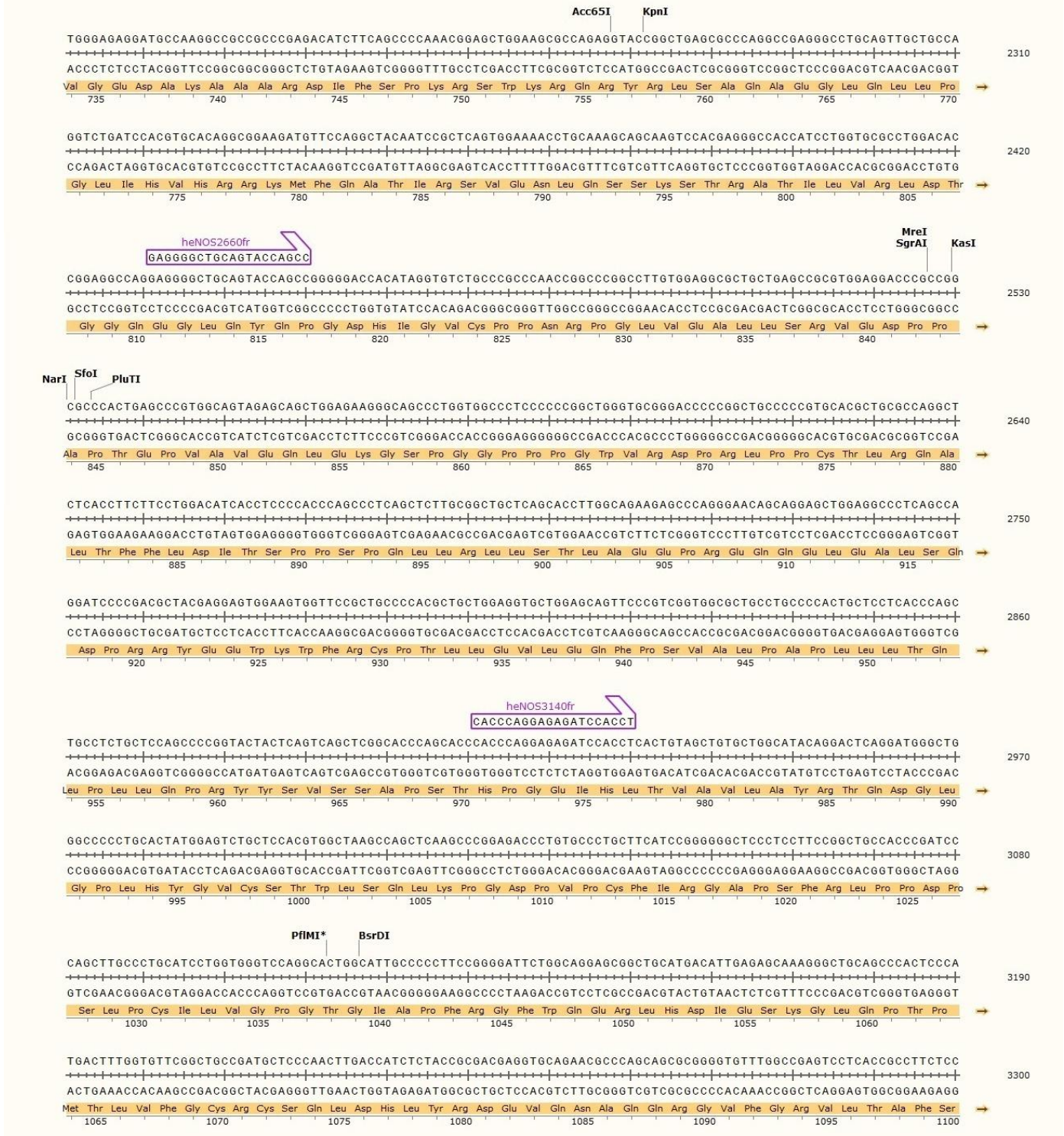

heNOS (cont'd – 4)

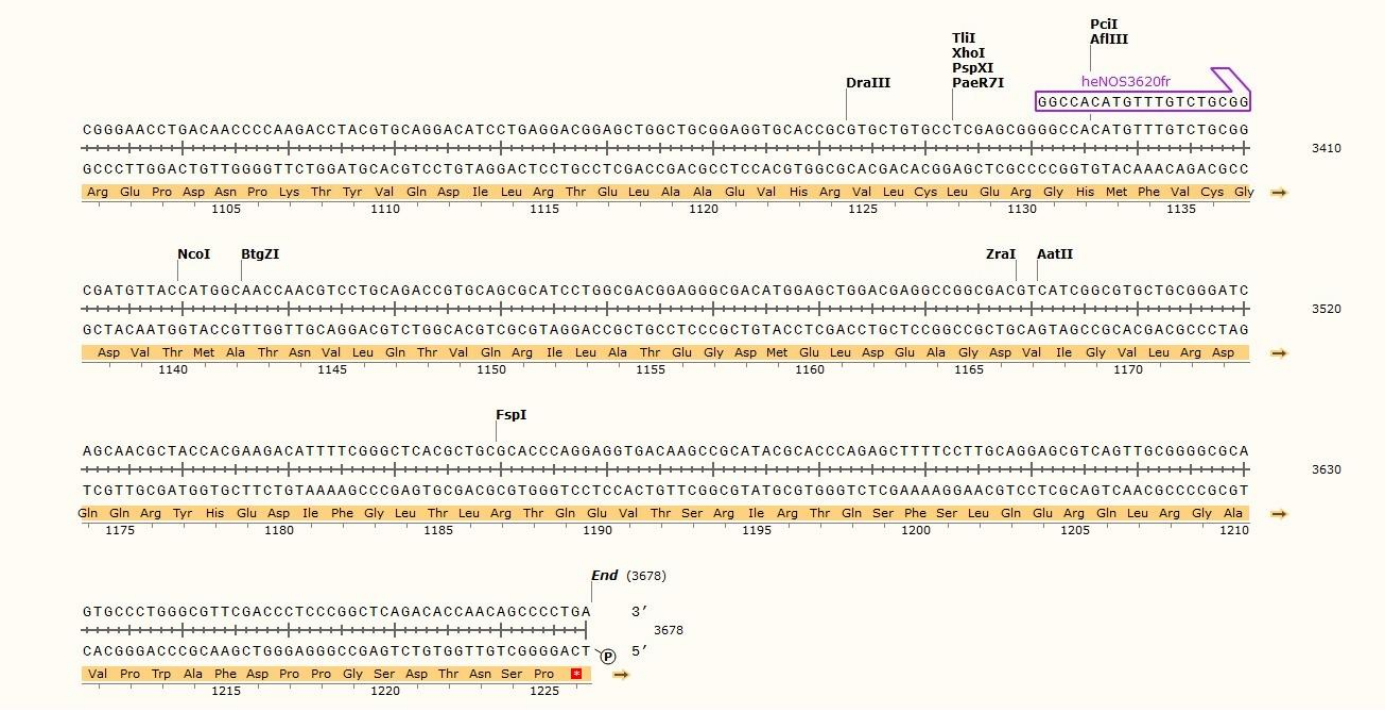

Sequencing summary of heNOS

DNA section	DNA sequencing	Primer to be used
1 – 1374	Complete	–
1375 – 1524	Incomplete	heNOS1280fr
1525 – 3678	Complete	–

No mutation was found in the sequencing results of heNOS.

Sequencing data of heNOS

T7

gggccggtaNattccctctagaataattttgtttaactttaagaaggagatataccatgggcagcagccatcNtcatcatcatcacagc
agcggcagagaaaacttgtatttccagggccatatgggcaacttgaagagcgtggcccaggagcctgggccaccctgcggcctgggg
ctggggctgggccttgggctgtgcggcaagcagggcccagccaccccggcccctgagcccagccgggccccagcatccctactccca
ccagcgccagaacacagccccccgagctccccgctaacccagcccccagaggggcccaagttccctcgtgtgaagaactgggaggtg
gggagcatcacctatgacaccctcagcgcccaggcgcagcaggatgggccctgcaccccaagacgctgcctgggctccctggtatttc
cacggaaactacagggccggccctccccggccccccggcccctgagcagctgctgagtcaggcccgggacttcatcaaccagtact
acagctccattaagaggagcggctcccaggcccacgaacagcggcttcaagaggtggaagccgaggtggcagccacaggcacctac
cagcttagggagagcgagctggtgttcggggctaagcaggcctggcgcaacgctccccgctgcgtgggccggatccagtgggggaag
ctgcaggtgttcgatgcccgggactgcaggtctgcacaggaaatgttcacctacatctgcaaccacatcaagtatgccaccaaccggg
gcaaccttcgctcggccatcacagtgttcccgcagcgctgccctggccgaggagacttccgaatctggaacagccagctggtgcgcta

cgcgggctaccggcagcaggacggctctgtgcgggggacccagccaacgtggagatcaccgagctctgcattcagcacggctgga
cccaggaaacggtcgcttcgacgtgctgccctgctgctgcagcNccagatgagccccaNactcttcttctgcctccgagctgtctgagt
gcNcctggagcacccNcacgctgagtgatgcagccctggctggcctggtacgNcctccgcaNgtcaacatgctgctggaatgggac
tggagttcctgcagccctcctcaNtgctgtactgggacttggaatcggNcaggaacttggttgacttactgtNaattctgagaatgact
tctNtctggaacNNg

heNOS801fr

tgcgtgggccggatccagtgggggaagctgcaggtgttcgatgcccgggactgcaggtctgcacaggaaatgttcacctacatctgca
accacatcaagtatgccaccaaccggggcaaccttcgctcggccatcacagtgttcccgcagcgctgccctggccgaggagacttccg
aatctggaacagccagctggtgcgctacgcgggctaccggcagcaggacggctctgtgcgggggacccagccaacgtggagatca
ccgagctctgcattcagcacggctggaccccaggaaacggtcgcttcgacgtgctgcccctgctgctgcaggccccagatgagccccc
agaactcttccttctgccccccgagctggtccttgaggtgcccctggagcaccccacgctggagtggtttgcagccctgggcctgcgctg
gtacgccctcccggcagtgtccaacatgctgctggaaattgggggcctggagttccccgcagccccccttcagtggctggtacatgagca
ctgagatcggcacgaggaacctgtgtgaccctcaccgctacaacatcctggaggatgtggctgtctgcatggacctggatacccggac
cacctcgtccctgtggaaagacaaggcagcagtggaaatcaacgtggccgtgctgcacagttaccagctagccaaagtcaccatcgt
ggaccaccacgccgccacggcctctttcatgaagcacctggagaatgagcagaag

heNOS1700fr

gggacNccagggagtgccgccagggcaccggcatcaccaggaagaagacctttaaagaagtggccaacgccgtgaagatctccgc
ctcgctcatgggcacggtgatggcgaagcgagtgaaggcgacaatcctgtatggctccgagaccggccgggcccagagctacgcaca
gcagctggggagactcttccggaaggcttttgatccccgggtcctgtgtatggatgagtatgacgtggtgtccctcgaacacgagacgc
tggtgctggtggtaaccagcacatttgggaatggggatcccccggagaatggagagagctttgcagctgccctgatggagatgtccgg
cccctacaacagctcccctcggccggaacagcacaagagttataagatccgcttcaacagcatctcctgctcagacccactggtgtcct
cttggcggcggaagaggaaggagtccagtaacacagacagtgcaggggccctgggcaccctcaggttctgtgtgttcgggctcggct
cccgggcatacccccacttctgcgcctttgctcgtgccgtggacacacggctggaggaactgggcggggagcggctgctgcagctggg
ccagggcgacgagctgtgcggccaggaggaggccttccgaggctgggcccaggctgccttccaggccgcctgtgagaccttctgtgtg
ggagaggatgccaaggccgccgcccgagacatcttcagccccaaacggagctggaagcgccagaggtaccggctgagcgcccagg
ccgagggcctgcagttgctgccaggtctgatccacgtgcacaggcggaagatgttNcaggctacaatccgctcagtggaaaacctgc
aagcagcaagtccacgagggccaccatcctggtgcgcctggacaNcggaggccaggaggggctgcagtaccagccgggacNcat
agtgtctgcNcgcNcaacggccggcttgtgagcgctgctgagcgcgtgagaccgcgNgccactgagcccgtgcagtaagcagctgg
agaagcagcctggtgtctccccgcNggtNNggacccggctgccNggaNgctggccagtNctacttNtctgacataNctccaccag
cctagctttgcgtgNagaccttggcgaaagtatgaatcgaacctgagctgccgaatcacgaacgctcNcaNagtgaatggttgcgcg
ctgagaca

heNOS2160fr

gacagtgcaggggccctgggcaccctcaggttctgtgtgttcgggctcggctcccgggcataccccacttctgcgcctttgctcgtgcc
gtggacacacggctggaggaactgggcggggagcggctgctgcagctgggccagggcgacgagctgtgcggccaggaggaggcctt
ccgaggctgggcccaggctgccttccaggccgcctgtgagaccttctgtgtgggagaggatgccaaggccgccgcccgagacatcttc
agccccaaacggagctggaagcgccagaggtaccggctgagcgcccaggccgagggcctgcagttgctgccaggtctgatccacgt
gcacaggcggaagatgttccaggctacaatccgctcagtggaaaacctgcaaagcagcaagtccacgagggccaccatcctggtgc
gcctggacaccggaggccaggaggggctgcagtaccagccgggggaccacataggtgtctgcccgcccaaccggcccggccttgtg

gaggcgctgctgagccgcgtggaggacccgccggcgcccactgagcccgtggcagtagagcagctggagaagggcagccctggtgg
ccctccccccggctgggtgcgggacccccggctgcccccgtgcacgctgcgccaggctctcaccttcttcctggacatcacctccccacc
cagccctcagctcttgcggctgctcagcaccttggca

heNOS2660fr

atttgNgtgtagctgttctgccgccaccggcggccttgtggaggcgctgctgagccgcgtggaggacccgccNgcgcccactgagccc
gtggcagtagagcagctggagaagggcagccctggtggccctcccccggctgggtgcgggacccccggctgcccccgtgcacgctg
cgccaggctctcaccttcttcctggacatcacctccccacccagccctcagctcttgcggctgctcagcaccttggcagaagagcccag
ggaacagcaggagctggaggccctcagccaggatccccgacgctacgaggagtggaagtggttccgctgccccacgctgctggaggt
gctggagcagttcccgtcggtggcgctgcctgccccactgctcctcacccagctgcctctgctccagccccggtactactcagtcagctc
ggcacccagcacccacccaggagagatccacctcactgtagctgtgctggcatacaggactcaggatgggctgggccccctgcactat
ggagtctgctccacgtggctaagccagctcaagcccggagaccctgtgccctgcttcatccgggggctccctccttccggctgccacc
cgatcccagcttgccctgcatcctggtgggtccaggcactggcattgccccttccggggattctggcaggagcggctgcatgacattg
agagcaaagggctgcagcccactcccatgactttggtgttcggctgccgatgctcccaacttgaccatctctaccgcgacgaggtgcag
aacgcccagcagcgcggggtgtttggccgagtcctcaccgccttctcccgggaacctgacaaccccaagacctacgtgcaggacatcc
tgaggacggagctggctgcggaggtgcaccgcgtgctgtgcctcgagcgggcNcatgtttgtctgcgcgatgttaccatggcaaccaa
cgtcctgcagaccgtgcagcgcatcctgcgacggagggcgacatgagctggacgagccggcgacgtcatcgcgtgctgcggatcagc
aacgctacNcgaagacttttcggctcNcgctgcgcacccagaggtgaNagcgcatacNcNccagaagcttttcttgcagNacgtc
agtgcgggNcatggcctgggcgattcgaccctccgtcgatcaacgccctgtaNtggaattcagcttcgaatctgacgctcaccacatg
gaaatccggcgNcataaaaagccgaaagaaacctat

heNOS3140fr

gNNcNNctgcaacaggactcaggatgggctgggcccctgcactatggagtctgctccacgtggctaagccagctcaagcccgga
gaccctgtgccctgcttcatccgggggctccctccttccggctgccacccgatcccagcttgccctgcatcctggtgggtccaggcact
ggcattgccccttccggggattctggcaggagcggctgcatgacattgagagcaaagggctgcagcccactcccatgactttggtgtt
cggctgccgatgctcccaacttgaccatctctaccgcgacgaggtgcagaacgcccagcagcgcggggtgtttggccgagtcctcacc
gccttctcccgggaacctgacaaccccaagacctacgtgcaggacatcctgaggacggagctggctgcggaggtgcaccgcgtgctg
tgcctcgagcggggccacatgtttgtctgcggcgatgttaccatggcaaccaacgtcctgcagaccgtgcagcgcatcctggcgacgg
agggcgacatggagctggacgaggccggcgacgtcatcggcgtgctgcgggatcagcaacgctaccacgaagacattttcgggctca
cgctgcgcacccaggaggtgacaagccgcatacgcacccagagcttttccttgcaggagcgtcagttgcggggcgcagtgccctggg
cgttcgaccctcccggctcagacaccaacagcccctgatatggaattcaagcttctcgagcaccaccaccaccaccactgagatccgg
ctgctaacaaagcccgaaaggaagctgagttggctgctgccaccgctgagcaataactagcataaccccttggggcctctaaacggg
tcttgagggttttgctgaaaggaggaactatatccggattggcgaatggacgcgcctgtagcgcgcattaagcgcggcgggtgtggt
gtacgcgcagcgtgacgctacactgcagcgcctagcgccgctcttcgcttctctcttctcgcccgtcgcgcttcccgtcagcNtaatcgg
gctccgtagtcgatatgctacgactcgacccaaactgatagggatgtNcgtatgacatNcctgaNaacgatcNcctgactggatcag
tcttatatgcacttgtcactgaaccgNacgattcgcatctggatttaaggattgcgNat

Blast results of heNOS

T7

Score	Expect	Method	Identities	Positives	Gaps	Frame
473 bits(1218)	3e-159	Compositional matrix adjust.	280/280(100%)	280/280(100%)	0/280(0%)	+3

```
Query  123  MGNLKSVAQEpgppcglglglglglcgKQGpatpapepsrapasllppapehsppssplT  302
            MGNLKSVAQEPGPPCGLGLGLGLGLCGKQGPATPAPEPSRAPASLLPPAPEHSPPSSPLT
Sbjct  1    MGNLKSVAQEPGPPCGLGLGLGLGLCGKQGPATPAPEPSRAPASLLPPAPEHSPPSSPLT  60

Query  303  QPPEGPKFPRVKNWEVGSITYDTLSAQAQQDGPCTPRRCLGSLVFPRKLQGRPSPGPPAP  482
            QPPEGPKFPRVKNWEVGSITYDTLSAQAQQDGPCTPRRCLGSLVFPRKLQGRPSPGPPAP
Sbjct  61   QPPEGPKFPRVKNWEVGSITYDTLSAQAQQDGPCTPRRCLGSLVFPRKLQGRPSPGPPAP  120

Query  483  EQLLSQARDFINQYYSSIKRSGSQAHEQRLQEVEAEVAATGTYQLRESELVFGAKQAWRN  662
            EQLLSQARDFINQYYSSIKRSGSQAHEQRLQEVEAEVAATGTYQLRESELVFGAKQAWRN
Sbjct  121  EQLLSQARDFINQYYSSIKRSGSQAHEQRLQEVEAEVAATGTYQLRESELVFGAKQAWRN  180

Query  663  APRCVGRIQWGKLQVFDARDCRSAQEMFTYICNHIKYATNRGNLRSAITVFPQRCPGRGD  842
            APRCVGRIQWGKLQVFDARDCRSAQEMFTYICNHIKYATNRGNLRSAITVFPQRCPGRGD
Sbjct  181  APRCVGRIQWGKLQVFDARDCRSAQEMFTYICNHIKYATNRGNLRSAITVFPQRCPGRGD  240

Query  843  FRIWNSQLVRYAGYRQQDGSVRGDPANVEITELCIQHGWT  962
            FRIWNSQLVRYAGYRQQDGSVRGDPANVEITELCIQHGWT
Sbjct  241  FRIWNSQLVRYAGYRQQDGSVRGDPANVEITELCIQHGWT  280
```

heNOS801fr

Score	Expect	Method	Identities	Positives	Gaps	Frame
476 bits(1224)	6e-163	Compositional matrix adjust.	253/253(100%)	253/253(100%)	0/253(0%)	+1

```
Query  1    CVGRIQWGKLQVFDARDCRSAQEMFTYICNHIKYATNRGNLRSAITVFPQRCPGRGDFRI  180
            CVGRIQWGKLQVFDARDCRSAQEMFTYICNHIKYATNRGNLRSAITVFPQRCPGRGDFRI
Sbjct  184  CVGRIQWGKLQVFDARDCRSAQEMFTYICNHIKYATNRGNLRSAITVFPQRCPGRGDFRI  243

Query  181  WNSQLVRYAGYRQQDGSVRGDPANVEITELCIQHGWTPGNGRFDVLPLLLQApdeppelf  360
            WNSQLVRYAGYRQQDGSVRGDPANVEITELCIQHGWTPGNGRFDVLPLLLQAPDEPPELF
```

```
Sbjct  244  WNSQLVRYAGYRQQDGSVRGDPANVEITELCIQHGWTPGNGRFDVLPLLLQAPDEPPELF  303

Query  361  llppelvlevplehptleWFAALGLRWYALPAVSNMLLEIGGLEFPAAPFSGWYMSTEIG  540
            LLPPELVLEVPLEHPTLEWFAALGLRWYALPAVSNMLLEIGGLEFPAAPFSGWYMSTEIG
Sbjct  304  LLPPELVLEVPLEHPTLEWFAALGLRWYALPAVSNMLLEIGGLEFPAAPFSGWYMSTEIG  363

Query  541  TRNLCDPHRYNILEDVAVCMDLDTRTTSSLWKDKAAVEINVAVLHSYQLAKVTIVDHHAA  720
            TRNLCDPHRYNILEDVAVCMDLDTRTTSSLWKDKAAVEINVAVLHSYQLAKVTIVDHHAA
Sbjct  364  TRNLCDPHRYNILEDVAVCMDLDTRTTSSLWKDKAAVEINVAVLHSYQLAKVTIVDHHAA  423

Query  721  TASFMKHLENEQK  759
            TASFMKHLENEQK
Sbjct  424  TASFMKHLENEQK  436
```

heNOS1700fr

Score	Expect	Method	Identities	Positives	Gaps	Frame
536 bits(1380)	0.0	Compositional matrix adjust.	283/287(99%)	286/287(99%)	0/287(0%)	+3

```
Query  21   QGTGITRKKTFKEVANAVKISASLMGTVMAKRVKATILYGSETGRAQSYAQQLGRLFRKA  200
            +GTGITRKKTFKEVANAVKISASLMGTVMAKRVKATILYGSETGRAQSYAQQLGRLFRKA
Sbjct  486  KGTGITRKKTFKEVANAVKISASLMGTVMAKRVKATILYGSETGRAQSYAQQLGRLFRKA  545

Query  201  FDPRVLCMDEYDVVSLEHETLVLVVTSTFGNGDPPENGESFAAALMEMSGPYNSSPRPEQ  380
            FDPRVLCMDEYDVVSLEHETLVLVVTSTFGNGDPPENGESFAAALMEMSGPYNSSPRPEQ
Sbjct  546  FDPRVLCMDEYDVVSLEHETLVLVVTSTFGNGDPPENGESFAAALMEMSGPYNSSPRPEQ  605

Query  381  HKSYKIRFNSISCSDPLVSSWRRKRKESSNTDSAGALGTLRFCVFGLGSRAYPHFCAFAR  560
            HKSYKIRFNSISCSDPLVSSWRRKRKESSNTDSAGALGTLRFCVFGLGSRAYPHFCAFAR
Sbjct  606  HKSYKIRFNSISCSDPLVSSWRRKRKESSNTDSAGALGTLRFCVFGLGSRAYPHFCAFAR  665

Query  561  AVDTrleelggerllqlgqgdelCGQEEAFRGWAQAAFQAACETFCVGEDAKAAARDIFS  740
            AVDTRLEELGGERLLQLGQGDELCGQEEAFRGWAQAAFQAACETFCVGEDAKAAARDIFS
Sbjct  666  AVDTRLEELGGERLLQLGQGDELCGQEEAFRGWAQAAFQAACETFCVGEDAKAAARDIFS  725

Query  741  PKRSWKRQRYRLSAQAEGLQLLPGLIHVHRRKMXQATIRSVENLQAA  881
            PKRSWKRQRYRLSAQAEGLQLLPGLIHVHRRKM QATIRSVENLQ++
Sbjct  726  PKRSWKRQRYRLSAQAEGLQLLPGLIHVHRRKMFQATIRSVENLQSS  772
```

heNOS2160fr

Score	Expect	Method	Identities	Positives	Gaps	Frame
402 bits(1033)	4e-135	Compositional matrix adjust.	230/230(100%)	230/230(100%)	0/230(0%)	+1

```
Query  1    DSAGALGTLRFCVFGLGSRAYPHFCAFARAVDTrleelggerllqlgqgdelCGQEEAFR  180
            DSAGALGTLRFCVFGLGSRAYPHFCAFARAVDTRLEELGGERLLQLGQGDELCGQEEAFR
Sbjct  637  DSAGALGTLRFCVFGLGSRAYPHFCAFARAVDTRLEELGGERLLQLGQGDELCGQEEAFR  696

Query  181  GWAQAAFQAACETFCVGEDAKAAARDIFSPKRSWKRQRYRLSAQAEGLQLLPGLIHVHRR  360
            GWAQAAFQAACETFCVGEDAKAAARDIFSPKRSWKRQRYRLSAQAEGLQLLPGLIHVHRR
Sbjct  697  GWAQAAFQAACETFCVGEDAKAAARDIFSPKRSWKRQRYRLSAQAEGLQLLPGLIHVHRR  756

Query  361  KMFQATIRSVENLQSSKSTRATILVRLDTGGQEGLQYQPGDHIGVCPPNRPGLVEALLSR  540
            KMFQATIRSVENLQSSKSTRATILVRLDTGGQEGLQYQPGDHIGVCPPNRPGLVEALLSR
Sbjct  757  KMFQATIRSVENLQSSKSTRATILVRLDTGGQEGLQYQPGDHIGVCPPNRPGLVEALLSR  816

Query  541  VEDPPAPTEPVAVEQLEKGSPGGPPPGWVRDPRLPPCTLRQALTFFLDIT  690
            VEDPPAPTEPVAVEQLEKGSPGGPPPGWVRDPRLPPCTLRQALTFFLDIT
Sbjct  817  VEDPPAPTEPVAVEQLEKGSPGGPPPGWVRDPRLPPCTLRQALTFFLDIT  866
```

heNOS2660fr

Score	Expect	Method	Identities	Positives	Gaps	Frame
554 bits(1427)	0.0	Compositional matrix adjust.	318/324(98%)	320/324(98%)	1/324(0%)	+2

```
Query  32    GLVEALLSRVEDPPAPTEPVAVEQLEKGSPGGPPPGWVRDPRLPPCTLRQALTFFLDITs  211
            GLVEALLSRVEDPPAPTEPVAVEQLEKGSPGGPPPGWVRDPRLPPCTLRQALTFFLDITS
Sbjct  808   GLVEALLSRVEDPPAPTEPVAVEQLEKGSPGGPPPGWVRDPRLPPCTLRQALTFFLDITS  867

Query  212   ppspqllrllstlAEEPREQQELEALSQDPRRYEEWKWFRCPTLLEVLEQFPSValpapl  391
            PPSPQLLRLLSTLAEEPREQQELEALSQDPRRYEEWKWFRCPTLLEVLEQFPSVALPAPL
Sbjct  868   PPSPQLLRLLSTLAEEPREQQELEALSQDPRRYEEWKWFRCPTLLEVLEQFPSVALPAPL  927

Query  392   lltqlpllqpRYYSVSSAPSTHPGEIHLTVAVLAYRTQDGLGPLHYGVCSTWLSQLKPGD  571
            LLTQLPLLQPRYYSVSSAPSTHPGEIHLTVAVLAYRTQDGLGPLHYGVCSTWLSQLKPGD
Sbjct  928   LLTQLPLLQPRYYSVSSAPSTHPGEIHLTVAVLAYRTQDGLGPLHYGVCSTWLSQLKPGD  987

Query  572   PVPCFIRGAPSFRLPPDPSLPCILVGPGTGIAPFRGFWQERLHDIESKGLQPTPMTLVFG  751
```

```
            PVPCFIRGAPSFRLPPDPSLPCILVGPGTGIAPFRGFWQERLHDIESKGLQPTPMTLVFG
Sbjct  988  PVPCFIRGAPSFRLPPDPSLPCILVGPGTGIAPFRGFWQERLHDIESKGLQPTPMTLVFG  1047

Query  752  CRCSQLDHLYRDEVQNAQQRGVFGRVLTAFSREPDNPKTYVQDILRTELAAEVHRVLCLE  931
            CRCSQLDHLYRDEVQNAQQRGVFGRVLTAFSREPDNPKTYVQDILRTELAAEVHRVLCLE
Sbjct  1048 CRCSQLDHLYRDEVQNAQQRGVFGRVLTAFSREPDNPKTYVQDILRTELAAEVHRVLCLE  1107

Query  932  RAHVCL-RDVTMATNVLQTVQRIL  1000
            R H+ +  DVTMATNVLQTVQRIL
Sbjct  1108 RGHMFVCGDVTMATNVLQTVQRIL  1131
```

heNOS3140fr

Score	Expect	Method	Identities	Positives	Gaps	Frame
500 bits(1287)	9e-170	Compositional matrix adjust.	241/241(100%)	241/241(100%)	0/241(0%)	+2

```
Query  14   RTQDGLGPLHYGVCSTWLSQLKPGDPVPCFIRGAPSFRLPPDPSLPCILVGPGTGIAPFR  193
            RTQDGLGPLHYGVCSTWLSQLKPGDPVPCFIRGAPSFRLPPDPSLPCILVGPGTGIAPFR
Sbjct  963  RTQDGLGPLHYGVCSTWLSQLKPGDPVPCFIRGAPSFRLPPDPSLPCILVGPGTGIAPFR  1022

Query  194  GFWQERLHDIESKGLQPTPMTLVFGCRCSQLDHLYRDEVQNAQQRGVFGRVLTAFSREPD  373
            GFWQERLHDIESKGLQPTPMTLVFGCRCSQLDHLYRDEVQNAQQRGVFGRVLTAFSREPD
Sbjct  1023 GFWQERLHDIESKGLQPTPMTLVFGCRCSQLDHLYRDEVQNAQQRGVFGRVLTAFSREPD  1082

Query  374  NPKTYVQDILRTELAAEVHRVLCLERGHMFVCGDVTMATNVLQTVQRILATEGDMELDEA  553
            NPKTYVQDILRTELAAEVHRVLCLERGHMFVCGDVTMATNVLQTVQRILATEGDMELDEA
Sbjct  1083 NPKTYVQDILRTELAAEVHRVLCLERGHMFVCGDVTMATNVLQTVQRILATEGDMELDEA  1142

Query  554  GDVIGVLRDQQRYHEDIFGLTLRTQEVTSRIRTQSFSLQERQLRGAVPWAFDPPGSDTNS  733
            GDVIGVLRDQQRYHEDIFGLTLRTQEVTSRIRTQSFSLQERQLRGAVPWAFDPPGSDTNS
Sbjct  1143 GDVIGVLRDQQRYHEDIFGLTLRTQEVTSRIRTQSFSLQERQLRGAVPWAFDPPGSDTNS  1202

Query  734  P  736
            P
Sbjct  1203 P  1203
```

phiNOS – human full-length Δ70 iNOS in pDS-78

Vector map

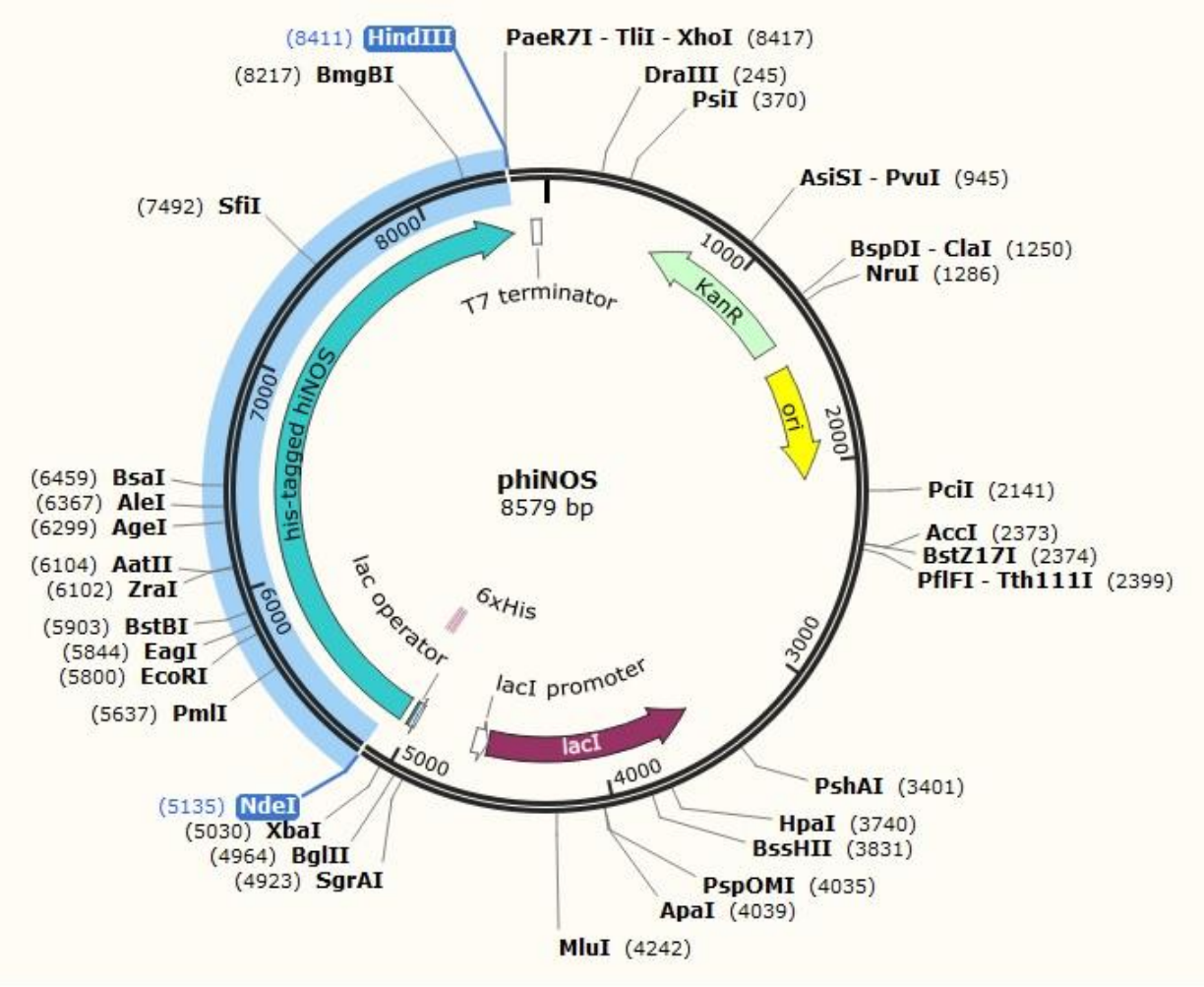

Sequence details of hiNOS

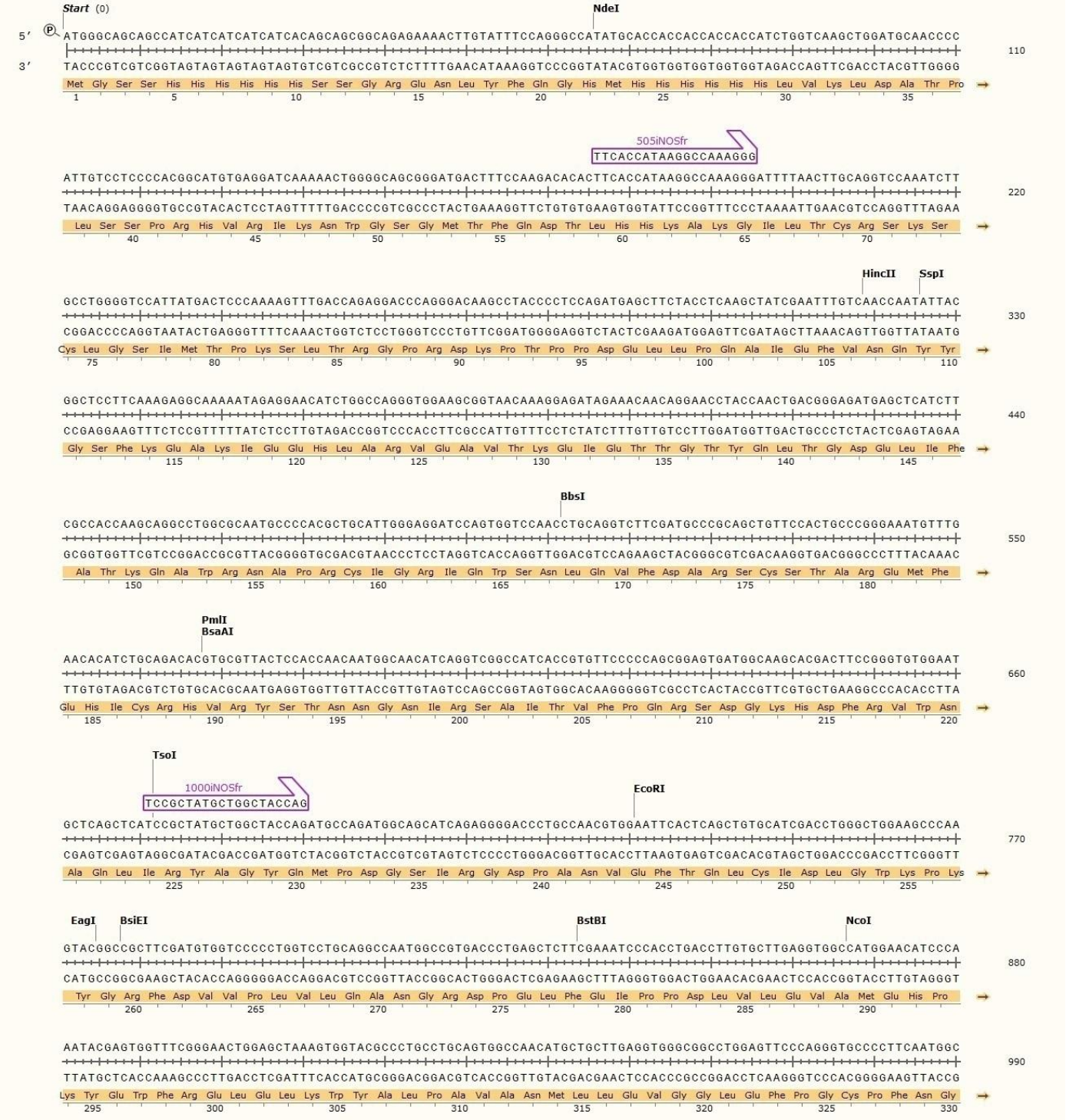

hiNOS (cont'd – 2)

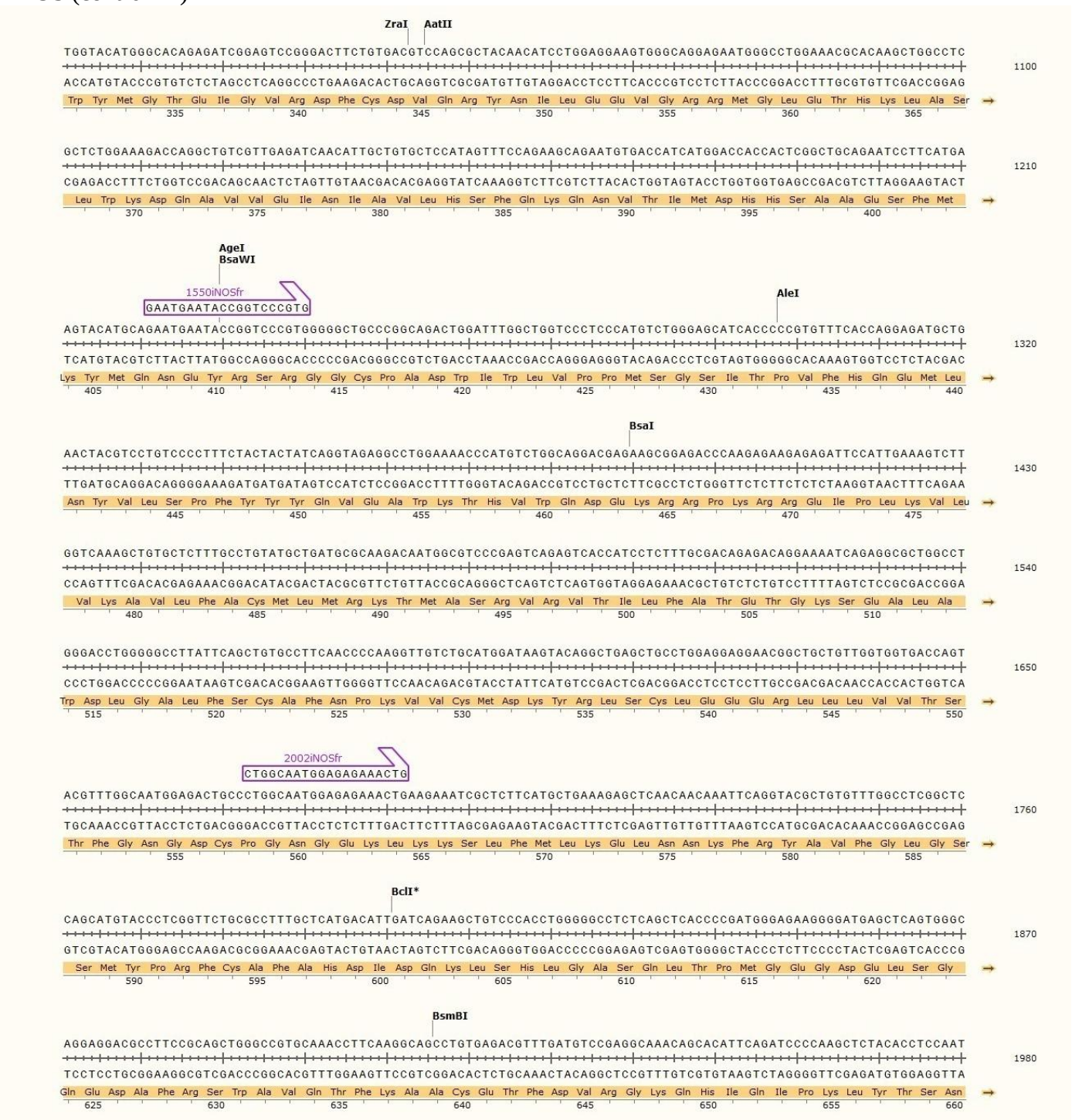

hiNOS (cont'd – 3)

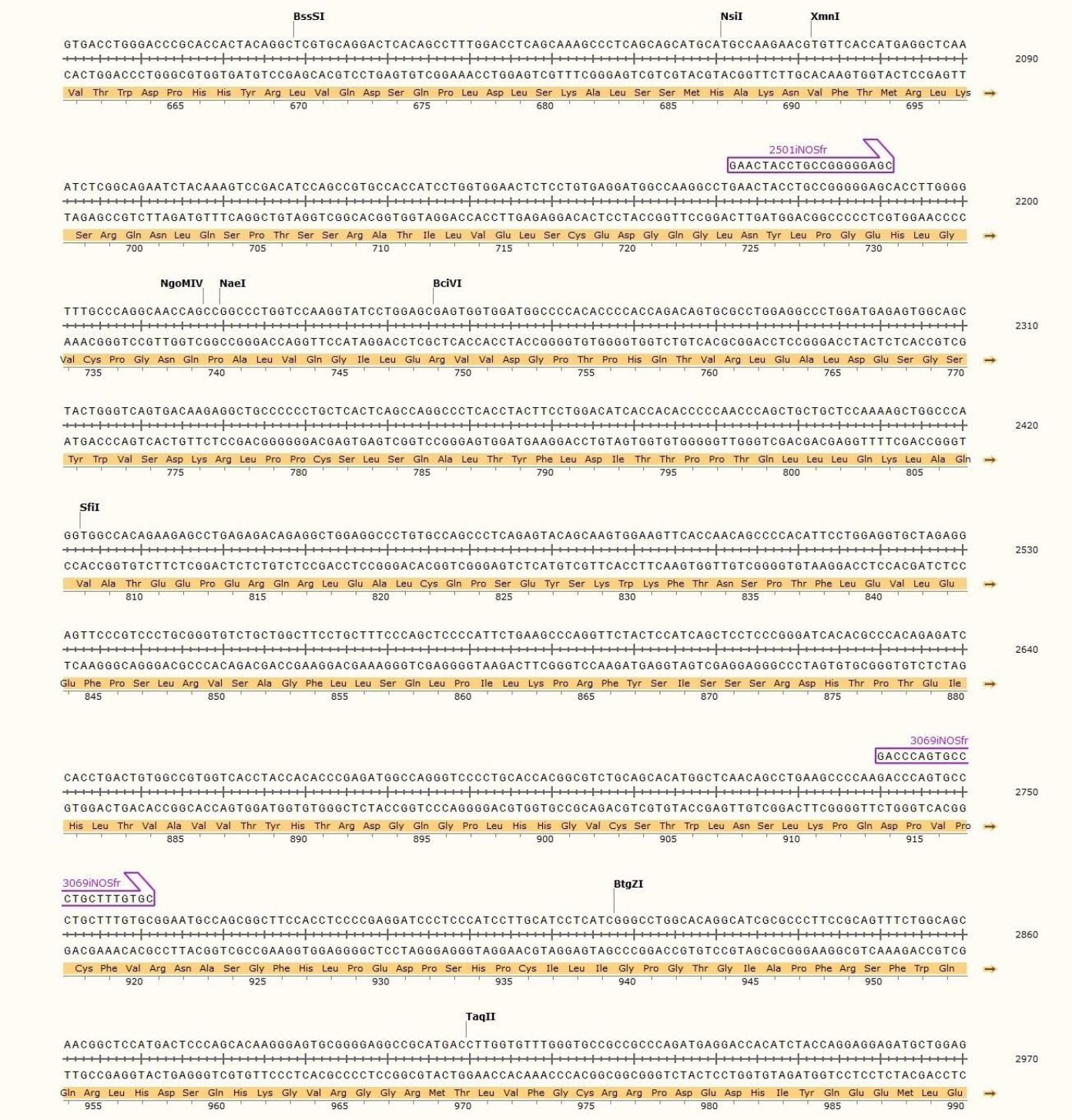

hiNOS (cont'd – 4)

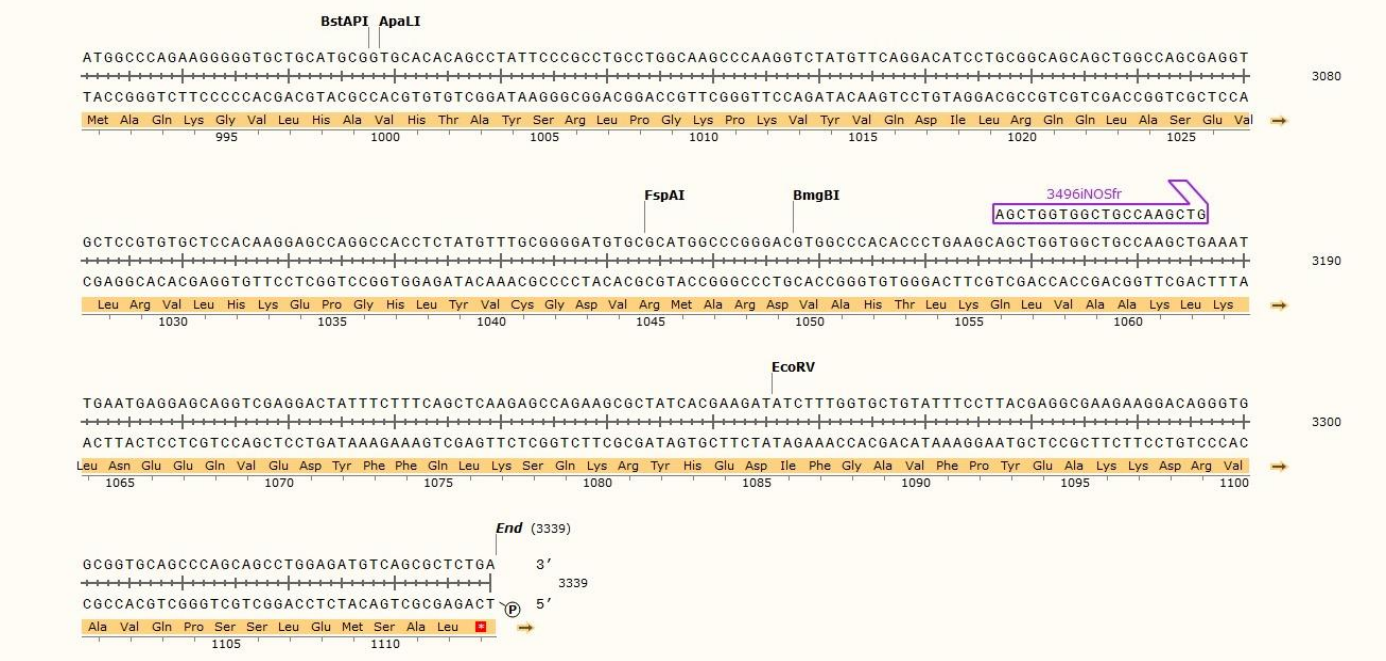

Sequencing summary of hiNOS

DNA section	DNA sequencing	Primers to be used
1 – 3339	Incomplete	pCWOri-fr 505iNOSfr 1000iNOSfr 1550iNOSfr 2002iNOSfr 2501iNOSfr 3069iNOSfr 3496iNOSfr

References

Alderton, W. K., Cooper, C. E., & Knowles, R. G. (2001). Nitric oxide synthases: structure, function and inhibition. *The Biochemical Journal*, *357*(Pt 3), 593–615.

Bretscher, L. E., Li, H., Poulos, T. L., & Griffith, O. W. (2003). Structural characterization and kinetics of nitric-oxide synthase inhibition by novel N5-(iminoalkyl)- and N5-(iminoalkenyl)-ornithines. *The Journal of Biological Chemistry*, *278*(47), 46789–97.

Fang, J., Ji, H., Lawton, G., & Xue, F. (2009). L337H Mutant of Rat Neuronal Nitric Oxide Synthase Resembles Human Neuronal Nitric Oxide Synthase toward Inhibitors. *Journal of medicinal Chemistry*, *52*(14), 4533–4537.

Fang, L., Jia, K. Z., Tang, Y. L., Ma, D. Y., Yu, M., & Hua, Z. C. (2007). An improved strategy for high-level production of TEV protease in *Escherichia coli* and its purification and characterization. *Protein expression and purification*, *51*(1), 102-9.

Garcin, E. D., Arvai, A. S., Rosenfeld, R. J., Kroeger, M. D., Crane, B. R., Andersson, G., … Getzoff, E. D. (2008). Anchored plasticity opens doors for selective inhibitor design in nitric oxide synthase. *Nature Chemical Biology*, *4*(11), 700–7.

Garcin, E. D., Bruns, C. M., Lloyd, S. J., Hosfield, D. J., Tiso, M., Gachhui, R., … Getzoff, E. D. Structural basis for isozyme-specific regulation of electron transfer in nitric-oxide synthase. *Journal of biological chemistry*, *279*(36), 37918-27.

Harper, S., & Speicher, D. W. (2011). Purification of proteins fused to glutathione S-transferaase. *Methods in molecular biology*, *681*, 259-80.

Hurshman, A. R., & Marletta, M. A. (2002). Reactions catalyzed by the heme domain of inducible nitric oxide synthase: evidence for the involvement of tetrahydrobiopterin in electron transfer. *Biochemistry*, *41*(10), 3439–56.

Iwasaki, T., Hori, H., Hayashi, Y., Nishino, T., Tamura, K., Oue, S., … Esumi, H. (1999). Characterization of mouse nNOS2, a natural variant of neuronal nitric-oxide synthase produced in the central nervous system by selective alternate splicing. *Journal of biological chemistry*, *274*(25), 17559-66.

Jeong, J.-Y., Yim, H.-S., Ryu, J.-Y., Lee, H. S., Lee, J.-H., Seen, D.-S., & Kang, S. G. (2012). One-step sequence- and ligation-independent cloning as a rapid and versatile cloning method for functional genomics studies. *Applied and Environmental Microbiology*, *78*(15), 5440–3.

Ji, H., Delker, S. L., Li, H., Martásek, P., Roman, L. J., Poulos, T. L., & Silverman, R. B. (2010). Exploration of the active site of neuronal nitric oxide synthase by the design and synthesis of pyrrolidinomethyl 2-aminopyridine derivatives. *Journal of Medicinal Chemistry*, *53*(21), 7804–24.

Joubert, J., & Malan, S. F. (2011). Novel nitric oxide synthase inhibitors: a patent review. *Expert opinion on therapeutic patents*, *21*(4), 537–60.

Kolesnikov, Y. A., Pan, Y., Babey, A., Jain, S., Wilson, R., & Pasternak, G. W. (1997). Functionally differentiating two neuronal nitric oxide synthase isoforms through antisense mapping: evidence for opposing NO actions on morphine analgesia and tolerance. *Proceedings of the National Academy of Sciences of the United States of America*, *94*(15), 8220-5.

Maddaford, S., Annedi, S. C., Ramnauth, J., Rakhit, S. (2009). Advancements in the Development of Nitric Oxide Synthase Inhibitors. *Annual Reports in Medicinal Chemistry*, *44*, 27-50.

McMillan, K., & Masters, B. S. S. (1995). Prokaryotic Expression of the Heme- and Flavin-Binding Domains of Rat Neuronal Nitric Oxide Synthase as Distinct Polypeptides: Identificationn of the Heme-Binding Proximal Thiolate Ligand as Cysteine-415. *Biochemistry*, *34*, 3686-3693.

Montgomery, H. J., Dupont, A. L., Leivo, H. E., & Guillemette, J. G. (2010). Cloning, Expression, and Purification of a Nitric Oxide Synthase-Like Protein form *Bacillus cereus*. *Biochemistry Research International, 2010*(2010), 1-4.

Nallamsetty, S., Kapust, R. B., Tozser, J., Cherry, S., Tropea, J. E., Copeland, T. D., & Waugh, D. S. (2004). Efficient site-specific processing of fusion proteins by tobacco vein mottling virus protease in vivo and in vitro. *Protein expression and purification*, *38*(1), 108-15.

Rafferty, S. P., Boyington, J. C., Kulansky, R., Sun, P. D., & Malech, H. L. (1999). Stoichiometric arginine binding in the oxygenase domain of the inducible nitric oxide synthase requires a single molecule of tetrahydrobiopterin per dimer. *Biochemical and Biophysical Research Communications*, *257*(2), 344-7.

Roman, L. J., Sheta, E. A., Martasek, P., Gross, S. S., Liu, Q., & Masters, B. S. S. (1995). High-level expression of functional rat neuronal nitric oxide synthase in *Escherichia coli*. *Proceedings of the National Academy of Sciences of the United States of America*, *92*, 8428-8432.

Sahdev, S., Khattar, S. K., & Saini, K. S. (2008). Production of active eukaryotic proteins through bacterial expression systems: a review of the existing biotechnology strategies. *Molecular and cellular biochemistry*, *307*(1-2), 249-64.

Salerno, L., Sorrenti, V., Di Giacomo, C., Romeo, G., & Siracusa, M. A. (2002). Progress in the Development of Selective Nitric Oxide Synthase (NOS) Inhibitors. *Current Pharmaceutical Design*, *8*, 177-200.

Schneider, E., & Clark, D. S. (2013). Cytochrome P450 (CYP) enzymes and the development of CYP biosensors. *Biosensors & bioelectronics, 39*(1), 1-13.

Spratt, D. E. (2008). Calmodulin Binding and Activation of Mammalian Nitric Oxide Synthase (Doctoral dissertation). University of Waterloo, Waterloo.

Vitecek, J., Lojek, A., Valacchi, G., & Kubala, L. (2012). Arginine-Based Inhibitors of Nitric Oxide Synthase: Therapeutic Potential and Challenges. *Mediators of Inflammation, 2012*(2012), 1-22.

Wang, W., & Malcom, B. A. (1999). Two-stage PCR protocol allowing introduction of multiple mutations, deletions and insertions using QuikChange Site-Directed Mutagenesis. *Biotechniques, 26*(4), 680-2.

Xue, F., Li, H., Fang, J., Roman, L. J., Martásek, P., Poulos, T. L., & Silverman, R. B. (2010). Peripheral but crucial: a hydrophobic pocket (Tyr(706), Leu(337), and Met(336)) for potent and selective inhibition of neuronal nitric oxide synthase. *Bioorganic & Medicinal Chemistry Letters, 20*(21), 6258–61.

Zelasko, S., Palaria, A., & Das, A. (2013). Optimizations to achieve high-level expression of cytochrome P450 proteins using *Escherichia coli* expression systems. *Protein expression and purification, 92*(1), 77-87.